AALBORG UNIVERSITY

Department of Energy Technology - Pontoppidanstræde 101
Aalborg University, Denmark

MASTER THESIS

COORDINATED CONTROL OF WIND TURBINES

Conducted by:
Cosmin-Eugen Bănceanu
Iulian Vrânceanu

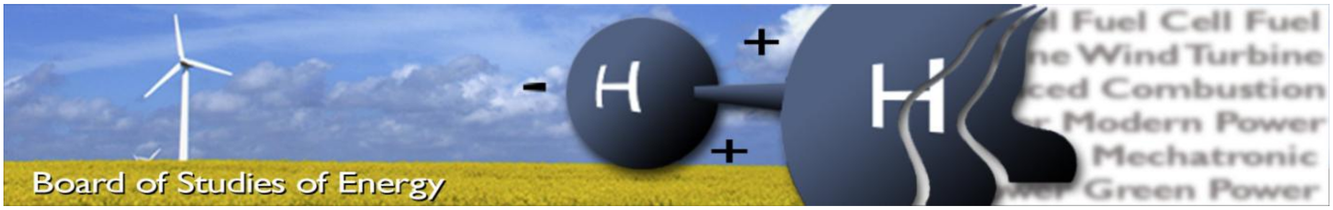

Title: Coordinated Control of Wind Turbines
Semester: 10th
Semester theme: **Master Thesis**

Project period: 01.02.2011 – 31.05.2011
ECTS: 30
Supervisors: **AAU:** Remus Teodorescu, Andrzej Grzegorz Adamczyk,
ABB: Adrian Timbus, Carsten Franke
Project group: WPS4 - 1052

SYNOPSIS:

Over the last ten years, the global wind energy capacity has increased rapidly and proved to be the fastest developing renewable energy technology and an important competitor to the traditional sources of energy. Design of Wind Power Plants (WPP) has evolved through time with the aim of becoming less expensive and producing energy more efficiently.

Due to the high penetration level of the wind energy into the grid, the TSOs start to impose severe grid codes requirements and expects from WPP to behave like a regular power plant. Therefore having an efficient and a reliable WPP controller is very important.

The main objective of this thesis is to develop a WPP Controller capable to fulfill the most demanding European grid codes, according to ENTSOE, and to control not only the wind turbines but also the ancillary devices (e.g. STATCOM). This thesis also investigates the optimal Q rating for the STATCOM, Capacitor Bank and the Grid Side Converter, based on a technical and economic analysis and different scenarios.

Moreover, the optimal dispatch was analyzed for different WPP control modes (delta, balance, etc) and different control objectives (losses minimization or life time optimization). Finally, a conventional power flow was implemented as well, in order to evaluate the optimal power flow with respect to a benchmark.

____
Cosmin-Eugen Bănceanu

____
Iulian Vrânceanu

Copies: 3
Pages, total: 83
Appendix: 5
Supplements: 1 CD

By signing this document, each member of the group confirms that all participated in the project work and thereby that all members are collectively liable for the content of the report.

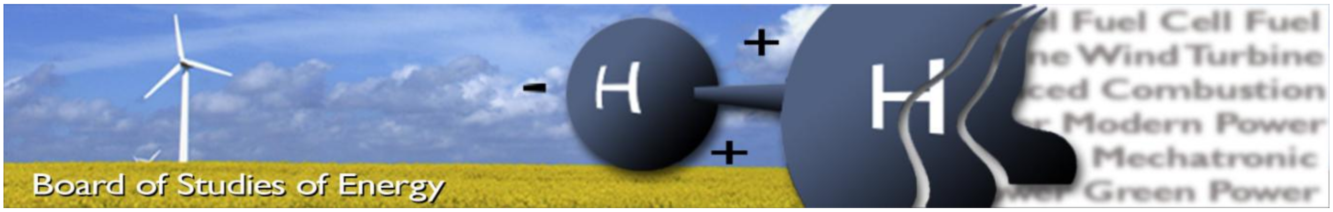

Preface

The present project entitled *Coordinated Control of Wind Turbines* was written by group WPS4-1052 in 10th Semester at the Department of Energy Technology, Aalborg University. This project has been carried out between 1st of February – 31th May 2011.

Reading Instructions

The references are shown in form of numbers put in square brackets. Detailed information about literature is presented in the References. While the format for equations is (X.Y) for figures and tables is X-Y, where X is the number of chapter and Y is the number of equation/figure/table.

Acknowledgement

We gratefully appreciate all the guidance and professional support from our supervisors Remus Teodorescu, Andrzej Grzegorz Adamczyk, Adrian Timbus and Carsten Franke which with their patience and generosity devoted valuable time during the project period.

Many thanks to all our colleagues at AAU - DET for their friendly companion and constructive discussions. In particular, we thank to Bogdan Ionut Crăciun, Cătalin Dâncan, Daniel Stroe and Irina Stan. Also we would like to express our appreciation for Tamas Kerekes for his cooperation, encouragement and full support during the entire MSc period.

Finally, we would like to thank to our families for their generous and continuous moral support in the past 2 years.

Aalborg, 1st of June 2011
GROUP 1052

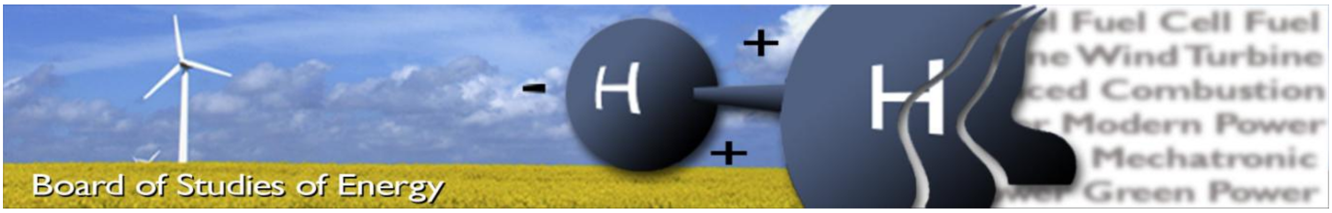

Table of contents

Nomenclature

List of abbreviations

AC	Alternative Current
CIM	Common Information Model
CN	Connectivity Node
DC	Direct Current
DFIG	Double Fed Induction Generator
DSO	Distribution System Operator
EMS	Energy Management System
ESS	Energy Storage System
EWEA	European Wind Energy Association
FACTS	Flexible AC Transmission System
FRT	Fault Ride Through
FSC	Full Scale
GSC	Grid Side Converter
IGBT	Insulated Gate Bipolar Transistor
OPF	Optimal Power Flow
PCC	Point of Common Coupling
PMSG	Permanent Magnet Synchronous Generator
SCADA	Supervisory Control And Data Acquisition
SCIG	Squirrel Cage Induction Generator
TN	Topological Node
TR	Terminal
TSO	Transmission System Operator
WF	Wind Farm
WRIG	Wound Rotor Induction Generator
WPP	Wind Power Plant
WT	Wind Turbine
WTS	Wind Turbine System
XML	Extensible Markup Language

List of Symbols

β	Pitch angle
C_p	Power Coefficient
f_{meas}^{PCC}	Frequency measured in PCC
$I_{C\max}, I_{L\max}$	Maxim Capacitive/Inductive Current
I_i	Current at each bus bar
I^{meas}	Measured Current
I_{stat}	STATCOM Current
L_g	Grid Inductance
Ω_{gen}^{meas}	Generator Speed Measured
P	Active power
P_{avail_i}, Q_{avail_i}	Available Active/Reactive Power Reference for the i^{th} WT

P_{bus_i}, Q_{bus_i}	Active/Reactive Power for the i^{th} bus
$P_{demand_i}, Q_{demand_i}$	Requested Active/Reactive Power Reference for the i^{th} WT
P_{in}, Q_{in}	Active/Reactive Power input
P_{grid}^{meas}	Grid Active Power measured
P_{out}, Q_{out}	Active/Reactive Power output
$P_{meas}^{PPC}, Q_{meas}^{PPC}$	Active/Reactive Power measured in PCC
P_{ref_i}, Q_{ref_i}	Active/Reactive Power Reference for the i^{th} WT
$P_{Qpenalties}$	Cost of the penalties paid during the WF lifetime
$P_{STATCOM+Cap.Banks}$	Price for the STATCOM and the Capacitor Bank
Q	Reactive power
$Q_{cap.bank}$	Rated Reactive Power of the Capacitor Bank
$Q_{C\max}, Q_{L\max}$	Maxim Capacitive/Inductive Reactive Power
$Q_{ind.capab\_j}, Q_{cap.capab\_j}$	Inductive/Capacitive Reactive Power capability of the j^{th} WT
$Q_{\min\_STATCOM}$	Minimum requested Rated Reactive Power of the STATCOM
$Q_{ST.+Cap.Banks}$	Reactive Power Capability of the STATCOM and Capacitor Bank
$Q_{STATCOM}$	Rated Reactive Power of the STATCOM
R_g	Grid Resistance
U_{grid}	Grid Voltage
U_{stat}	STATCOM Voltage
V_{ang_j}, V_{mag_j}	Voltage Angle/Magnitude at each bus bar
V_{DC}^{meas}	DC Voltage measured
V_{DC}^{ref}	DC Voltage reference
V_i	Voltage at each bus bar
v_{PCC}	PCC Voltage
V_{meas}^{PCC}	PCC Voltage measured
x_0	Initial Condition of the Optimization Problem
x_{opt}	Optimal solution of the Optimization Problem
Y_{bus}	Admittance matrix
Z_g	Grid Impedance

Chapter 1 Introduction

This chapter realizes a short overview regarding the wind turbine technologies. Various wind turbine (WT) trends are highlighted and different grid codes requirement are presented with the purpose to underscore their importance in the integration of the wind energy. Later on the problem is defined, the objectives are listed, the project limitations are mentioned and finally the project outline summarizes the structure and content of the report.

1.1 Background and motivation

Over the last 30 years, wind power has emerged as the most promising renewable resource for its rapid developments in disciplines such as aerodynamics, structural dynamics, mechanics as well as power electronics. In spite of the phenomenal growth and development in the last decades, the WT industry keeps moving forward in order to increase the efficiency and controllability of the wind turbines and to improve the integration to the power grid [1].

The present wind power share of the world's electricity generation is of 1.6%, but a bigger share up to 8.4% in 2019 was indicated by the forecasts and the predictions presented in [2]. The European Wind Energy Association scenario shows that over the next ten years, wind energy could meet one fifth of the EU's electricity demand in 2020, one third in 2030, and half by 2050 (see Figure 1-1) [3].

Figure 1-1Expected increase in EU`s share of electricity provided by wind power [3]

As a result of this scenario, high level of wind power (>30%) should be integrated into large inter-connected power systems and major issues can appear if the existing power systems are not properly redesign. Penetration levels in the electricity sector have already reached 21% in Denmark, 7% in Germany and about 12% in Spain. Achievements are even more impressive at the regional level. For example in the north German state of Schleswig-Holstein the installed wind capacity has over 2500 MW enough to meet 36% of the region's total electricity demand, while in Navarra, Spain, 70% of consumption is met by wind power [4].

From Figure 1-2 it can be observed that in future, many countries around the world are likely to experience similar penetration levels, as wind power is an interesting economic alternative in areas with appropriate wind speeds.

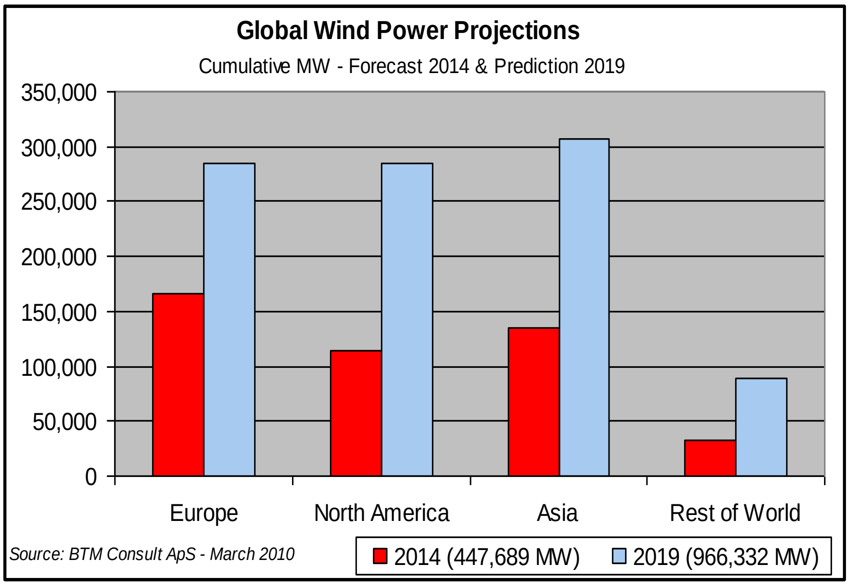

Figure 1-2 Global wind power projections [2]

1.1.1 Trends in Wind Power

The past years shows that the wind power industry is a well defined and profitable business. That's why each year a lot of resources are involved in order to improve and extend the efficiency and the installed power of the wind turbines.

An increasing trend is to remove dispersed single wind turbine in favor of concentrated wind turbines in large wind farms. Both onshore and offshore wind farms are quickly developing in a global scale.

In Europe, offshore wind energy becomes attractive, because of higher and constant wind speed and more space than onshore wind energy. Land structures and forests affect the wind flow. The strongest wind forces to drive the WT for maximal energy output are available over the sea. Offshore turbines thus produce more electricity per installed generation capacity than onshore wind power plants. However, the cost of offshore wind farms are about 30-60% higher than onshore wind farms of same capacity. In addition to the higher maintenance cost, the cost difference between onshore and offshore wind farm is due to the cost of foundations and the grid connection [5]. Furthermore, site access is limited in time as it is highly dependent on weather conditions. These conditions require a high degree of technical robustness and reliability for offshore wind turbines. From an environmental point of view regarding noise emissions and visual impacts, the footprint of an offshore WF is smaller than an onshore WF. In the future offshore wind farms will provide a large part of the power projections presented in Figure 1-2, today however, the market is dominated by onshore wind farms [6].

As large wind plants are likely to contribute to significant shares of the energy, they also bring new challenge in system operation. These challenges include connection of large wind farms to weak grids, securing power quality, power fluctuations and changes in operating strategies of conventional power plants. This trend to adapt new grid stability requirements for WTs means that WTs topology must have built-in capacity to support the grids by remaining connected in case of a grid faults. The DFIG topologies clearly are the most dominant concept but there is, however, an increasing trend for PMSG topologies using a full scale converter due to their increased capability regarding the grid code compliance.

While the wind turbine market continues to be dominated by conventional gear-driven wind turbine systems, the direct drive or one-stage gear is more attractive due to higher overall efficiency and availability of omitting the gear-box.

1.1.2 Grid codes requirements

Wind generation has become a substantial share of the total power generation. As a result, WTs have started to affect the stability of electric power systems, by interacting with conventional power plants. Therefore, the WT has to meet special regulations imposed by the TSO in order to operate without affecting the system stability.

Grid codes are technical documents containing rules governing the operation, development and use of the power system. Taking into consideration the large number of requirements and the purpose of this section, only the most relevant ENTSOE grid codes are presented. These requirements are divided in two main categories: *Normal operation* and *under grid disturbance* [7].

A. Normal operation grid requirements

Frequency and Voltage deviations

A Wind Power Plant (WPP) should maintain its operating frequency and voltage, at the point of common coupling (PCC), within a range around the rated values. From Figure 1-3 it can be seen that this requirement specifies the amount of time in which the WPP should operate for certain deviations of the frequency or voltage [8].

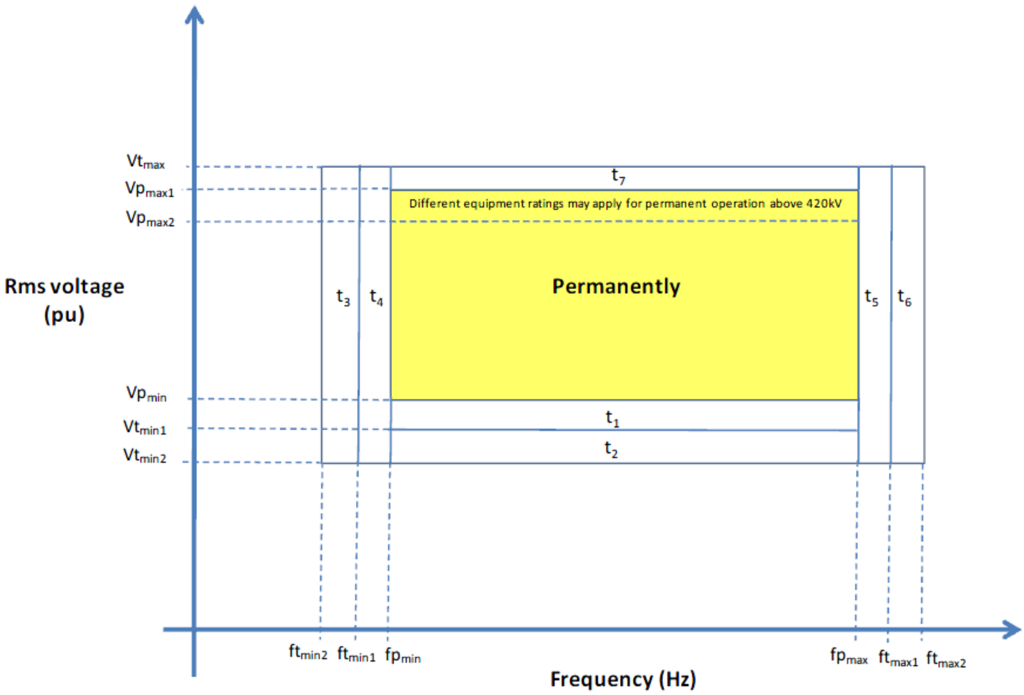

Figure 1-3 ENTSOE Voltage – Frequency operation window for 400kV [8]

The minimum and maximum frequency and voltage values for permanent ($f_{p\min}$ and $f_{p\max}$; $V_{p\min}$, $V_{p\max 1}$ and $V_{p\max 2}$) and temporary ($f_{t\min 1}$, $f_{t\min 2}$, $f_{t\max 1}$ and $f_{t\max 2}$; $V_{t\min 1}$, $V_{t\min 2}$ and $V_{t\max}$) operation are defined in Appendix B, as well as the required durations (t_1 to t_7) of temporary operation.

Active Power Control

Through this requirement the TSO imposes to the WF to behave as much as possible as a conventional power plant. This grid requirement can be divided in two, depending on the level of control in which the WPP is involved: the first case is when the WPP is in the secondary control and it has to provide only the amount of power requested by the TSO; the second case is when the WPP is in the primary control and it has to participate in frequency control [7].

When system frequency is above or below the nominal value it means there is too much or too less generated power in the system, compared to the load. The system operators prefers to have a plant capable of offering the so called "spinning reserve"; it means that the plant should be available and ready to respond to frequency change by reducing or increasing their output automatically. Wind cannot be boosted in the same way as the steam in the traditional plant. For some wind plant, the technical solution is to operate under the available output power, so by adjusting the blade pitch a boost will be obtained, see Figure 1-4.

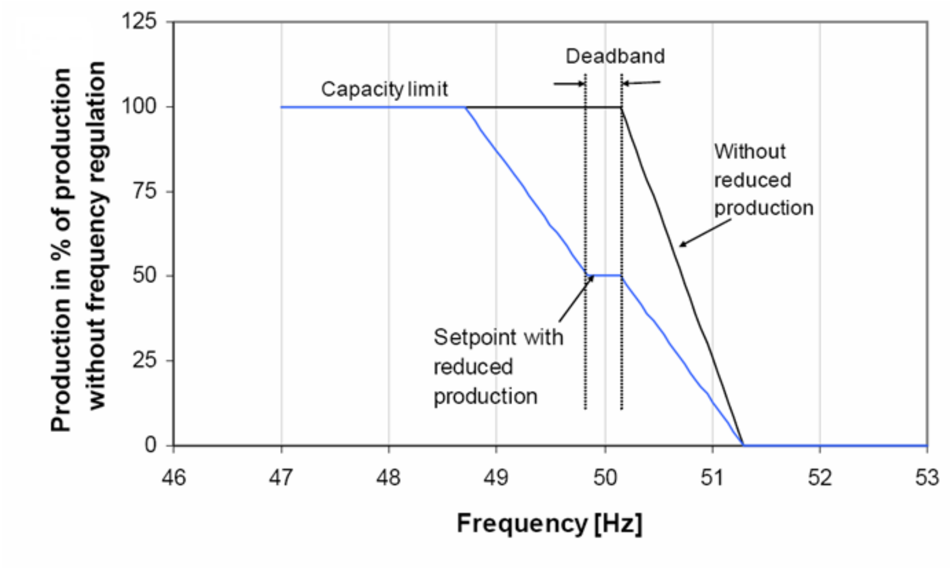

Figure 1-4 Active power and frequency control of a WT

Reactive Power Control

According to this grid code, the WF has to provide reactive output regulation, often in response to power system voltage variations, same as the conventional power plants. Based on ENTSOE "each Network Operator will define a U-Q profile of any shape in whose boundaries a wind farm will be required to provide reactive power at its nominal active power. This U-Q profile has to be within an envelope, the red box in Figure 1-5, where the dimensions and the position are defined according to each Network Operator. Nevertheless, the red box cannot be outside the green box of the Figure 1-5" [8].

The $Q / P_{\max}$ range and the range of steady state voltage level are defined in Appendix B. Moreover when operating at an active power output below the maximum active power ($P < P_{\max}$), it must be possible to operate the WF in every possible operating point in accordance with P-Q diagram in Figure 1-6.

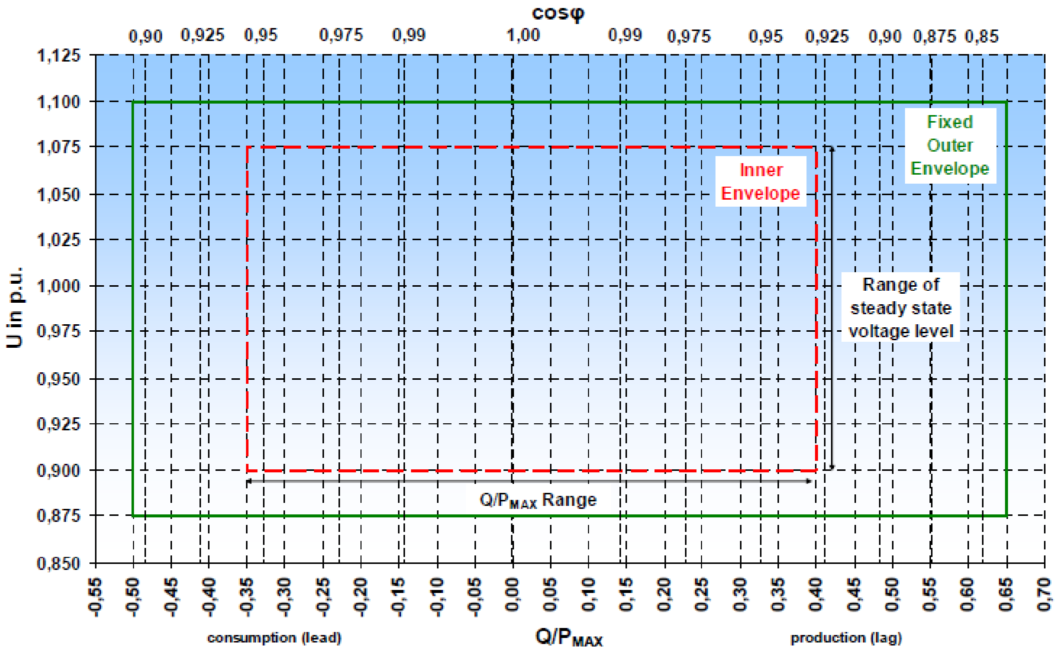

Figure 1-5 ENTSOE Reactive power capability at maximum active power diagram [8]

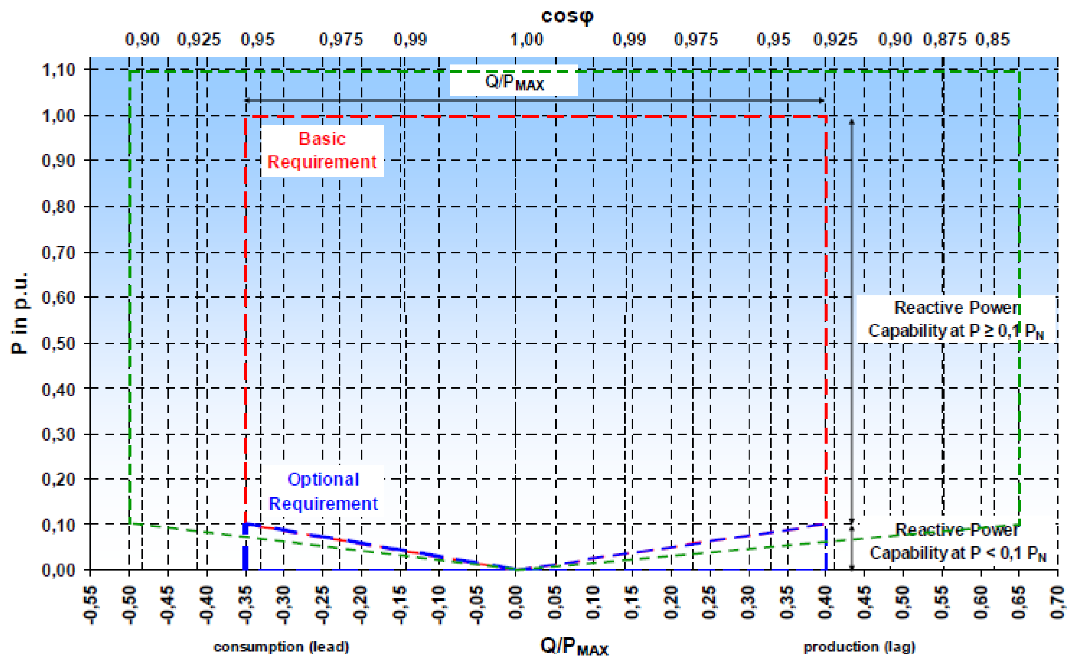

Figure 1-6 ENTSOE P-Q capability diagram [8]

B. Under grid disturbances requirements

All the grid codes share in common the relatively new requirements for WFs to contribute to grid stability. The main goals are to ride through momentary network faults and in the same time to provide grid support.

TSOs are imposing the FRT capability of WTs due to the fact that when a disturbance appear, if the WF is immediately disconnected, instead of helping the system to regain its stability will affect even more the electrical grid. Therefore, WFs must withstand voltage dips to a value of 0% of the nominal voltage for a specified duration. Such requirements are described by a voltage vs. time characteristic, denoting the minimum required immunity of the wind power plant as shown in Figure 1-7 [7].

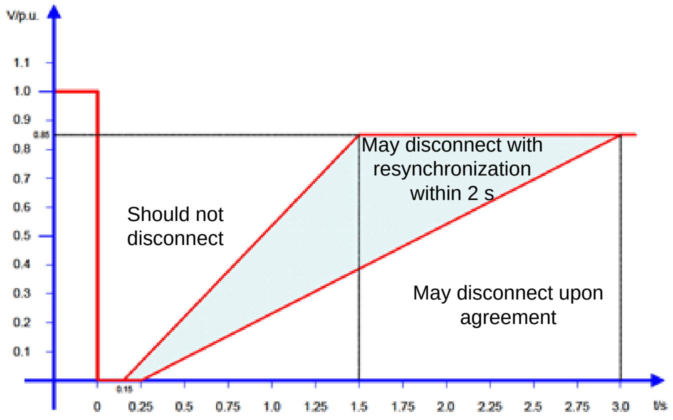

Figure 1-7 ENTSOE WF LVRT for voltage levels at 110kV or above [8]

Moreover in the case of a voltage deviation, through voltage control the WF must be capable of providing the requested reactive current based on Figure 1-8 (at least 2 % of the rated current per percent of the voltage deviation) [8].

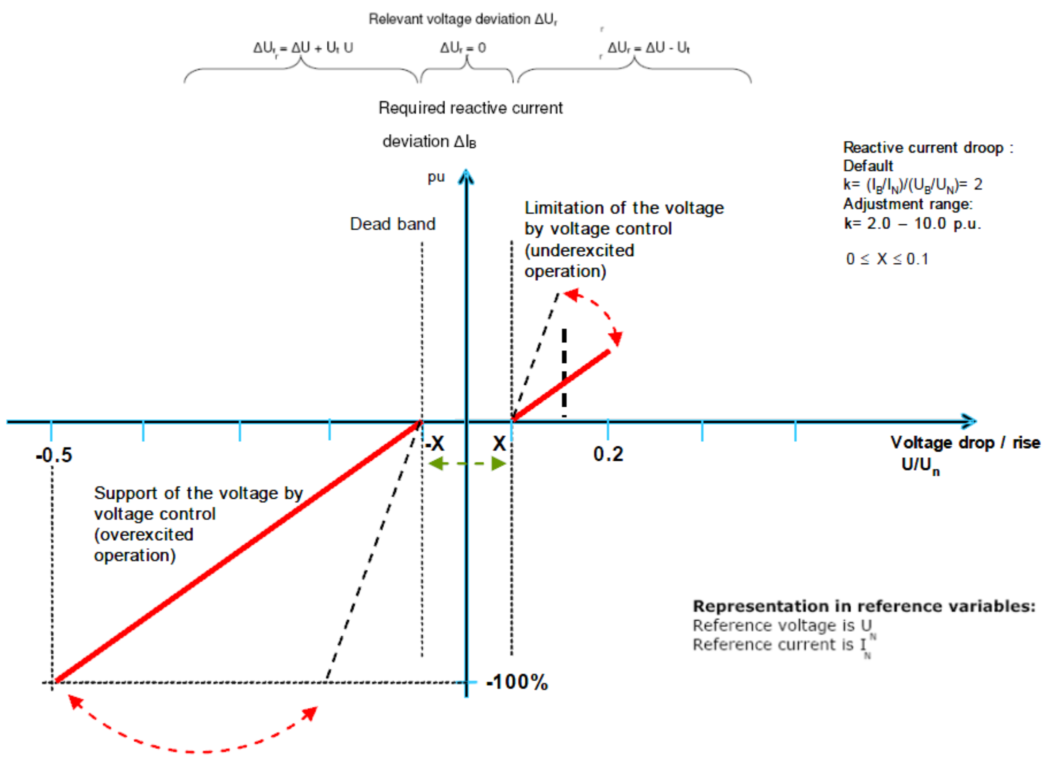

Figure 1-8 Principle of voltage support during fault [8]

1.1.3 WT topologies and their capability with respect to grid codes

The most commonly applied wind turbine configurations are classified both by their ability to control speed and by the type of power control they use. The advantages and disadvantages of each topology and their capability with respect to grid codes requirements are highlighted below.

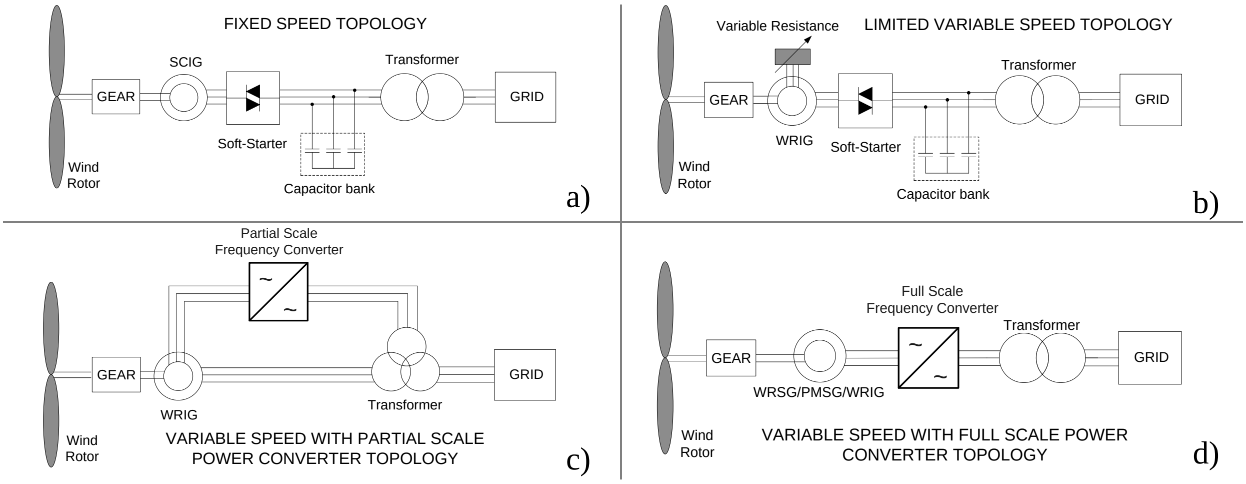

Figure 1-9 WT topologies

A. Fixed speed wind turbine topology

This configuration uses a squirrel cage induction generator (SCIG) directly connected to the grid through a transformer (see Figure 1-9a). Since the SCIG always draws reactive power from the grid, this configuration uses a capacitor bank for reactive power compensation. A smoother grid connection is achieved by using a soft-starter.

Due to its fixed speed operation, all the wind fluctuations are converted into mechanical fluctuations and consequently into electrical power fluctuations. In case of a weak grid, these can yield voltage fluctuations (flickers) at the point of common coupling (PCC). The fixed-speed wind turbine draws varying amounts of reactive power from the utility grid (unless there is a capacitor bank), which increases the line losses. Thus the main drawbacks of this concept are the following: it does not support any speed control, it requires a stiff grid and its mechanical construction must be able to tolerate high mechanical stress [9].

B. Limited variable speed wind turbine topology

The Optislip concept, which has been applied by the Danish manufacturer Vestas since the 1990s, is actually the limited variable speed concept with a multi-stage gearbox. A wound rotor induction generator (WRIG) with variable rotor resistance defines this WT topology (see Figure 1-9b).

The OptiSlip feature allows the generator to have a variable slip (changed by modifying the total rotor resistance) which gives smaller fluctuations in the drive train torque and in the output power.

The advantages of this generator concept are a simple circuit topology, no need for slip rings and an improved operating speed range compared with the SCIG. However, it still requires a reactive power compensation system. Also, the speed range is typically limited to 0–10 %, as it is dependent on the size of the variable rotor resistance and the slip power is dissipated in the variable resistance as losses.

It can be concluded that both fixed speed topologies cannot meet the grid codes demands regarding the reactive power capability unless some FACTS devices are used. Further on, due to the fact that the stator is directly connected to the grid the above topologies are very sensitive to grid faults therefore protection devices should be utilized [10].

C. Variable-speed wind turbine topology

Variable-speed wind turbines are designed to achieve maximum aerodynamic efficiency over a wide range of wind speeds. Using this kind of system it is possible to continuously adapt the rotational speed of the wind turbine to the wind speed. Contrary to a fixed-speed system, a variable-speed system keeps the generator torque fairly constant and the variations in wind are absorbed by changes in the generator speed.

There are two main topologies of WT as presented in the following part.

a) Variable-speed with partial-scale power converter

This configuration, known as the doubly fed induction generator (DFIG) concept, corresponds to the limited variable speed wind turbine with a wound rotor induction generator (WRIG) and partial scale frequency converter on the rotor circuit, as illustrated in Figure 1-9c.

The stator is directly connected to the grid, but in order to control the rotor frequency and thus the rotor speed, its rotor is connected to grid through a power converter. Depending on the size of the frequency converter (usually rated at approximately 25-30% of nominal generator power) this WT topology can operates in a wide speed range. Typically, the variable speed range is +30% around the synchronous speed, which makes this concept attractive and popular from economic point of view [11]. If the generator runs super-synchronously, the electrical power is delivered to the grid through both the rotor and the stator. If the generator runs sub-synchronously, the electrical power is delivered into the rotor from the grid.

An advantage of this concept over the Optislip concept is the rotor energy, which can be fed into the grid by the power converter, instead of being dissipated. Moreover, the functionalities provided by the capacitor bank and the soft starter, reactive power compensation and smooth grid connection, are performed by the power converter system.

On the other hand one of the drawbacks of this system is the multi-level gearbox which introduces additional losses, noise, maintenance costs and inevitable need for slip rings.

But the main disadvantage of DFIG is that it’s very sensitive to grid disturbance, especially for the voltage dip, due to the fact that the stator is directly connected to the grid.

The voltage dip could cause over voltage and over current in the rotor windings and consequently damaged the rotor side converter. To provide a DFIG with good fault ride through (FRT) the WT and the power converter should have the ability to protect itself, without disconnecting during faults. In order to fulfill this requirement, a crowbar (used to bypass the converter by short-circuiting the rotor windings) is needed to offer extra protection [12].

b) Variable-speed with full-scale power converter

The synchronous machine, it is probably most suited for full power control as it is connected to the grid through a power converter (see Figure 1-9d).

The synchronous generator is much more expensive and mechanically more complicated than an induction generator of a similar size. However, it has one clear advantage compared with the induction generator, namely, that it does not draw a reactive magnetizing current from grid.

The magnetic field in the synchronous generator can be created by using permanent magnets or with a conventional winding. This WT concept can be used for direct-drive applications without the need of a gearbox if the synchronous generator has a suitable number of poles, depending on the operating speed of the WT rotor.

Since the generator rotor is directly connected on the hub of the turbine rotor the DD generator rotates at a low speed. To deliver a certain power, the lower speed makes it necessary to produce a higher torque.

The full-scale power converter can perform smooth grid connection over the entire speed range, not only in a limited range as in the case of the partial scale converter. Since all the generated power has to pass through the power converter, the cost and the power losses in the power electronics are the main drawbacks of this topology.

The power converter has two primary goals: to act as an energy buffer (DC-link) for the power fluctuations caused by the wind energy and for the transients coming from the grid side and enables the system to control active and reactive power.

When a disturbance occurs in the external grid, one effect can be the appearance of a voltage dip at the AC output terminals of the WT. The maximum active power that the WT can provide is modified proportionally to the voltage dip. In normal operation, the power produced by the generator passes through the power converter into the grid. When a voltage dip occurs, in order to compensate the AC voltage and keep the power constant the grid side converter increases the current. However, due to the current limitation, the excess power from the generator that cannot be delivered to the grid must flow into the DC capacitor causing an overvoltage in the DC link. An excessive DC link voltage will damage both the rectifying and inverting converters, so protective action must be taken. As a result, a braking resistor is inserted in the DC circuit to dissipate the excess energy and restore the balance [10].

However, the power extracted by the WT blades cannot be reduced as quickly. The most obvious attempt to reduce the energy imbalance is to pitch the turbine blades to reduce the captured wind power. This will mean that the energy imbalance decreases during the voltage dip. Therefore when abnormal voltage is measured at the AC terminal of the grid side converter, the pitch controller is requested to increase the pitch angle of the blades to reduce the energy imbalance.

The combined control of a DC circuit braking resistor, the pitch angle and the full scale converter ensure a good protection of the mechanical and power electronic components and allows the wind turbine to remain connected despite the occurrence of voltage dips.

Compared with the DFIG system, the grid-fault ride-through capability for this topology has a better efficiency and is less complex. Therefore variable speed WT concepts with a full-scale power converter are more attractive [13]. Moreover the reactive power requirements can be fulfilled through the power converter control for both DFIG and full scale concepts.

1.1.4 Project Motivation

The main trends of modern WF are clearly the variable speed operation and a grid connection through a full scale power converter. However, large wind installations are requested to behave like a conventional power plant (frequency control, reactive power capability, FRT, etc). Consequently, the control of the wind power plant needs to be carefully designed to meet the requirements from system operators in terms of grid code compliance and participation in grid controls.

This research project analyzes the possibility of implementing a wind power plant controller in order to meet grid requirements in different Europeans countries. The amount of wind energy supplied to the electrical network is considerably increasing, therefore having an efficient and a reliable WF controller is very important. The project also investigates the necessary controls for the WF with the aim of minimizing the power losses inside the WF grid and maximizing the WF life time.

Modeling the WF controller using MATLAB software and performing the simulations helps to achieve a better understanding of the overall system. Furthermore it was possible to compare the behavior of the WF controller for different control modes imposed by TSOs. These comparisons will provide useful information’s which ultimately will indicate if the WF controller implemented in MATLAB it is suitable for a real time implementation.

1.2 Objectives

The main objectives of this project are the followings:

- WPP modeling in CIMTool through a series of XML files (e.g. WF Topology, WF Equipment and WF Measurements etc.).
- Definition of control objectives (WF grid losses minimization, life time optimization etc.) and implementation in MATLAB of a WF controller.

- Implementation in MATLAB of a few control strategies for the plant to show compliance with grid codes in Europe.
- Define a method for finding the optimal reactive power ratings for the WTs grid side convertor, capacitor banks and STATCOM in PCC.

1.3 Limitations

During the project development several limitations had to be considered. Thus, the most important limitations of this project were summed up and are presented as follows:

- A hypothetical conventional power flow was considered due to the limited literature regarding the conventional WT references dispatch in a WPP.
- Simple life time coefficients were considered due to limited information in the literature regarding the WT's life time.
- The possibility to control an energy storage system (ESS) in the PCC wasn't considered due to lack of time.
- Due to lack of time voltage and frequency WF control wasn't implemented.
- Simulations that utilize a real wind profile were limited from 1 year period to only 1 month or less due to long simulation times.

1.4 Project Outline

This project is structured in six chapters and studies the coordinated control of the WTs for different WF control modes and different control objectives.

In the first chapter a short overview regarding the wind turbine technologies is realized. Various WT trends are highlighted and different aspects of the ENTSOE grid code requirement are presented. Moreover the problem is defined, the objectives are listed and project limitations are mentioned.

The second chapter presents a brief description of the complete model for a WPP including the WTs with the associated controls, the WF Topology, the power transformers, STATCOM and ac lines. The focus is mainly on the modeling of the WF from the power system point of view using standardized model structure to have a robust implementation.

In Chapter 3, first the WT control objectives were highlighted followed by the presentation of the WF controller objectives. Next an optimization problem is formulated for a specified study case. Finally, the new WF Power Management System (including the TSO, WF Controller and the WF) is briefly presented.

In the first part of Chapter 4 a short overview regarding the FACTS Controllers is presented, followed by a description of the STATCOM. In the last part, the first two study cases for this project are presented. The effects of increasing/decreasing the STATCOM, capacitor banks and WTs grid side converters Q rating are highlighted from a technical and economic point of view.

The aim of Chapter 5 is to evaluate the performance, of the WF Controller implemented in MATLAB, for different study cases. In the first part of the chapter the behavior of the WF Controller is analyzed for different WF control modes (normal, balance, etc.). Than the study cases are extended for real wind profiles and beside WF losses minimization a new control objective is introduced based on life time optimization.

Chapter 6 summarizes the work presented along this thesis. The main conclusions are deduced based on the results achieved. As a final point, the directions for future work are outlined.

Chapter 2 Modeling of the Wind Power Plant

In this chapter the method of modeling a WPP using CIMTool and MATLAB software is described. In the first part of the chapter a small introduction in the basics of CIM is realized followed by a description of the WTs together with the Transformer, the AC line, the STATCOM and the rest of the equipment belonging to the WPP. The WPP Topology and the WPP Measurements are presented in the last part of the chapter.

More and more requirements for grid connection of WTs and WPPs were established by TSOs (Transmission System Operator) in order to improve the grid stability. The simulation of WPPs became popular to verify the performance based on the scope of analysis. Therefore, models of the WPPs of different complexity were developed depending on the different points of interest. The objective of this chapter is to develop a simplified WPP model in order to study the capability of the WF Controller in fulfilling the requirements imposed by the TSO.

The WPP model was developed based on the IEC6140-25 standard series. This standard focuses on the communication between WPP and SCADA systems and is designed for a client-server communication environment. A more detailed description of this concept is presented in Figure 2-1.

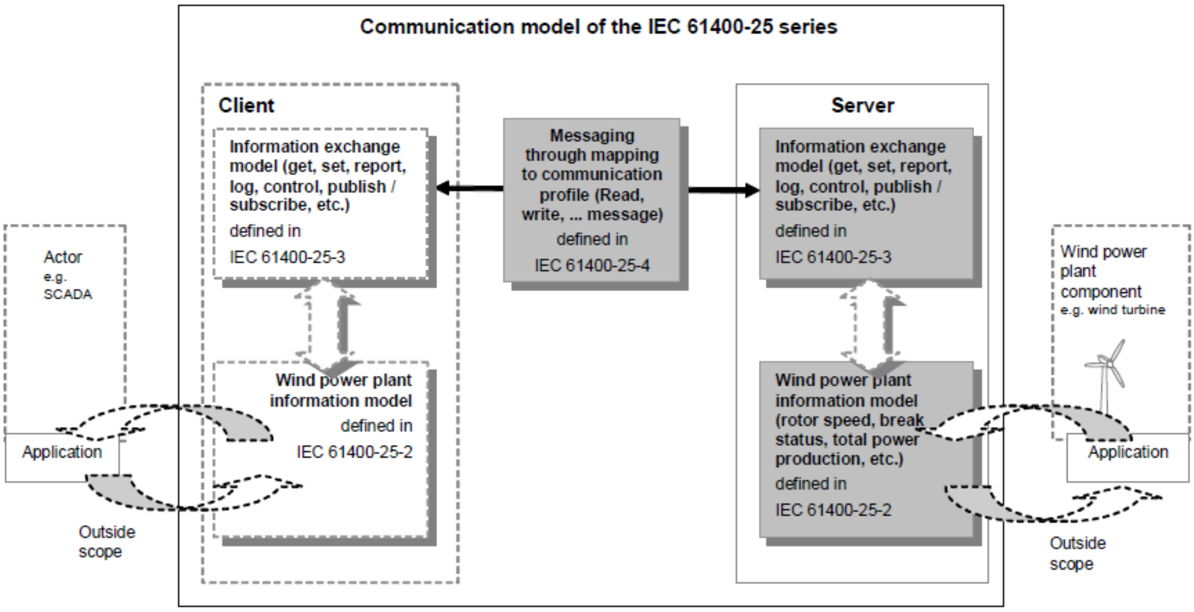

Figure 2-1 Conceptual communication model of the IEC61400-25 Standard [14]

The key element in this communication is represented by the standardized self-description WPP information model (contained by an XML file). This information model offers the necessary contents for the information exchange that takes place during the monitoring and control process between client and server.

The IEC6140-25 series utilizes the concept of virtualization. Through this approach the information found in the real components is modeled and an overview image of the real world can be provided to the WPP automation system. The conceptual overview is depicted in Figure 2-2.

From the bellow figure it can be observed that the real components from the right side of figure are transposed into a virtual model in the middle of the figure.

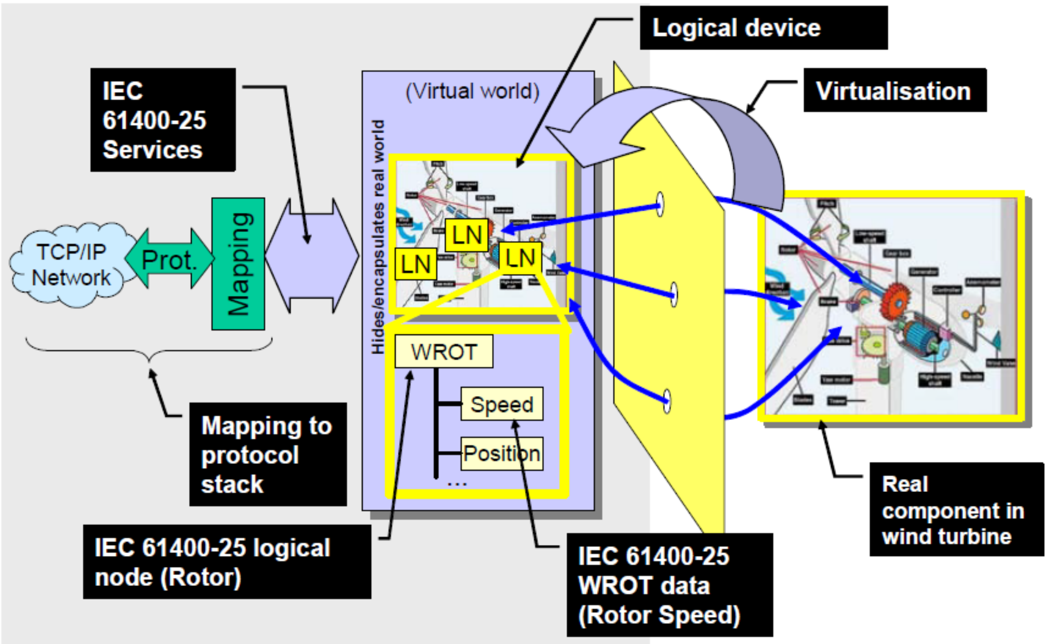

Figure 2-2 Modeling approach [14]

A logical node can contain based on its functionality a list of data (e.g. rotor speed, rotor position). The logical nodes are modeled and defined from a conceptual application point of view and are collected in a logical device (e.g. a WT).

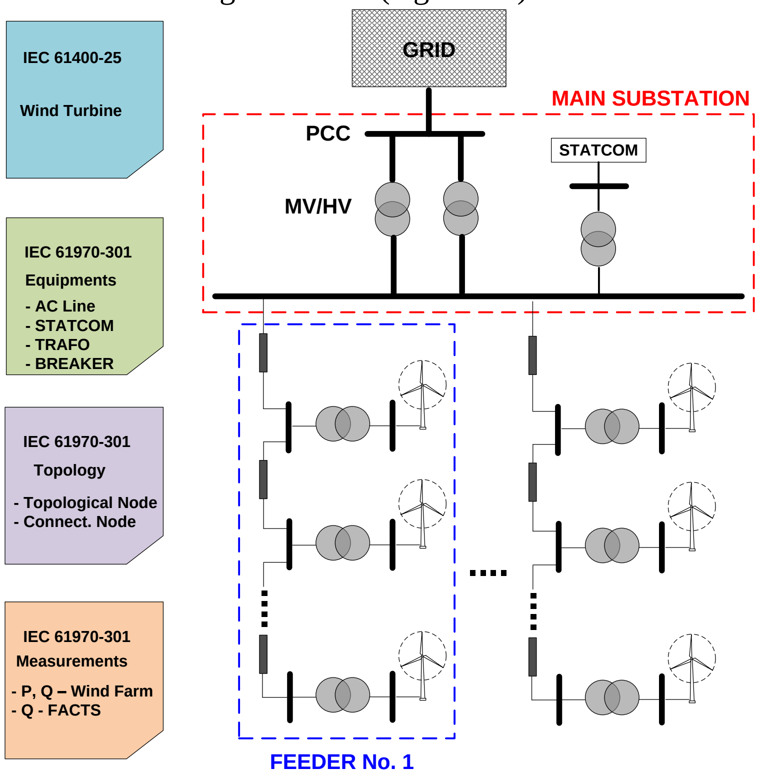

Figure 2-3 WPP model including the main components

The complete model of a WPP including all its components (e.g. WT, Transformers, AC line etc.) and its correspondents XML (extensible markup language) files is depicted in Figure 2-3. It should be stated that only the necessary information from the standard was used in the modeling. In addition the data classes specified in the standards were modeled to a certain extent to simplify the internal model. Moreover a detailed presentation of each component is realized in the following section.

2.1 Basics of CIM modeling

As it was mentioned on the beggining of the chapter, one of the software utilized to develop the WPP model is CIMTool. With this software a schema of the common information model (CIM) can be build, schema wich is used to derive and validate an instance of the model. One assumption that was made is that the WPP was seen as a power system distribution network.

The CIM is an abstract model that represents all the major equipments in an electric system. The CIM facilitates the integration of energy management system (EMS) or other systems concerned with different aspects of power system operations, such as generation or distribution management.

In order to make a model easier to design, understand and review the CIM is divided into a set of packages. For the WPP modeling the information used can be found in several IEC61970-301 packages such as: Topology (where the connections between the equipments are defined), Meas (describes the dynamic measurements), Core, Wires etc. Moreover each package is divided in a series of classes. A class is the description of an object found in the real world, such as a power transformer, generator, etc. that needs to be represented as part of the overall power system model. Therefore, particular equipment in a power system with a unique identity is modeled as an instance of the class to which it belongs. The parameters of the physical equipment are defined through the attributes associated to each class [15].

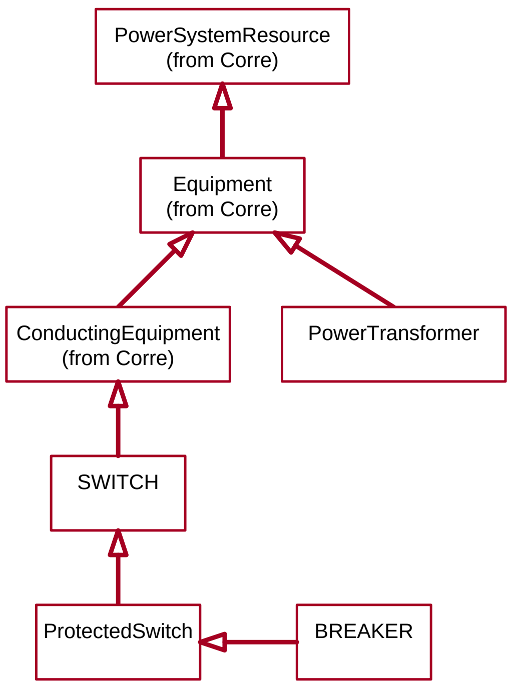

Figure 2-4 Example of generalization [15]

Moreover, relationships between classes make known how they are structured in terms of each other. CIM classes are interconnected in three ways: generalization, simple association and aggregation. The mentioned relationships are described below together with some small examples.

As it is mentioned in the IEC61900-321 standard "*A generalization is a relationship between a more general and a more specific class.*" The more specific class can contain only additional information. Generalization provides for the specific class to inherit attributes and relationships from all the classes above it.

In Figure 2-4 an example of generalization is presented and it can be seen that a Breaker is a more specific type of Protected Switch, which in turn is a more specific type of Switch, which is a more specific type of Conducting Equipment, etc. From the same figure it can be also observed that in a similar way a Power Transformer is another specific type of Equipment.

Moreover, based on [15] "an association is a conceptual connection between classes". Each association has two roles each role also has multiplicity/cardinality, which is an indication of how many objects may participate in the given relationship. The proposed example for this type of relationship is an association between a Tap Changer and a Regulation Schedule, see [15]. Multiplicity is shown at both ends of the association. In this example, a Tap Changer object may have 0 or 1 Regulation Schedules, and a Regulation Schedule may belong to 0, 1, or more Tap Changer objects.

Figure 2-5 Example of simple association [15]

Finally, aggregation is a special case of association which indicates that one class is "part of" the other class. The part class does not inherit from the whole class as in generalization. As shown in Figure 2-6 an aggregation relation exists between the Transformer Winding class and the Tap Changer class. While a Tap Changer can be a member of exactly one Transformer Winding, a Transformer Winding can contain any number (but at least one) of Tap Changers [15].

Figure 2-6 Example of aggregation [15]

2.2 Modeling of the WT

Considering the purpose of this thesis some assumptions and trade-offs were made, when the model of the WT was developed. It was considered that the WT and all its subsystems behave ideally; therefore the WT was modeled as a PQ generator. This PQ generator is based on the WT PQ capability curve, which is presented in Figure 2-7.

From the bellow figure it can be seen that when the WT is operating at its rated active power, the reactive power capability it's only 10% from the rated active power. When the WT doesn't produce any active power, the maximum reactive power capability of the WT is 90% from the rated active power. For some study cases, where the size of the grid side converter is variable, the percentages which give the WT reactive power capability will fluctuate accordingly with the given conditions. A detailed schema of the WT model developed in CIMTools is depicted in Appendix D.

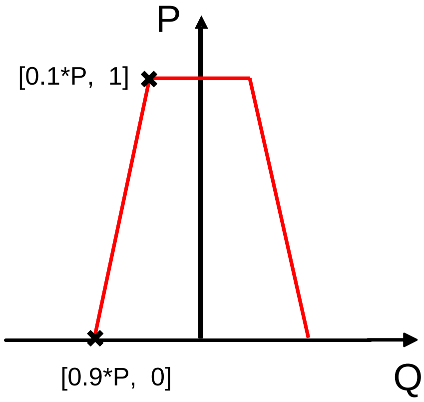

Figure 2-7 Wind turbine PQ capability curve

Wind Model

An important component of the WT model, that has to be mentioned together with its assumptions, is the wind model. Many wind models, with higher accuracy and complexity, have been developed in order to obtain the real behavior of the wind [16], but a deep analyze of the wind profile is beyond the objective of this project.

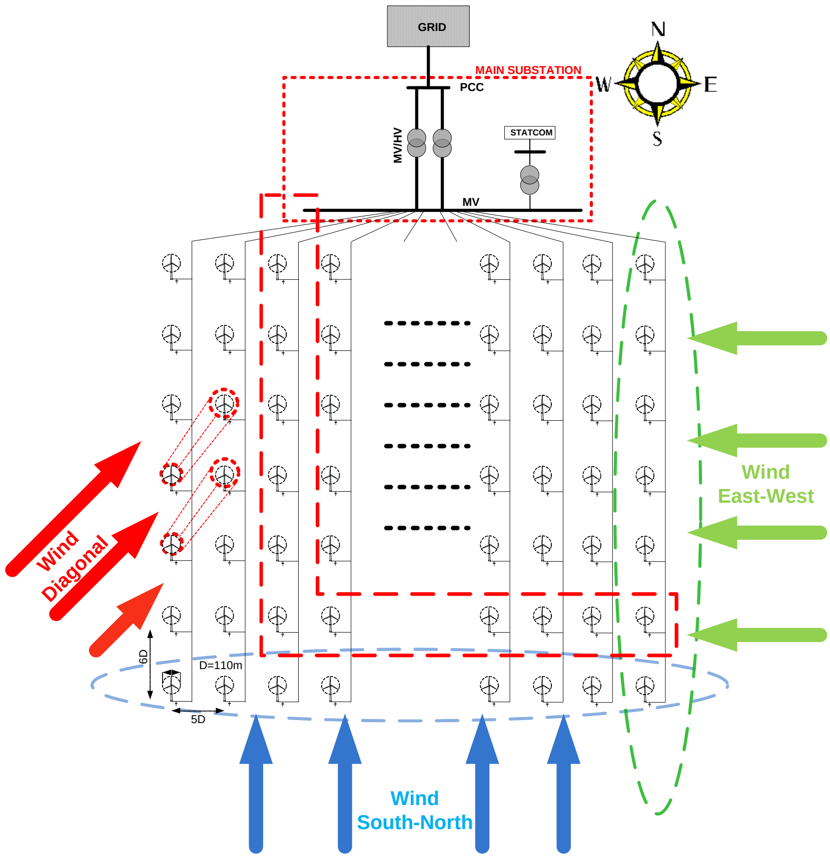

Figure 2-8 Wind directions and WF layout

In some study cases it was enough to consider the wind as a simple constant wind speed value. But in other cases taking into consideration that in a WF the wind speeds at the individual WTs have different values since there are strong interactions between WTs, the *wake effect* was considered. In general, the wake effect has a three dimensional character, but such representation is too complex and is beyond the purpose of this report. Therefore a simplified representation of the wake effect it is used based on [17], in which the wind speed is decreased with a certain percentage (2-4%) after every row/column of the WF.

The wind profiles depend on the direction of the incoming wind to the farm and also on the structure of the farm. In Figure 2-8 are presented the different wind directions associated with the WF layout.

From the above figure it can be remarked that the wind directions can be reduced to three main directions: South-North direction, East-West direction and Diagonal (NE, NW, SE and SW). For example when the wind blow from the South-North direction, the WTs of the first row perceive different values of the wind speed, deviated with 0.1% from the initial value. The next rows of the WF receive different wind speeds due to the wake effect. The same principle applies for the other two wind directions (East-West and Diagonal).

The Power profile for the WT based on the wind speed is presented in Figure 2-9. Four different regions can be distinguished from the power profile depicted in the mentioned figure:

- *Region 1* wind-speed bellow the cut-in speed (3m/s)
- *Region 2* wind speed between the cut-in speed and the rated wind speed (13m/s)
- *Region 3* wind speed between the rated wind speed and the cut-off speed (25m/s)
- *Region 4* wind speed above cut-off speed

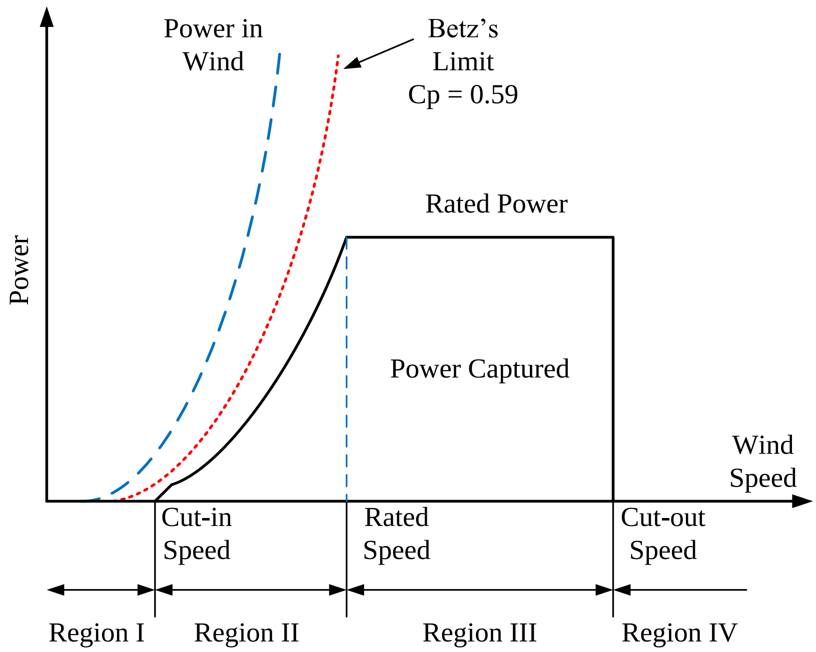

Figure 2-9 WT Power profile

2.3 Modeling of the WPP Equipment

Power Transformer

The main functions of a Power Transformer are voltage level conditioning and galvanic insulation of the two connected circuits. In order to connect the WPP system to the grid, in this thesis due to high power level, two transformers are used at the PCC to increase the voltage level.

In Figure 2-10 a portion of the Wires class diagram which models a Power Transformer device is presented. As shown, a Power Transformer is a specialized class of Equipment, which is a specialized class of a Power System Resource, as is Conducting Equipment and Tap Changer. Therefore the Power Transformer is inheriting attributes from both Equipment and Power System Resource.

As it can be observed from the below figure, the Power Transformer has a Transformer Winding, which is modeled with an aggregation type of relationship using a diamond symbol to point from the part class to the whole class. Moreover, the Transformer Winding has other relationships as well:

- a generalization relationship with Conducting Equipment;
- an association relationship with the Winding Test class, such that a Transformer Winding object may be Tested from 0, 1, or more Winding Test objects;
- an aggregation relationship with the Tap Changer class, such that a Transformer Winding object may have 0, 1, or more Tap Changer objects associated with it.

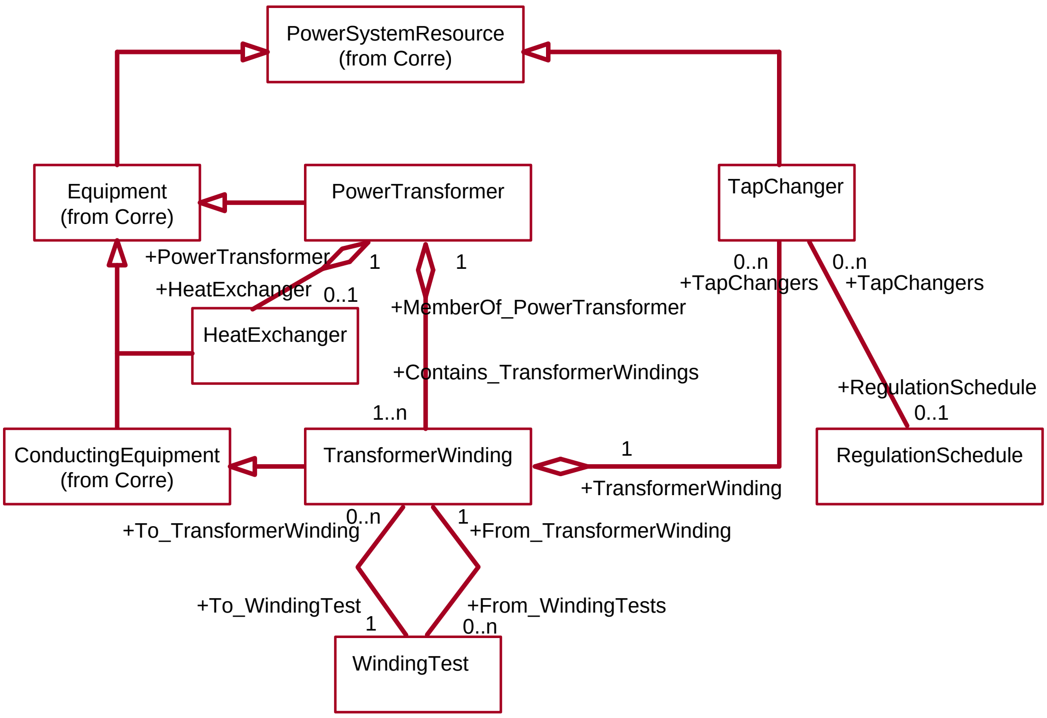

Figure 2-10 Power transformer model [15]

The Power Transformer is modeled through its Windings and its Tap Changer. The modeling of the Winding Transformer is based on the following parameters: rated apparent power, rated voltage, windings resistance and windings reactance. The resistance and the reactance of the windings are expressed in per unit values (see Appendix C). The Tap Changer is modeled considering the following parameters: neutral voltage, number of high steps, number of low steps and step voltage increment. The parameters were chosen based on the fact that the maximum voltage variation that can be produced by Tap Changer is around ± 15% from its rated value (see Appendix C).

AC Line

The AC Line is modeled as a PI section (see Figure 2-11). In the single PI line model, R is the total line resistance, L is the total line inductance and C is the equivalent line capacitance at the beginning and at the end of the line. In the equivalent drawing y is the admittance of the line and *B* is the susceptance of the line. For the exact parameters values for each AC Line segment of the WPP, depending on the apparent power limit, see Appendix C.

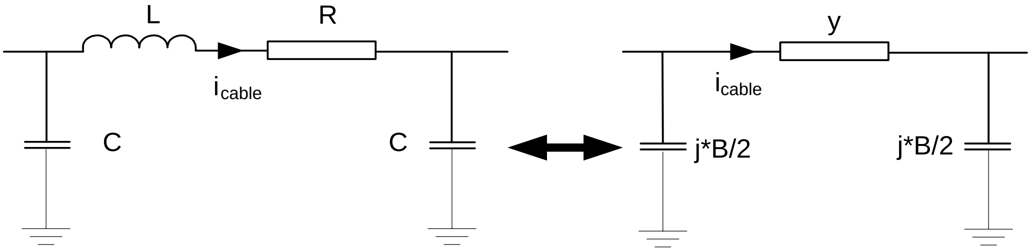

Figure 2-11 Standard PI model

A part of the Wires class diagram which models an AC Line is depicted in Figure 2-12. As shown, an AC Line is a specialized class of Conductor, which is a specialized class of Conducting Equipment, which in its turn is a specific class of Equipment etc. As presented before, this is shown by using the generalization type of relationship, which uses an arrow to point to the general class. Therefore the AC Line is inheriting attributes from all its superior classes. For a more detailed description of the relationships between classes see Appendix D.

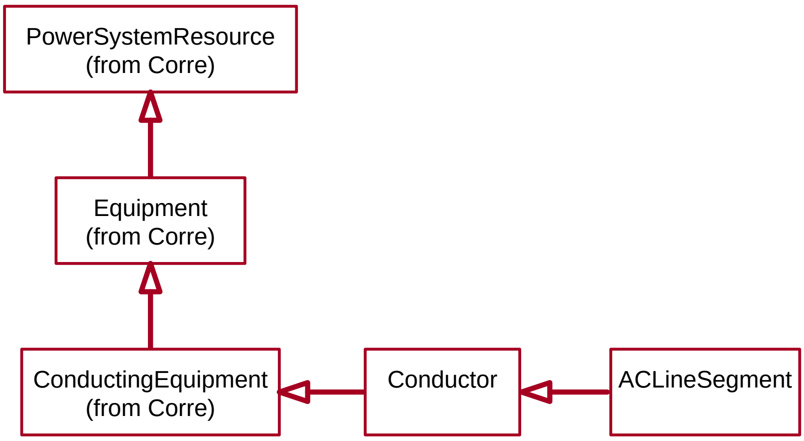

Figure 2-12 AC Line model [15]

STATCOM

STATCOM is a voltage-source converter based device, which converts a DC input voltage into an AC output voltage in order to compensate the active and reactive needs of the system [18].

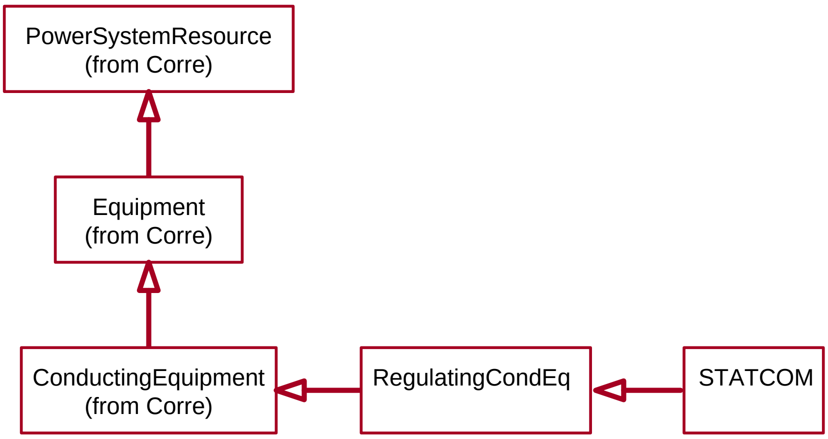

Figure 2-13 STATCOM model [15]

The STATCOM is presented in the same manner as the previous components were described, as a portion of the Wires class diagram. As depicted in Figure 2-13, a STATCOM is a specialized class of *RegulatingCondEq*, which is a specialized class of Conducting Equipment, which in its turn is a specific class of Equipment etc. The relationship that describes this situation is the Generalization type, which also makes the STATCOM to inherit all the attributes of the above classes.

The model of the STATCOM is based on parameters such as: capacitive ratings, inductive ratings and its control mode (see Appendix C). The STATCOM can operate in voltage mode or reactive power mode. For the proposed model the operating mode is selected to be reactive power mode, therefore the references for the STATCOM are given in terms of reactive power.

Electrical Grid

The proposed model of the grid is based on the Thevenin equivalent circuit. The equivalent circuit is shown in Figure 2-14.

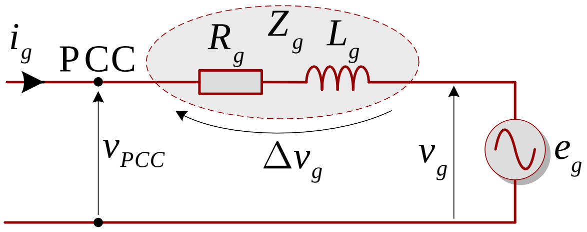

Figure 2-14 The equivalent Thevenin circuit of the grid

In the Equation (2.1) is described the relation between the voltage at point of common coupling v_{PCC} and the grid voltage v_g.

$$v_{PCC} = v_g + \Delta v_g = v_g + i_g \cdot Z_g \tag{2.1}$$

Usually, the grid impedance is mainly inductive therefore the grid impedance is mostly considered as:

$$Z_g = R_g + j \cdot \omega \cdot L_g \tag{2.2}$$

Depending on the value of the grid impedance, the grid can be stiff (low grid impedance) or weak (high grid impedance) [19]. The grid impedance is an important parameter, based on which the value of the capacitor bank was selected for the next study cases. Considering this parameter was possible to analyze the impact of the capacitor bank on the PCC voltage (voltage variation maintained between the admitted limit of 10%) [20].

2.4 Modeling of the WPP Topology and WPP Measurements

Topology is the logical definition of how equipment is connected via closed switches. This package is an extension to the Core Package that in association with the Terminal class models Connectivity, that is the physical definition of how equipment is connected together [15].

In order to understand easier the principle used to develop the WPP Topology in CIMTool the definition of certain terms is presented in the following section:

Terminal: An electrical connection point to a piece of conducting equipment.

Connectivity Node: Are points where terminals of conducting equipment are connected together with zero impedance.

Topological Node: A set of connectivity nodes that, in the current network state, are connected together through any type of closed switches, including jumpers.

Measurement: Any measured, calculated or non-measured non-calculated quantity.

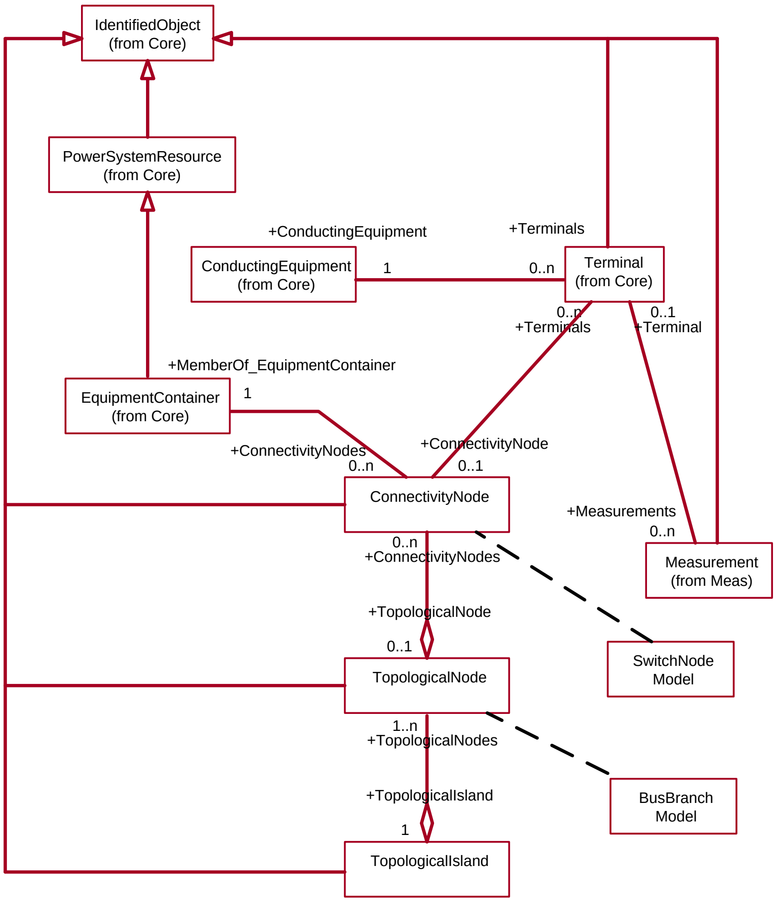

Figure 2-15 Connectivity model [15]

In Figure 2-15 a simplified Topology class diagram which is used for modeling the connectivity between different types of Conducting Equipment is presented. For modeling the WPP topology Terminal and Connectivity classes are defined. A Terminal belongs to one Conducting Equipment and it can be connected to a Connectivity Node, which is a point where terminals of conducting equipment are connected together with zero impedance. Further on, a Connectivity Node may have any number of terminals connected, and may be a member of a Topological Node (i.e. a bus). Moreover any piece of equipment may contain Measurements (e.g. a substation may have temperature measurements and door open indications, a transformer may have oil temperature, etc.).

Some Measurements represent quantities related to a particular sensor location in the network, (e.g. a voltage transformer at a busbar) and the sensing position is difficult to be captured. Therefore, by associating the Measurement with the Terminal the sensing location in the network topology is obtained. The location is defined by the connection of the Terminal to ConductingEquipment [15].

A more specific example is depicted in Figure 2-16, where the WT connection of one WPP feeder associated with its measurements is presented together with its Terminals (TN), Connectivity Nodes (CN) and its Topological Nodes (TN).

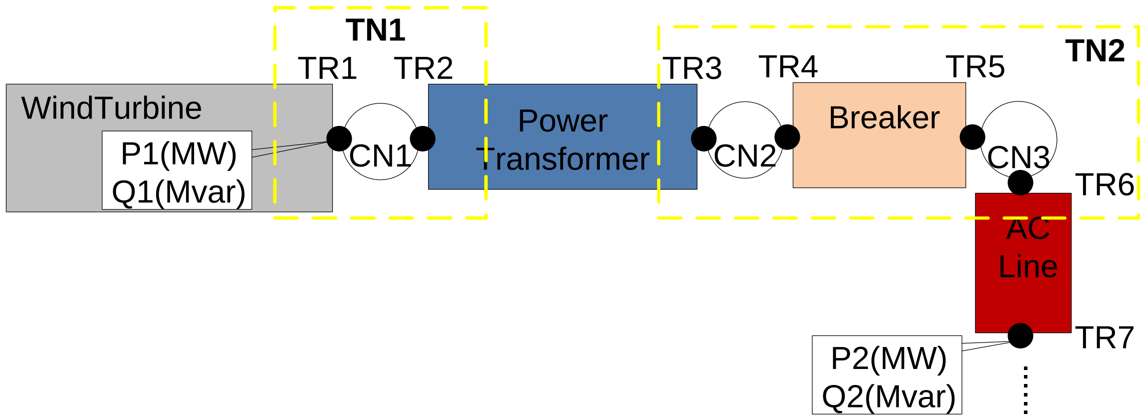

Figure 2-16 WT connectivity and measurements association [15]

Measurements are represented by square callouts where the arrow points to a Terminal. From the Figure 2-16 it can be observed that P1 and Q1 are connected to the right Terminal belonging to Wind Turbine and are drawn inside its box, showing that are part of this equipment. For the case of P2 and Q2 it can be seen that they don't belong to any equipment, meaning that the measurements can be long to a Voltage Level or to a Substation.

Using the model presented in the above figure, all the equipments of the WPP are connected, and by synchronizing their connections with the measurements the overview image of the real WPP is obtained in CIMTool. Further on by transposing the necessary information into XML files, the WPP controller can communicate with the WPP and it can perform its desired operations of maintenance or control.

Chapter 3 Wind Farm Control

This chapter is focused on describing the control technique implemented in MATLAB for the WF controller. First the WT control objectives are highlighted followed by the presentation of the WF controller objectives. Finally the emphasis is over the WF Controller and the implementation algorithm for the proposed control objectives.

3.1 WT Control Objectives

In any process, control has two main objectives: protection and optimization of operation. Furthermore, when applied to a WT system (WTS), control becomes more important, in all aspects, as the main characteristic of a WTS is that it deals with the highly variable, intermittent and unpredictable nature of the wind [21]. Although wind is one of the most well-developed and economical sources of renewable energy, advances in control can still improve wind turbine technology. Increases in wind turbine size have led to increases in both cost and structural complexity compared to turbines of past decades leading to new control problems. Since the primary goal for a WT is to produce the most electricity at the lowest cost, control schemes that reduce cost by improving structural loads or by increasing the efficiency of the turbine are beneficial to the wind-energy industry [22].

The three most common actuators used for WT control are the yaw drive, the blade-pitch drive, and the generator. The yaw drive aligns the rotor and nacelle with the wind direction at any given time but typically operates slowly on large turbines. Due to its slowness, the yaw drive is not of particular interest to control engineers. The blade pitch actuators can be electromechanical or hydraulic and are used to position the blades to a desired angular position to achieve various control objectives. Finally, the generator control is achieved using power electronics, therefore is a good candidate for minimizing drive train stresses and increasing efficiency[22].

Further on, since the topology proposed for this project is based on a FSC power converter, the control structure of the WTS can be divided into two main systems: a WT control and the grid converter control (see Figure 3-1). The WT control typically contains a pitch control and a generator converter control. While the generator converter controls the speed of the rotor so that the power is maximized, the pitch controller objective is to modify the angle of attack of the rotor blades so the output power of the wind turbine can be controlled. Further on the grid converter usually controls the voltage on the DC-link and also the reactive power delivered to the grid. Overall the following objectives of a WT control system can be highlighted:

- to control the wind captured power for speeds larger than the rated speed;
- to maximize the extracted power from the wind as long as the constraints regarding the speed and the captured power are met;
- to comply with rigorous power quality standards (e.g. power factor, harmonics, flickers, *etc.*);
- to transfer the electrical power to the grid at an imposed level, for wide range of wind velocities;
- to protect the WTS and, at the same time, to offer active grid support during grid faults [21].

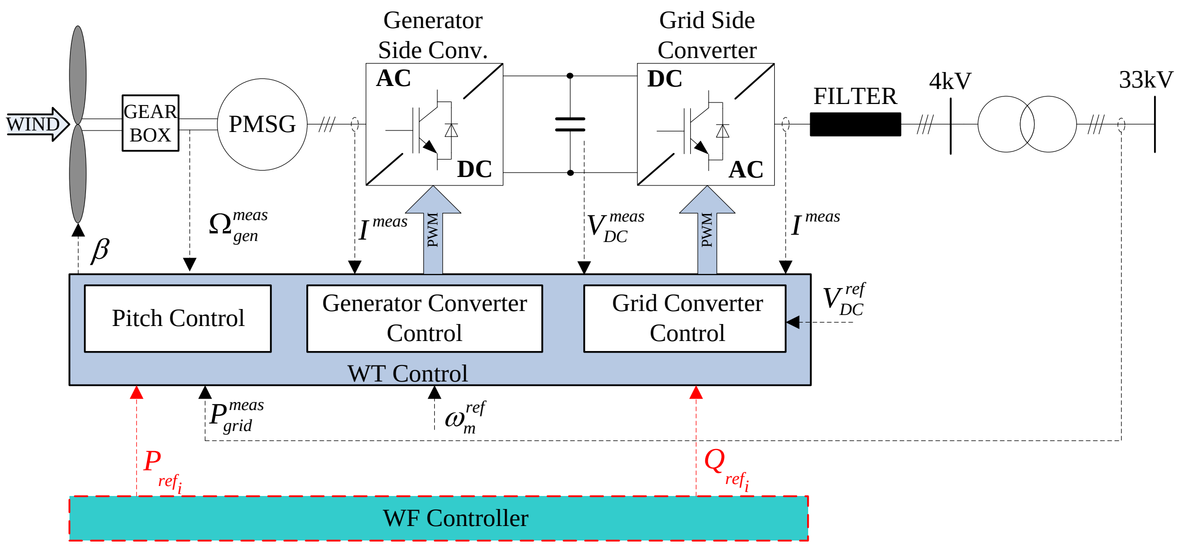

Figure 3-1 Overall Control Structure of a WTS

A detailed description for each control loop presented above can be realized, but is not the purpose of this project. As it was stated also in Chapter 2 the modeling of the WT was based only on the PQ capability curve (see Figure 2-7) and the power profile curve (see Figure 2-9). Therefore for the study cases the WT control was considered ideal: the references in P and Q are the same with the measured P and Q at the 4kV bus bar.

3.2 WF Control Objectives

With the rapid development of wind power generation, large capacity wind farms are built up and integrated into transmission network. The effect of wind farms on the grid becomes more serious and more extensive. As a consequence operators have the increasing expectation that wind turbines should function in some ways similar to the conventional power plants. Moreover, a precise Power Management System that controls the communications between Distribution System Operator (DSO), wind farm and WT has to be developed.

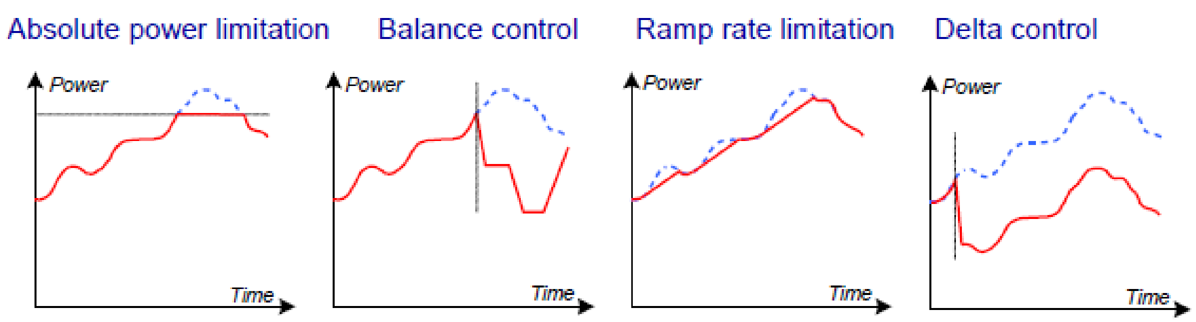

Figure 3-2 TSO References

From a control perspective, the complexity of large scale wind farms has been handled by separating the control into two levels. The first level is the network operator giving references for the whole farm. The second level of the control is the WF Controller and it deals with the fulfillment of the farm reference from the system operator and the distribution of the turbine references. Figure 3-3 illustrates a typical diagram of a wind farm control. It has as input signals: demands from the system operator, measurements from the PCC and available power from the wind turbines [23]. The references from the system operator are (see also Figure 3-2):

- power ramp rate limiter, that decides how fast the wind farm production should be adjusted. Normally this control can be used in conjunction with the others when the wind farm faces high wind speeds and the network operator would like to limit the power variations on the grid.
- balance control, the operator asks the wind farm controller to decrease or increase the production at specific levels.
- delta control, where the operator asks the wind farm controller to reserve an amount of available power as given by the prediction of the available power from the wind farm controller. This actually means that the operator requests a power reserve.
- frequency and voltage control [24].

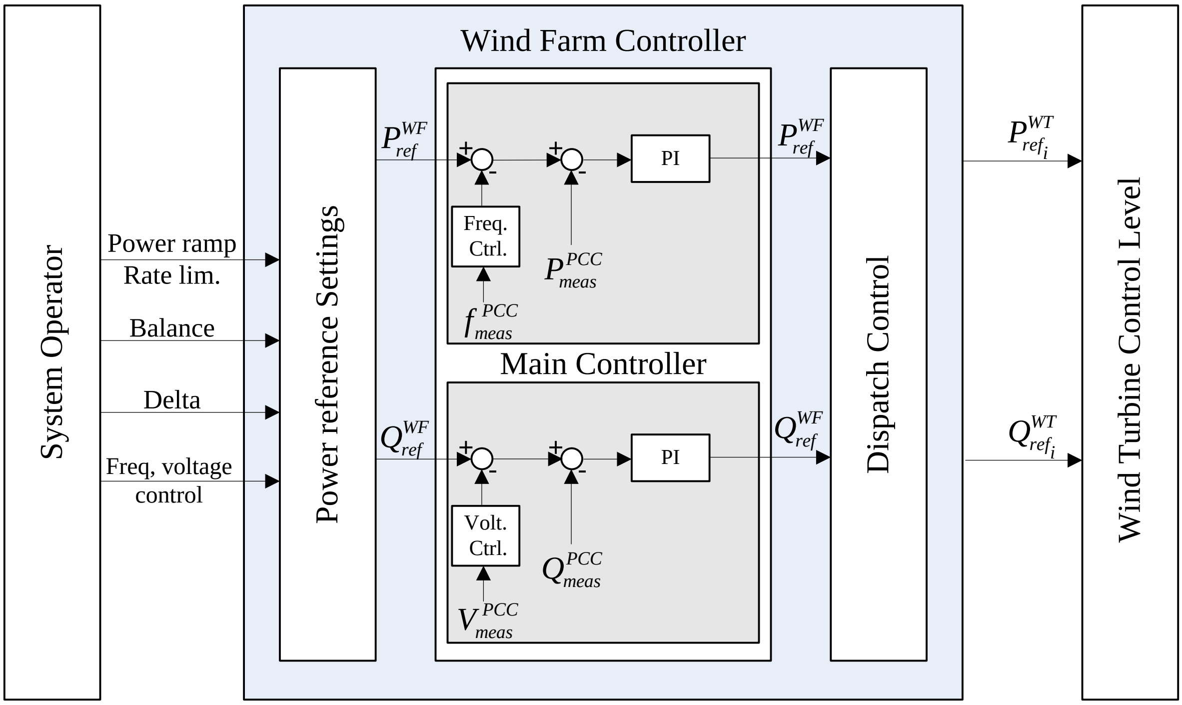

Figure 3-3 Structure of a Typical Power Management System [24]

Typically the wind farm control system contains a power reference settings block, a main controller and a dispatch function block. The power reference settings block, uses the system operator references and elaborates the references for active and reactive power, as illustrated in Figure 3-3. If necessary, these reference signals can be adjusted by the subordinated control loops (frequency and voltage), in order to support the power system control of frequency and voltage of the PCC. In our case, when only the wind farm's active and reactive power production is in focus, the frequency and voltage subordinated control loops are neglected. Further a dispatch function block converts the power reference signals from the controller into power reference signals for each individual wind turbine of the wind farm [23].

As it can be seen also in Figure 3-1 the control structure of the WTS receives two references P_{ref_i} and Q_{ref_i} from the WF Controller. It is assumed that the conventional dispatch control uses a simple way for distributing the farm active and reactive power references to all wind turbines and it is based on the proportional distribution. The references can be calculated by the following equations:

$$\begin{cases} P_{ref_i} = P_{demand} \cdot \dfrac{P_{avail_i}}{P_{avail}} \\ Q_{ref_i} = Q_{demand} \cdot \dfrac{Q_{avail_i}}{Q_{avail}} \end{cases} \tag{3.1}$$

where: P_{ref_i} is the power reference for the i^{th} wind turbine, P_{demand} is the requested active power from the network operator, P_{avail_i} is the available power at the i^{th} wind turbine and P_{avail} is the total available power at the farm by $P_{avail} = \sum_{i=1}^{n} P_{avail_i}$, where n is the number of wind turbines in the farm. (similar for reactive power Q) [24].

Further on, as stated also in the project objectives, the highlight is over the methodology of generating the optimal reactive an active power references for the WTs based on a specified control objective.

3.3 Implementation of the WF Controller

Usually a wind farm layout is defined by the wind turbines, cables and the main substation position. WTs are connected to each other in a cascade manner through the power cables, forming several feeders that are connected in the main substation, as illustrated in Figure 3-4.

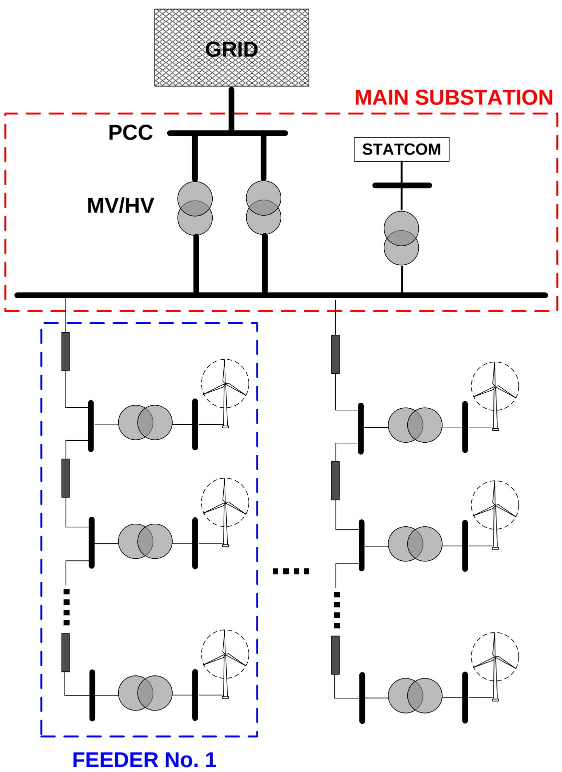

Figure 3-4 WF Layout

For a large WF with tens of WTs, active and reactive power losses are expected due to long cables and large number of power transformers. Therefore when a certain set point regarding active and or reactive power is requested by the TSO at the wind park PCC, it is important to determine what should be the optimal active and reactive power generation levels of each WT unit (based on the WF control objective) such that the WF is capable to fulfill the system operator demand [25].

The next section describes the algorithm to allocate these generation amounts based on different WF control objectives.

3.3.1 Standard Optimization Problem

Optimization is a mathematical process in which a search is activated that aims at a best value of an objective function that is optimal [26]. In a general sense, through optimization the optimal value for an objective function is searched while the constraints imposed are satisfied. Depending on the function definition the optimal value can be either a maximum or a minimum.

For a power system the objective function can involve different aspects like: minimization of generation cost, minimization of power losses, security or stability of the system. In standard form, the objective function can be written as $F(x)$ where F is a scalar function and x is the vector of variables, including both state variables and control variables. In optimal power flow problem, while the state variables can be represented by the voltage magnitudes and angles the control variables corresponds to tap changer positions, active and reactive power output of generators etc [26].

For the power system optimization problems, the equality constraints are written as $g(x)=0$ where x and g are vector functions. The most common example for a set of equality constraints is actually the set of nonlinear power-flow equations. Further on, the introduction of limits for both state and control variables leads to inequality constraints. The inequality can be a continuous function or a discrete or continuous variable and it is written as: $h(x)\leq 0$ where x and h are vectors or vector functions [26]. The inequality constraints may be for example: bounds on voltages or power levels, or that the line loading not exceeding thermal or stability limits.

Thus a standard optimization problem can be given as:

$$\min F(x) \tag{3.2}$$

subject to:

$$g(x)=0 \tag{3.3}$$

$$h(x)\leq 0 \tag{3.4}$$

where all vectors and vectors functions can be continuous, discrete or a combination [26].

3.3.2 Optimal Power Flow for a WF

The optimal power flow (OPF) problem is to fulfill a certain objective over power network variables under certain constraints. While the variables may include real and reactive power outputs, bus voltages and angles, the objective may be the minimization of generation cost, minimization of power losses, maximization of WF life time etc. Moreover, the constraints may be bounds on voltage magnitudes and angles or active and reactive power output from the WTs.

The proposed example for this sub-chapter aims to obtain a minimum deviation between the total active and reactive powers delivered by the wind farm to the grid as required by the TSO. Further on the Problem Formulation Process is presented based on [27].

Step 1: Problem Statement

Maintain the desired active and reactive power references imposed by the TSO in the WF PCC considering in the same time the losses minimization in the WF grid.

Step 2: Data and Information Collection

- the number of WTs in the WF is 100;
- WF layout, bus numbering, voltage levels are based on Figure 3-5;
- while the rated active power for the WT and rated reactive power capability for the STATCOM are predefined, the reactive power capability for the WTs is derived based on the PQ capability curve (see Figure 2-7);
- ratio tap changers for the MV/HV power transformers were not considered;
- wind speed and wake effect values are considered;
- parameters for cables and transformers are predefined;

Step 3: Identification/Definition of the design variables

For state variables, the voltage angle V_{ang_j} and magnitude V_{mag_j} for each bus bar in Figure 3-5 were considered. Moreover for the control variables, active (P_i) and reactive power reference (Q_i) for each WT and reactive power reference for STATCOM (Q_{202}) were defined. It can be concluded that the design variable vector is the following:

$$x_{opt} = [V_{mag\_j}, V_{ang\_j}, \mathrm{P}_i, Q_i, Q_{202}] \text{ where } j = \overline{1:203}, i = \overline{1,3:199} \tag{3.5}$$

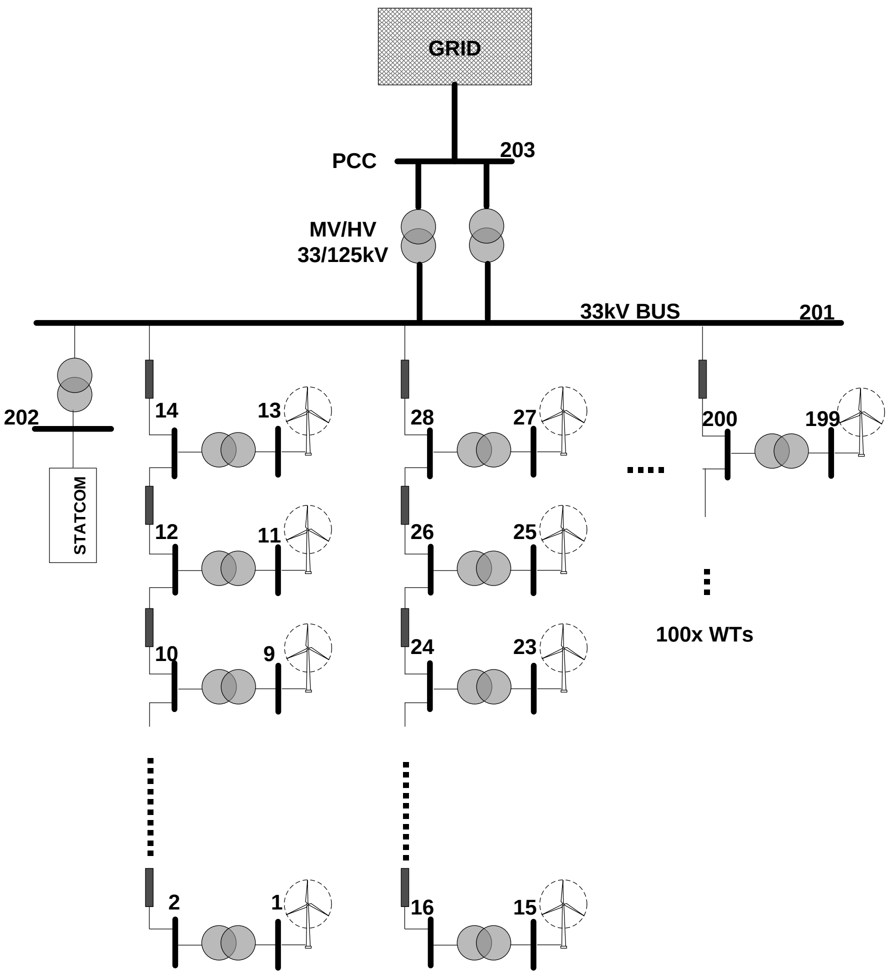

Figure 3-5 WF Configuration

Step 4: Identification of Criterion to be optimized

Based on the problem statement presented at Step 1 the following objective function is proposed:

$$\min f(x) = |Q_{dem} + Q_{203}| + |P_{dem} + P_{203}| \tag{3.6}$$

where: P_{dem} and Q_{dem} are imposed by the TSO. It should be mentioned that the following convention was used for the power flow: P_{in}, Q_{in} for a bus bar were considered negative and P_{out}, Q_{out} positive.

Step 5: Identification of Constraints

Step 5.1: Identification of Equality Constraints

As presented above, for the equality constraints the following load flow relations are considered:

$$V_i = V_{mag\_i} \cdot e^{jV_{ang\_i}} \text{ for } i = \overline{1:203} \tag{3.7}$$

$$\begin{bmatrix} I_1 \\ \dots \\ I_i \end{bmatrix} = \begin{bmatrix} Y_{11} & & Y_{1i} \\ & & \\ Y_{i1} & & Y_{ii} \end{bmatrix} \cdot \begin{bmatrix} V_1 \\ \dots \\ V_i \end{bmatrix} \tag{3.8}$$

where V_i, I_i are the voltage and currents at each bus bar, $i = \overline{1:203}$ and Y_{ii}, Y_{ij} are the admittance matrixes mutual or self components;

$$\begin{cases} S_i = V_i \cdot I_i^* \\ P_{bus\_i} = real(S_i) \quad \text{for } i = \overline{1:203} \\ Q_{bus\_i} = imag(S_i) \end{cases} \tag{3.9}$$

Moreover the PCC bus is modeled as a slack bus (see Equation(3.10)) and all other buses are modeled as PQ buses. For the even buses $i = \overline{2,4:200}$ and bus number 201 P and Q were considered 0 (see Equation(3.11)).

$$\begin{cases} V_{mag\_203} = 1 \\ V_{ang\_203} = 0 \end{cases} \tag{3.10}$$

$$\begin{cases} P_{bus\_i} = 0 \\ Q_{bus\_i} = 0 \end{cases} \text{ for } i = \overline{2,4:200,201} \tag{3.11}$$

For STATCOM bus (number $i = 202$) and WTs buses ($i = \overline{1,3:199}$), P_{bus_i} and Q_{bus_i} should be equal with P_i, Q_i from Equation(3.5) to assure that the optimal solution found matches with the power flow equations Equation(3.7) to (3.9). Considering also that the active power in the STATCOM bus should be 0, the last equality constraint imposed were the following:

$$\begin{cases} P_{bus\_202} = 0 \\ Q_{bus\_202} = Q_{202} \end{cases} \tag{3.12}$$

$$\begin{cases} P_{bus\_i} = P_i \\ Q_{bus\_i} = Q_i \end{cases} \text{ for } i = \overline{1,3:199} \tag{3.13}$$

Step 5.2: Identification of Inequality Constraints

For the state variables, Equation (3.14) expresses the limits for voltage magnitude and angle of all the buses presented in Figure 3-5.

$$\begin{cases} 0.9 < V_{mag\_i} < 1.1 \\ -\pi/4 < V_{ang\_i} < \pi/4 \end{cases} \text{for } i = \overline{1:203} \tag{3.14}$$

Further on, limits for active and reactive power capability for each WT and for the STATCOM were required:

$$\begin{cases} 0 < P_{bus\_i} < P_{avail\_j} \\ -Q_{ind.capab\_j} < Q_{bus\_i} < Q_{cap.capab\_j} \\ -Q_{STATCOM\_ind.rat} < Q_{bus\_202} < Q_{STATCOM\_cap.rat} \end{cases} \text{for } j = \overline{1:100} \text{ and } i = \overline{1,3:199} \tag{3.15}$$

where: P_{avail_j} is the available power of the j^{th} WT and depends on wind speed (see power profile curve Figure 2-9) ; $Q_{ind.capab\_j}$ and $Q_{cap.capab\_j}$ is the reactive power capability of the j^{th} WT and is conditioned by the active power delivered by the j^{th} WT based on PQ capability curve (see Figure 2-7) and Q_{bus_202} is the reactive power delivered/consumed by the STATCOM and it is limited by his rated inductive and capacitive values.

It should be mentioned that through this constraints presented above from Equation(3.7) to (3.15) the WF grid power losses minimization is achieved due to the Y_{bus} matrix and *fmincon* function. Therefore no additional changes are required in the initial cost function.

Step 6: Initial Conditions

Finally, for the initial conditions a *flat start* was considered based on the following values:

$$x_0 = [V_{mag\_j}, V_{ang\_j}, \mathrm{P}_i, Q_i, Q_{202}] \text{ for } j = \overline{1:203}, i = \overline{1,3:199} \tag{3.16}$$

where: $V_{mag\_j} = 1$, $V_{ang\_j} = 0$ and $\mathrm{P}_i = Q_i = Q_{202} = 0$

The optimal power flow algorithm presented above represents the base structure for the future study cases presented in Chapter 5. Later on, this power flow algorithm will suffer slightly changes based on the WF Control Mode (e.g. normal, delta etc.) and WF Controller objectives (e.g. WF grid losses minimization, life time optimization) specific for each study case.

Finally, in Figure 3-6 the structure of the new Power Management System is presented. The implementation in MATLAB, of the WF controller was realized according to this figure.

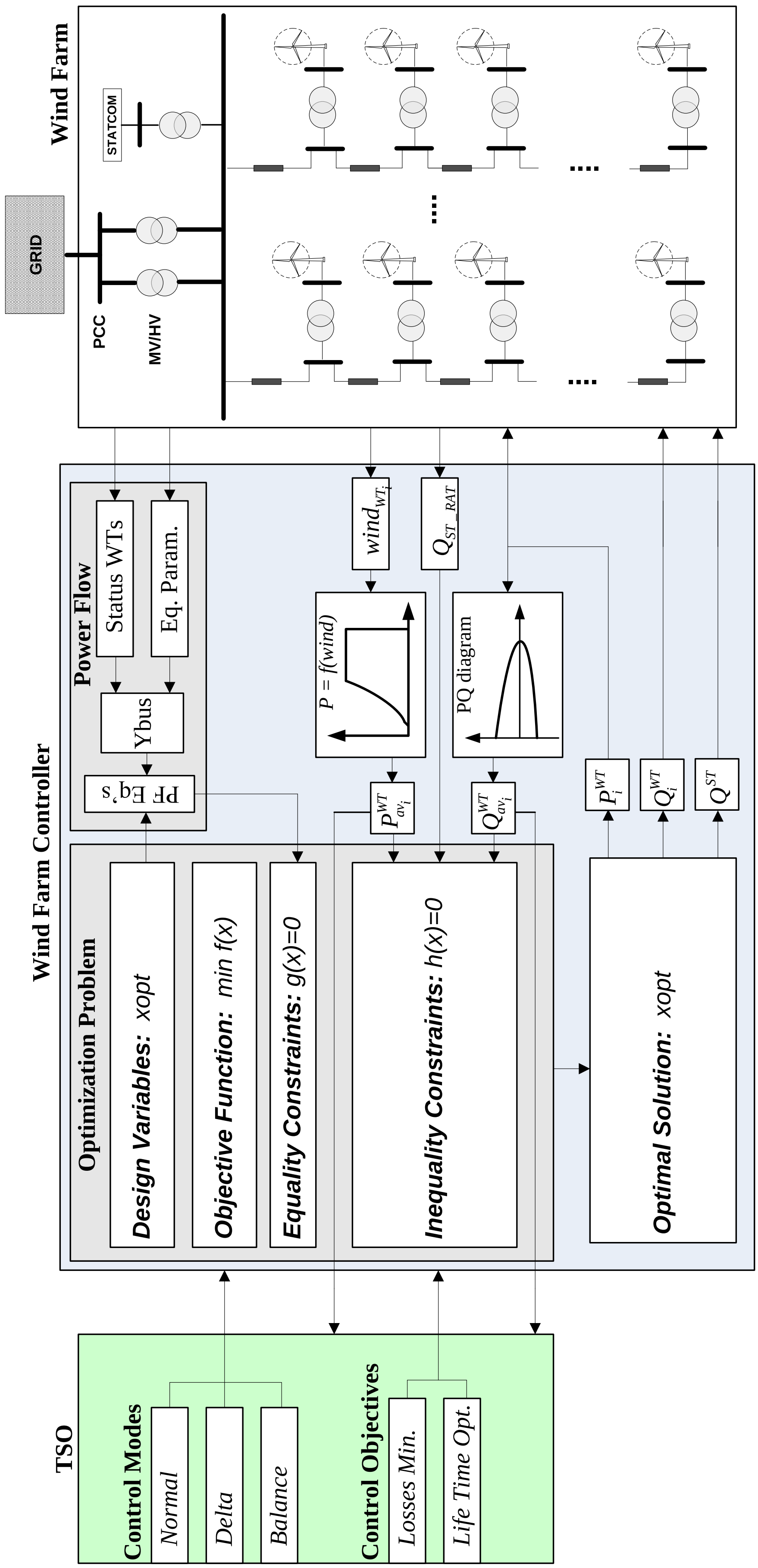

Figure 3-6 Structure of the Power Management System

Chapter 4 Reactive Power Capability of a Wind Power Plant

In the first part of this chapter a short overview regarding the FACTS Controllers is presented, followed by a brief description of the STATCOM. In the last part the effects of a STATCOM over a WPP from a technical and economical point of view are highlighted.

4.1 Overview of FACTS

In recent years, severe requirements have been placed on the transmission network, and these requirements will continue to increase because of the increasing number of nonconventional generator plants. Several factors such as increased demands on transmission and the need to provide open access to generating companies and customers have reduced the security of the system and the quality of supply. The cost of transmission lines and losses, as well as difficulties encountered in building new transmission lines, would often limit the available transmission capacity.

These problems have necessitated a change in the traditional concepts and practices of power systems. There are emerging technologies available, which can help system operators to deal with above problems [28].

Flexible AC Transmission System (FACTS) is one aspect of the power electronics revolution that happened in all areas of electric energy. These controllers provide a better adaptation to varying operational conditions and improve the usage of existing installations. FACTS controller is defined as a power electronic-based system that provide control of one or more AC transmission system parameters (series impedance, shunt impedance, current, voltage, phase angle).
The FACTS controllers are mainly used for the following applications:

- Power flow control,
- Increase of transmission capacity,
- Voltage control,
- Reactive power compensation,
- Stability improvement,
- Power quality improvement,
- Power conditioning,
- Flicker mitigation,
- Interconnection of renewable and distributed generation and storages.

Using the advantages offered by the power electronic devices the FACTS controller provides a smoother operation and an increased lifetime of the system(less maintenance), compared to the conventional devices which are mechanical switched [28]. In general, FACTS controllers can be divided into four categories:

- Series Controllers
- Shunt Controllers
- Combined series-series Controllers
- Combined series-shunt Controllers

A more detailed classification of the FACTS controllers is presented in Figure 4-1.

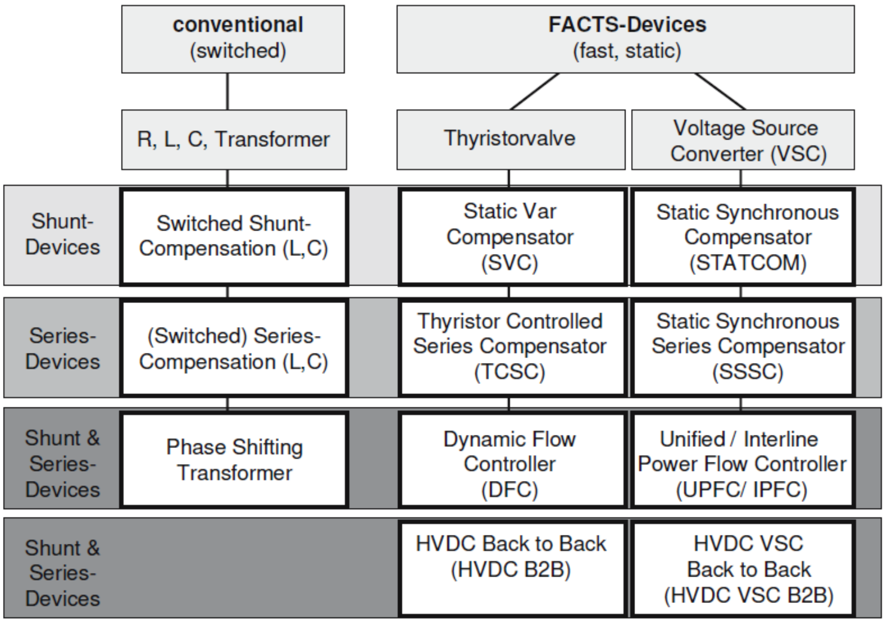

Figure 4-1 Overview of major Facts controller [29]

The first column in Figure 4-1 contains the conventional devices build out of fixed or mechanically switchable components. From this figure it can be also observed that the FACTS controllers are divided in two categories. While the first category is represented by the old generation of controllers based on the well proven thyristor valve technology, the second category is represented by the new Voltage Source Converter technology based mainly on the Insulated Gate Bipolar Transistors (IGBT) [29].

For a WPP one of the requirements imposed by the TSO, through the new grid codes, is the reactive power compensation at the PCC during normal or abnormal conditions operation. Since the purpose of the application is to control the voltage at and around the point of connection by injecting reactive current (leading or lagging), the Shunt devices proved to be the most suitable solution [28].

4.2 Reactive Power Compensator Devices

Capacitor Bank

Capacitor Bank consists of a number of shunt capacitors switched mechanically to provide reactive power, and its installation and maintenance is relatively inexpensive. Installing such a device in the load area or at the point that they are needed will increase the voltage stability. One of the drawbacks of this device is that it provides bulk reactive power which results in poor voltage regulation and incapibility to establish a stable operating point beyond a certain level of compensation [10]. As it can be observed from Figure 4-2, the reactive power delivered by the Capacitor Bank is proportional to the square of the terminal voltage (during low voltage conditions Var support drops) [18].

An important fact that has to be considered when a Capacitor Bank is utilized is the size of each capacitor in order to avoid large voltage transients. The impact of the Capacitor Bank over the voltage stability was analyzed based on the analytical method presented in [20].

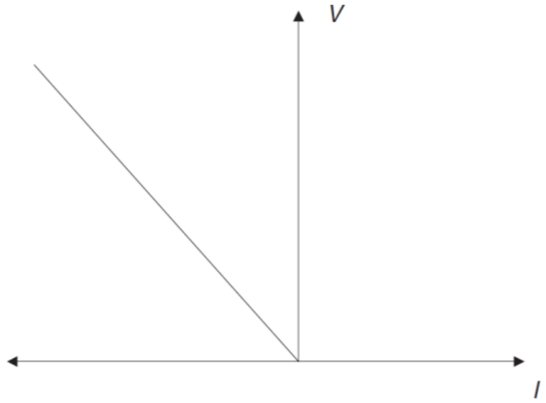

Figure 4-2 V-I Characteristic of a Capacitor Bank

Static Synchronous Compensation – STATCOM

To enhance a Wind Power Plant with ability to deliver or absorb reactive power from the grid, the STATCOM is the device which despite its higher price presents the following majors advantages compared with other devices:

- The maximum compensating current is maintained independently of the system voltage;
- The maximum reactive power output decrease linear with the voltage decrease;
- Harmonic generation can be internally very low (multilevel converter) and may require no-filtering;
- Maximum theoretical delay is negligible [28].

STATCOM tipically consists of an inverter, a DC capacitor and a coupling transformer, see Figure 4-3.

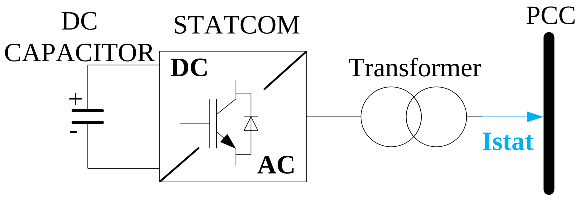

Figure 4-3 Schematic representation of a STATCOM [29]

Assuming that no active power is exchanged between STATCOM and the grid (lossless operation) the voltage of the controller is in phase with the grid voltage. If the compensator voltage magnitude is smaller than the voltage at the connection node current will flow from the grid to STATCOM. In this case the reactive power will be consumed. If the situation is opposite the reactive power will be delivered to the grid.Schematic representation of this principle is presented using phasor diagrams in Figure 4-4 [29].

A STATCOM injecting reactive current is supporting the grid voltage. Comparably when STATCOM is absorbing reactive current it is decreasing the grid voltage. In the first case controller behaves as an overexcited generator or capacitor and in the second case STATCOM behaves as an under excited generator or inductor [29].

The STATCOM is essentially an alternating voltage source with the corresponding *V-I* and *V-Q* characteristics shown in Figure 4-5.

These show that the STATCOM can be operated over its full output current range even at very low system voltage levels. In other words, the maximum capacitive or inductive output current of the STATCOM can be maintained independently of the ac system voltage, and the maximum VAr generation or absorption changes linearly with the ac system voltage [28].

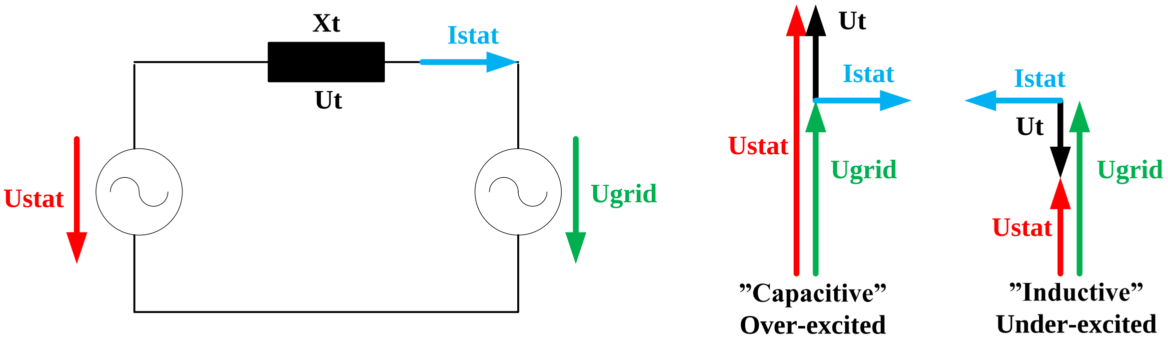

Figure 4-4 Equivalent circuit representation of a STATCOM [29]

In all applications the practical requirements, needs and benefits have to be considered carefully to justify the investment into a complex new device. The majority of the WPP developers are looking for the cheapest solution to fulfill the requirements imposed by the TSO. Since all the devices present drawbacks and advantages, a combination of them seems to be the suitable solution. A method that can help the WPP to support the grid with reactive power is the over sizing of the WTs Grid Side Converter. Therefore in order to find the optimal solution for different scenarios, a technical and economic analysis of different combination of the above presented devices and methods are presented in the next section.

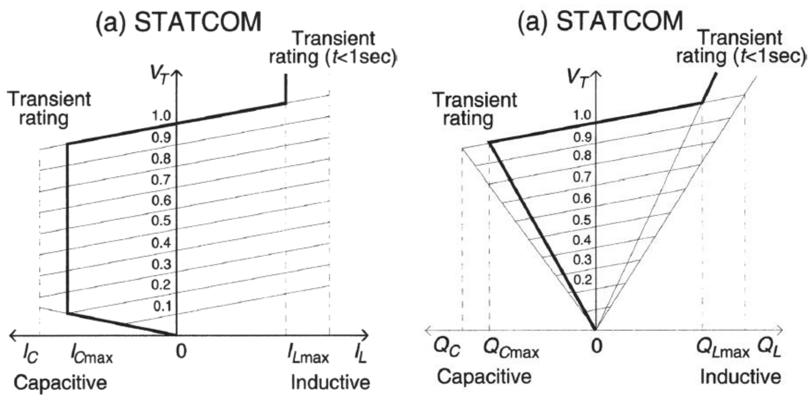

Figure 4-5 V-I and V-Q characteristic of a STATCOM [28]

4.3 Technical and Economic Analysis of a WPP Reactive Power Capability

Reactive power supply is essential for a reliable operation of the WF and the associated electric transmission system. Inadequate supply of reactive power can lead to penalties from TSO for not providing the requests imposed or worst can become the cause of voltage collapses in the WF grid.

Several generation and network devices, including generators, capacitors, static VAR compensators, and STATCOMs can be used for providing the necessary reactive power in the WFF PCC. However, WTs equipped with a full scale power converter also have the capability of producing reactive power and voltage support based on the grid side converter Q rating. While the potential for distributing reactive power with the WTs grid side converters or a STATCOM is great, the costs are higher in comparison with other conventional technologies, such as capacitors. However, not all these technologies are capable of providing the same kind of reactive power support. Grid side converters or STATCOMs can provide dynamic support capabilities that static device such as capacitors banks cannot fulfill. Therefore, when the optimal Q rating for different compensators is analyzed the percentage of static and dynamic reactive power capability desired has to be defined first. Since the dynamic reactive power control it is more effective but also more expensive than providing reactive support in bulk form, for finding an optimal Q rating for the compensator devices both economic and technical aspects have to be considered [30].

4.3.1 Technical and Economic Analysis Assumptions

As presented above, reactive power devices can be characterized as dynamic or static depending on their location and functionality. Static reactive power supply is most commonly found in the WF PCC and it is provided by capacitors, load tap changers on transformers, and reactors. In the following analysis only capacitor banks were considered while load tap changers for transformers are proposed as one of the objectives for the further work. However, static reactive power supply cannot respond to load changes rapidly. Therefore due to this primary disadvantage of static reactive reserves, the interest for the dynamic reactive reserves increased rapidly in the past years [30].

Moreover, in this project the following devices were considered for dynamic reactive power capability:

1. Pure Reactive Power Compensator (STATCOM) in the WF PCC
2. Oversized WTs Grid Side Converter

An inverter that is connected with a distributed energy device such as a WT can provide dynamic control of real and reactive power. Although conventionally the range of the reactive power supply from such devices is limited, it is possible to upgrade the inverters to supply reactive power in a much larger range. Over sizing of the inverter will significantly increase the range of reactive power supply but the main disadvantage is that cost increases as the reactive power ability is increased.

It can be concluded that the optimal allocation of reactive power capability for a given WF will be defined by 3 devices:

- WTs grid side converter
- STATCOM
- Capacitor banks in PCC

Since the economical scope of this analysis is to minimize the capital costs for the above devices the range of prices per kVAr where considered based on Figure 4-6 and [31-32].

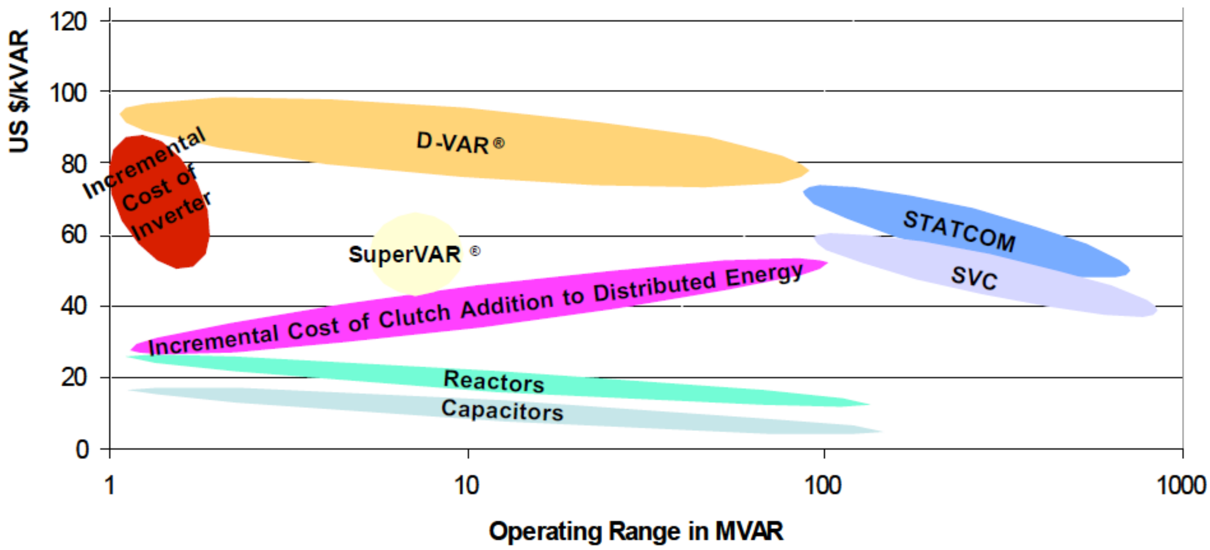

Figure 4-6 Average Costs of Reactive Power Technologies [30]

Moreover two types of study cases are presented. While for the first study case, the fulfillment ratio (FFR) of the WF based on TSO Q requests is less than 100%, for the second study case the optimal Q ratings for the WF compensators will always be capable of fulfilling all TSO request.

4.3.2 Study Case 1: WF Reactive Power capability for different FFRs

For this Study Case the WTs grid side converters Q capability was considered fixed, and it was defined by the conventional PQ curve presented in Figure 2-7. First, the following procedure was used for finding the necessary Q capability of the STATCOM and Capacitor Banks in the PCC. For a wind speed from 0 to 30 m/s, for each wind sample the following steps were performed:

- based on wind speed and wake effect assumptions P and Q capability of each WT were found and then imposed at each WT bus bar
- next the power factor was increased from 0.85 to 1 (only capacitive power factor was considered)
- than the power flow algorithm was performed and the Q capability of the STATCOM and Capacitor Banks were defined as a function of wind speed and power factor as presented in Equation (4.1) and Figure 4-7.

$$Q_{ST.+Cap.Banks} = f(wind, PF) \tag{4.1}$$

It can be said that the bellow plot validates the expectations regarding the evolution of the necessary Q capability based on wind speed and power factor. As it can be seen, when wind speed increases (between 9 m/s and 13 m/s), WTs Q capability decreases therefore the necessary $Q_{ST.+Cap.Banks}$ increases. Bellow cut in wind speed and above cut out wind speed the WTs Q capability is very high (based on PQ capability curve in Figure 2-7) hence the necessary $Q_{ST.+Cap.Banks}$ is 0.

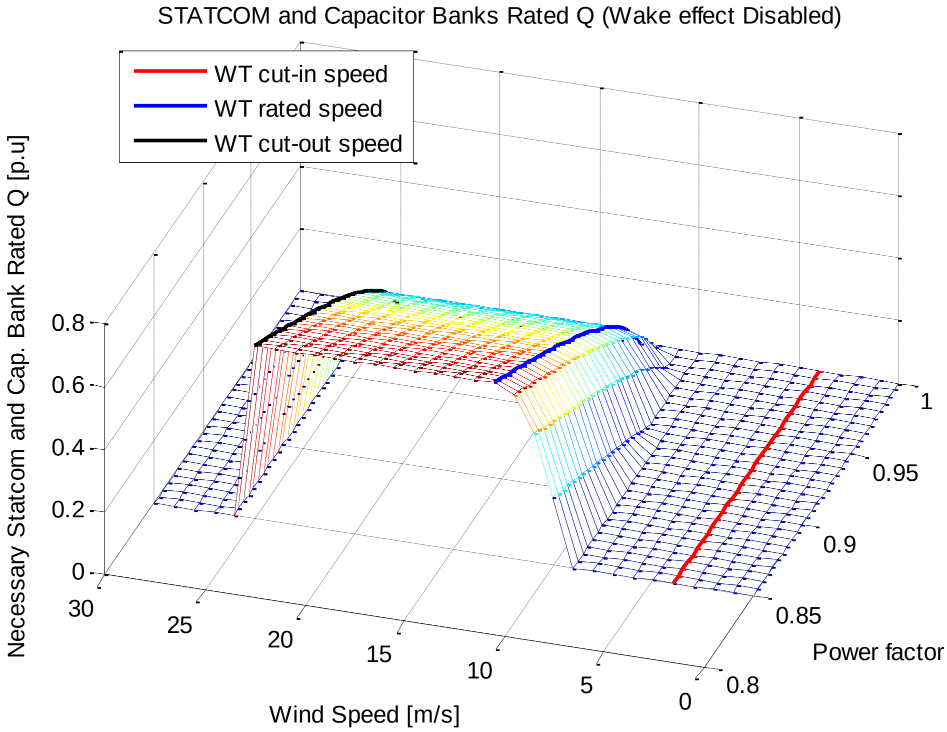

Figure 4-7 Necessary STATCOM and Cap. Bank Q capability

Similar behavior can be observed between cut-in wind speed and 9 m/s when the WTs are still capable of providing the necessary Q for the requested power factor by TSO. Moreover, when the power factor decreases, TSO Q request increases therefore the necessary

$Q_{ST.+Cap.Banks}$ will increase as well. It should be stated also that in the above figure the wake effect was disabled, if not, slightly changes would appear based on the magnitude of the wake coefficients.

In Figure 4-8 the necessary $Q_{ST.+Cap.Banks}$ was plotted for the rated wind speed. As it can be seen, for the lowest power factor requested (0.85) the maximum necessary $Q_{ST.+Cap.Banks}$ was around 0.55 p.u.

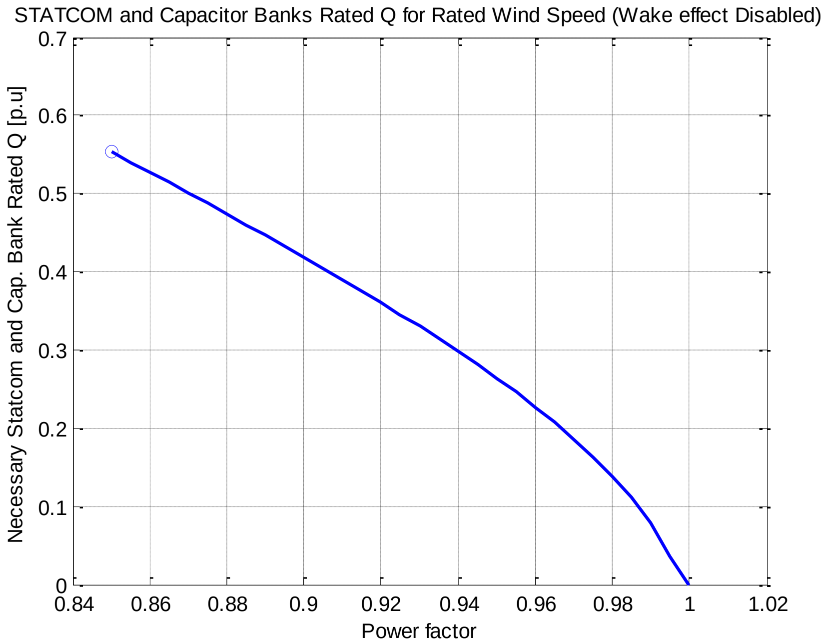

Figure 4-8 Necessary STATCOM and Capacitor Bank Q capability at rated wind speed

Moreover in Figure 4-9 a predefined $Q_{ST.+Cap.Banks}$ rating of 0.4 p.u was chosen. Above rated $Q_{ST.+Cap.Banks}$ the instances when the WF is not capable of providing the necessary PF requested by TSO can be observed. Contrarily bellow the predefined $Q_{ST.+Cap.Banks}$ the situations when the WF is capable of fulfilling the request can be viewed.

Based on this principle, the fulfillment ratio (FFR) for a predefined $Q_{ST.+Cap.Banks}$ is defined as:

$$\mathrm{FFR} = \left(1 - \frac{\sum \text{instances when PF is not fulfilled}}{\sum \text{total instances}}\right) \cdot 100 \tag{4.2}$$

Based on Equation (4.2) the FFR of a predefined $Q_{ST.+Cap.Banks}$ is derived as shown in Figure 4-10. It can be said that the results obtained validates the expectations regarding the evolution of the FFR. When the $Q_{ST.+Cap.Banks}$ rated Q is increased the overall FFR of the WF is increased also. The 100% FFR is reached when $Q_{ST.+Cap.Banks}$ is equal with the maximum presented in Figure 4-8.

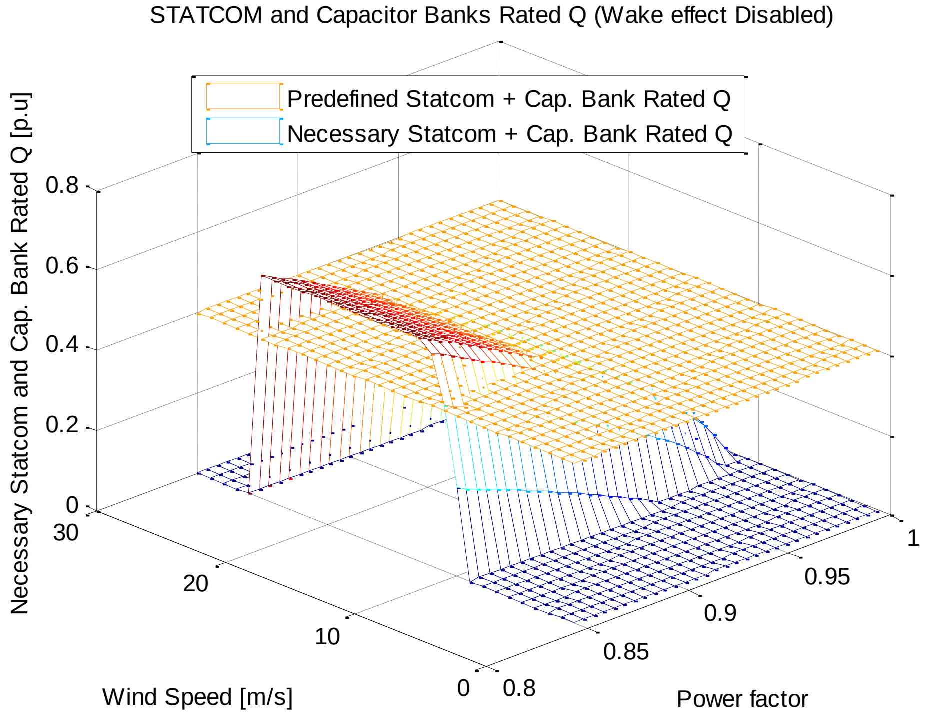

Figure 4-9 Predefined STATCOM and Cap. Bank Q capability

Moreover the algorithm presented above was extended on a real wind profile of a 1 year period. Based on the results obtained (see Figure 4-11) and the assumptions considered for the simulations the optimal Q sizing of the STATCOM and Capacitor Bank were derived for three different objectives:

- selection of the highest necessary $Q_{ST.+Cap.Banks}$ and therefore the WF will always be capable of providing the necessary power factor requested by TSO;
- selection of a lower $Q_{ST.+Cap.Banks}$ and paying the penalties imposed by TSO for not providing the requested power factor;
- selection of a lower $Q_{ST.+Cap.Banks}$ and decreasing the active power references of the WTs in order to increase their Q capability and to obtain a FFR of 100%;

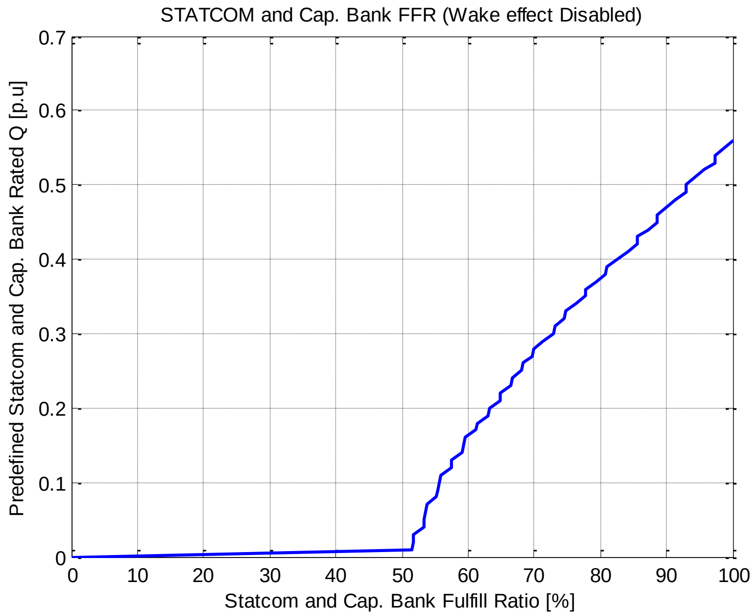

Figure 4-10 STATCOM and Capacitor Bank fulfillment Ratio

For this study case the following assumptions were considered: the life time of the WF was considered around 20 years and therefore the results obtained over 1 year were extended over 20 years, the TSO power factor request was changed every 2 hours (see subplot no. 2 in Figure 4-11), all WTs were considered available and STATCOM and capacitor bank prices were considered based on Figure 4-6 and [31-32].

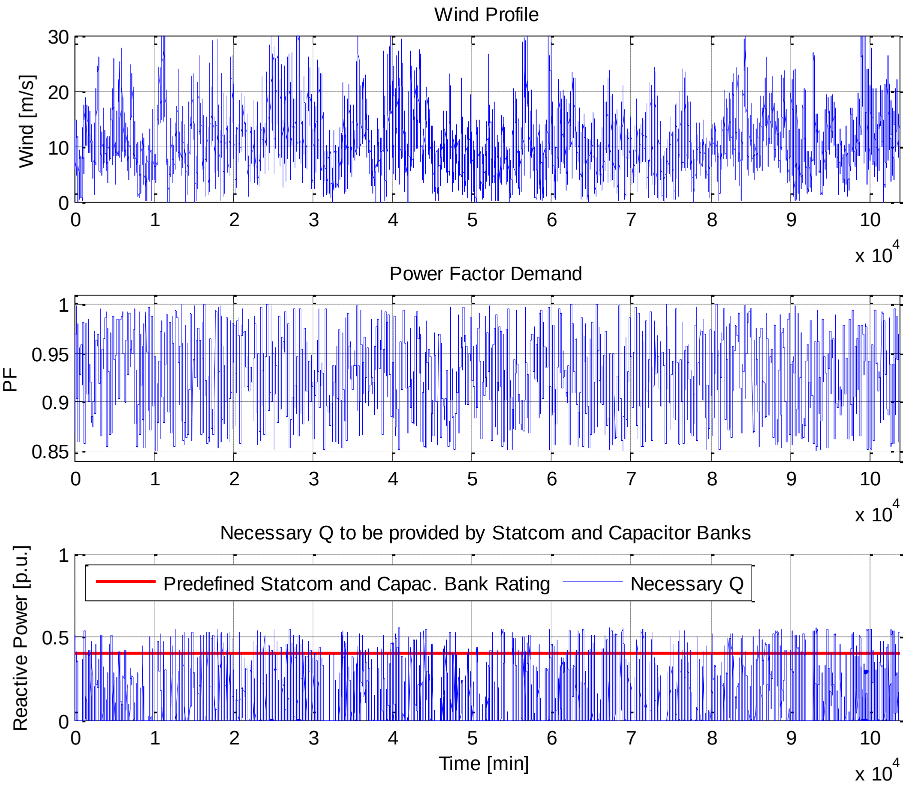

Figure 4-11 Necessary $Q_{ST.+Cap.Banks}$ for 1 year real wind profile

Based on the results obtained in last subplot in Figure 4-11 and based on a predefined constant penalty price from TSO for not providing the requested power factor, the following dependency were plotted in Figure 4-12:

- price evolution of the STATCOM and Capacitor Bank when the $Q_{ST.+Cap.Banks}$ rating is variable;
- Q penalties paid in 20 years for a variable $Q_{ST.+Cap.Banks}$ rating;

As it can be seen, if a lower $Q_{ST.+Cap.Banks}$ rating is chosen, the price for the STATCOM and capacitor bank is lower but the penalties are higher. On the other hand if a higher $Q_{ST.+Cap.Banks}$ is chosen the price paid for the devices is higher but the penalties are lower. Therefore, in order to find the optimal $Q_{ST.+Cap.Banks}$ rating an optimization problem was defined where $x_{opt} = [Q_{ST.+Cap.Banks}]$ and the objective function was considered as shown bellow:

$$\min f(x) = \mathrm{P}_{STATCOM+Cap.Bank} + P_{Qpenalties} \tag{4.3}$$

where $\mathrm{P}_{STATCOM+Cap.Bank}$ is the STATCOM and capacitor bank price and $\mathrm{P}_{Qpenalties}$ is the costs of the penalties paid during the lifetime.

The optimal $Q_{ST.+Cap.Banks}$ found was around 0.45 as shown also in Figure 4-12. Moreover the same principle can be applied for the study case when active power decreasing is considered and as it can be seen in Figure 4-13 the optimal $Q_{ST.+Cap.Banks}$ found was around 0.55.

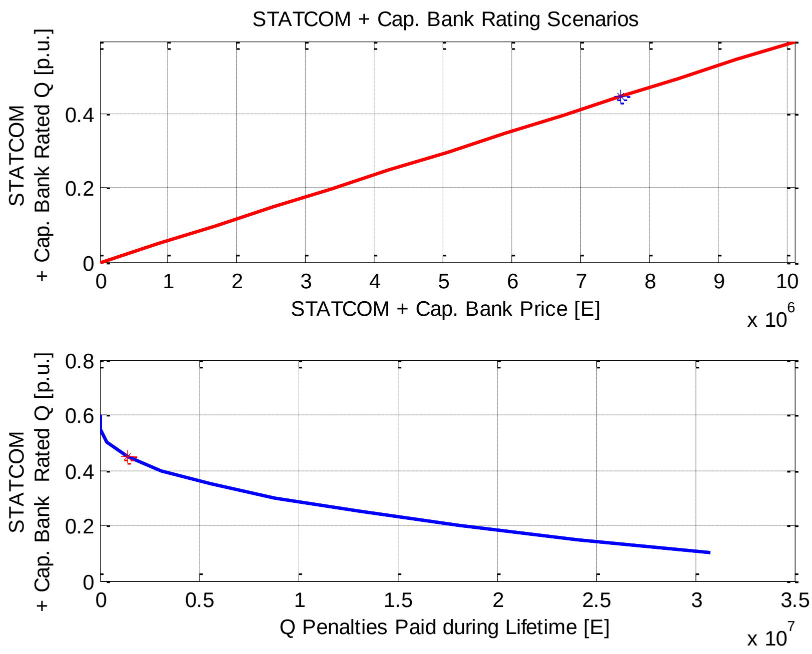

Figure 4-12 Scenarios for STATCOM and Capacitor Bank Rated Q depending on Q penalties

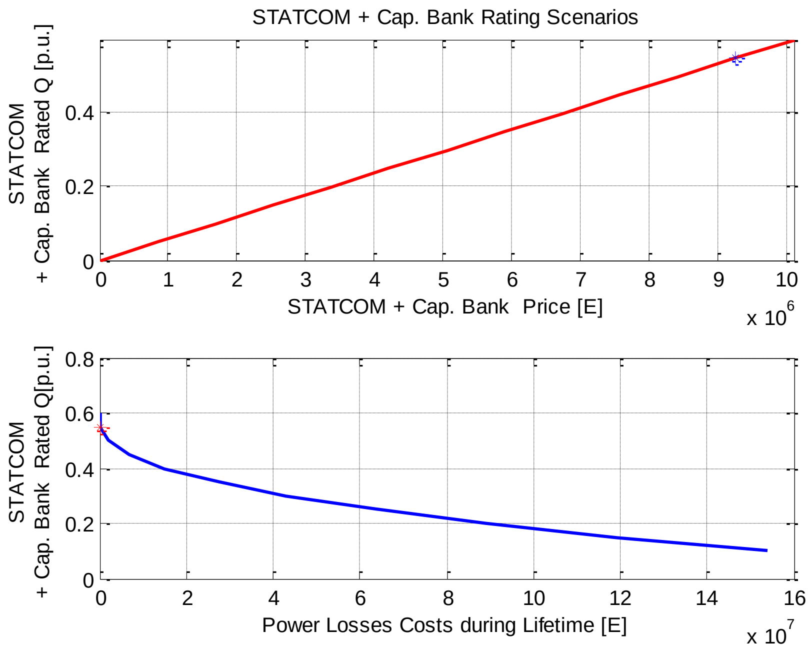

Figure 4-13 Scenarios for STATCOM and Capacitor Bank Rated Q depending on P losses costs

Analysis of Results

From the results obtained above the following conclusions are highlighted:

- for the assumptions considered, choosing the highest $Q_{ST.+Cap.Banks}$ rating is not the optimal way;
- the optimal $Q_{ST.+Cap.Banks}$ based on the assumptions presented above was obtained when paying penalties for not providing the necessary Q imposed by TSO;
- decreasing the WTs active power references with the intention of increasing their Q capability is not an cost effective method; Based on the results in Figure 4-13 the optimal $Q_{ST.+Cap.Banks}$ is almost the same with the highest $Q_{ST.+Cap.Banks}$ rating in Figure 4-8;

Finally it can be concluded the optimal $Q_{ST.+Cap.Banks}$ found is 0.45 however the following problems should be considered for a real study case.

Evaluating the economics of reactive power compensation is a complex procedure which implies different aspects. For example, the cost of providing reactive power includes capital costs as well as operating costs, such as operating expenses. In this study case only the capital cost was considered. Moreover constant penalties cost and power losses cost were considered. For a more realistic study case costs for both active power losses and reactive power penalties should be based on a detailed spot market profile.

However, based on [30] for the reactive power there are no standard models or analysis tools for this type of study (e.g. there are no fully functioning markets yet in U.S.). As a result, literature or data about penalties costs was difficult to find. To study the economic benefits of using an under rated $Q_{ST.+Cap.Banks}$ for reactive power support in WF PCC, it is necessary to developed a much more detailed cost profile for the penalties based also on the overall effects caused in the electrical grid.

Considering these aspects it can be concluded that choosing a $Q_{ST.+Cap.Banks}$ rating with a FFR smaller that 100% is a delicate and risky tasks therefore the next study cases are based only on a 100% FFR with the purpose of obtaining more realistic results.

4.3.3 Study Case 2: WF Reactive Power capability for a FFR of 100%

In this sub-chapter three study cases are presented. For the first study case the grid side converter, and both STATCOM and capacitor banks are variable. After that, in the second study case STATCOM is excluded and an optimal grid side converter and capacitor bank are determined. Finally, for the last study case the grid side converter will remain constant, similar with the previous study case presented in Chapter 4.3.2.

a. <u>Optimization of STATCOM, Cap. Banks and WTs grid side converter Q capability</u>

Until now $Q_{ST.+Cap.Banks}$ rating was defined as a function of wind speed and power factor request by TSO (see Equation(4.1)). However for this study case, $Q_{ST.+Cap.Banks}$ rating is defined as a function of three variables:

$$Q_{ST.+Cap.Banks} = f(wind, PF, GSC) \tag{4.4}$$

where PF is the power factor and GSC is the grid side converter Q capability at rated active power (the upper point of the WTs PQ capability curve in Figure 2-7). Since there is an additional parameter (GSC) a new procedure was used for finding the necessary Q capability of the STATCOM and Capacitor Banks in the PCC. For a GSC parameter starting from 0.1 to 0.8 and a wind speed starting from 0 to 30 m/s, for each pair $[GSC, wind]$ the following steps were performed:

- based on wind speed and wake effect assumptions P and Q capability of each WT were found and then imposed at each WT bus bar;
- next the power factor was increased between 0.85 to 1 (capacitive) and then from 0.9 to 1 (inductive). Later on the lagging power factor will impose indirectly the ratio between static and dynamic reactive power compensation;
- then the power flow algorithm was performed and the Q capability of the STATCOM and Capacitor Banks were defined as a function of wind speed, power factor and GSC as presented in Equation (4.4);

Based on this algorithm the $Q_{ST.+Cap.Banks}$ rating was defined as a function of wind speed and GSC (see Figure 4-15) or as a function of power factor and GSC (see Figure 4-14).

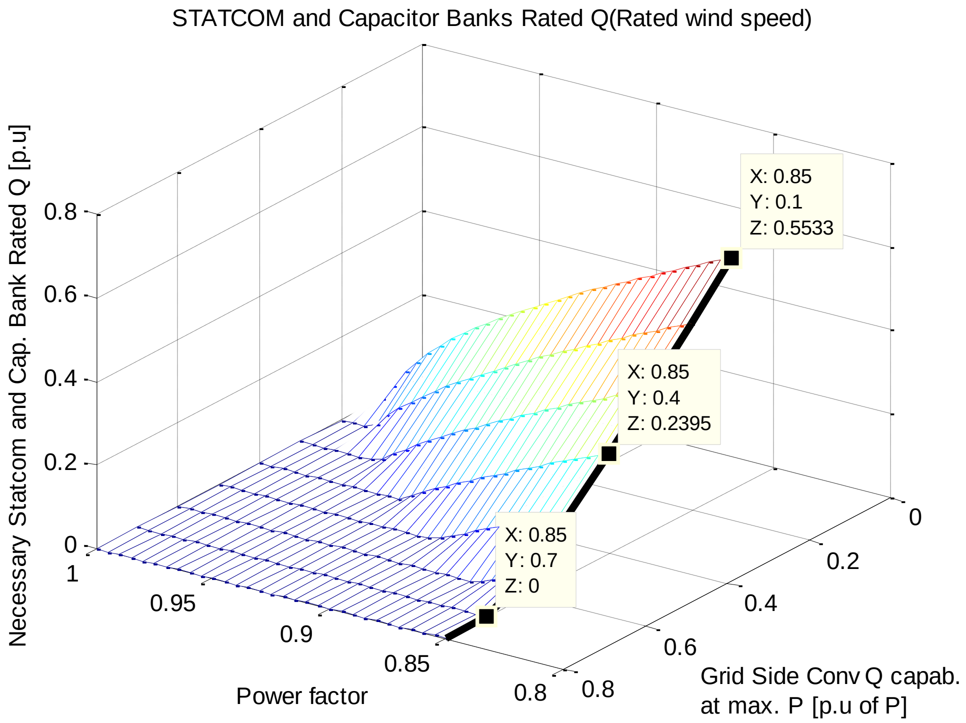

Figure 4-14 Necessary STATCOM and Cap. Bank Q capability for a PF=0.85

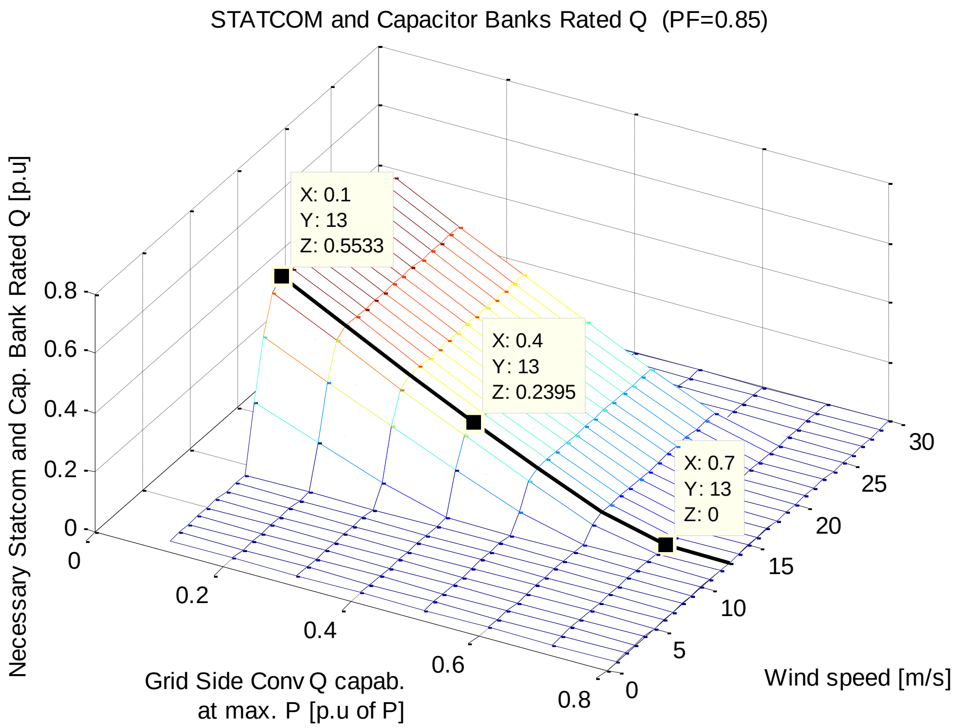

Figure 4-15 Necessary STATCOM and Cap. Bank Q capability at rated wind speed

It can be said that both plots validates the expectations concerning the evolution of the necessary $Q_{ST.+Cap.Banks}$ capability based on wind speed, power factor and GSC. As it can be seen in Figure 4-14, when the grid side converter Q capability increases (GSC from 0.1 to 0.8), the necessary $Q_{ST.+Cap.Banks}$ is decreasing. It can be observed that for a GSC of 0.7 - 0.8 the necessary $Q_{ST.+Cap.Banks}$ is 0 since the WTs are capable of providing the requested power factor in any conditions. Moreover when the power factor decreases, the Q requested is increasing and therefore the necessary $Q_{ST.+Cap.Banks}$ will always increase. For Figure 4-15 while the GSC evolution has the same effect over $Q_{ST.+Cap.Banks}$ as presented above, the wind speed evolution from 0 to 30 m/s causes the same consequences as presented in Chapter 4.3.2.

Moreover in both figures a black line is plotted defining $Q_{ST.+Cap.Banks} = f(GSC)$ for a PF = 0.85 and rated wind speed. Based on this curve, presented also in Figure 4-16, a new optimization problem is developed.

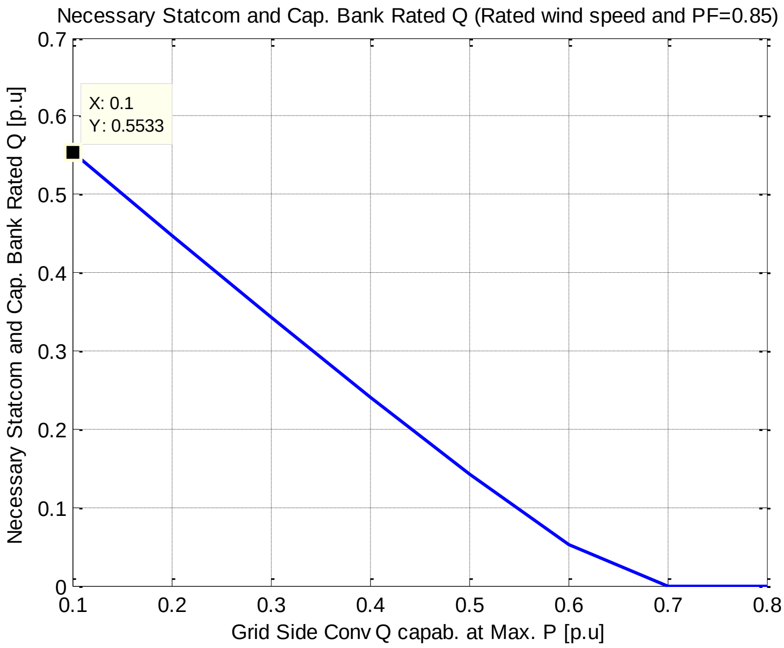

Figure 4-16 Necessary STATCOM and Cap. Bank Q capability at rated wind speed and PF=0.85

The proposed optimization problem for this study case aims to minimize the costs of WF`s equipment (STATCOM, capacitor banks, etc.) and in the same time deliver the necessary reactive power in the WF PCC as requested by TSO. Further on the Problem Formulation Process is presented based on [27].

Step 1: Problem Statement

Find the optimal Q ratings for WTs grid side converters, STATCOM and capacitor banks by minimize the costs involved.

Step 2: Data and Information Collection

- while the rated active power for the WT is predefined, the reactive power capability for the WTs is derived based on the PQ capability curve (see Figure 2-7);
- ratio tap changers for the MV/HV power transformers were not considered;
- wake effect values are not considered;
- parameters for cables and transformers are predefined;

Step 3: Identification/Definition of the design variables

The design variable vector is the following:

$$x_{opt} = [Q_{STATCOM}, Q_{cap.bank}, GSC] \tag{4.5}$$

where $Q_{STATCOM}$ and $Q_{cap.bank}$ are the rated reactive powers and GSC is the grid side converter's Q capability at rated active power.

Step 4: Identification of Criterion to be optimized

Based on the problem statement presented at Step 1 the following objective function is proposed:

$$\min f(x) = P_{STATCOM} + P_{Cap.banks} + P_{WTs\_GSC} + P_{cables} \tag{4.6}$$

where P stands for price. Cables prices were also considered since the cable parameters might change when the grid side converter Q rating is changing. Price of the WTs power transformer were considered fixed and therefore it is not a part of the optimization problem.

Step 5: Identification of Constraints

Step 5.1: Identification of Equality Constraints

As presented above in Figure 4-16 the relation between $Q_{STATCOM}$, $Q_{cap.bank}$ and GSC has to be imposed.

$$Q_{STATCOM} + Q_{cap.bank} = f(GSC) \tag{4.7}$$

Imposing this constraint, it can be guaranteed that the optimal point x_{opt} will always be positioned on the blue line plotted in Figure 4-16.

Before presenting the inequality constraints it should be stated that the optimization problem is based on a curve (see Figure 4-16) that gives the dependency between the Q capabilities of the devices only for a capacitive power factor (0.85 to 1). In order to consider also the inductive power factor a new dependency curve is considered as shown in Figure 4-17.

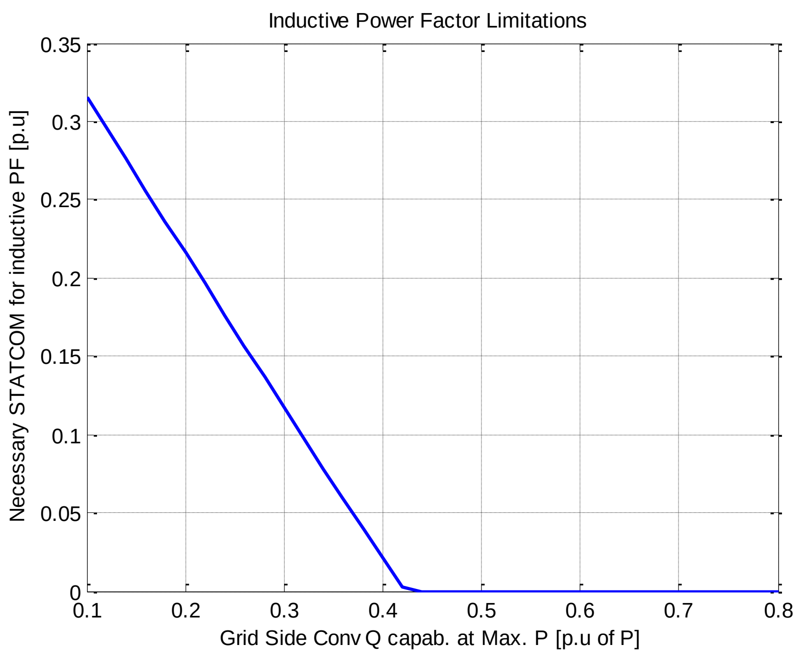

Figure 4-17 Inductive power factor limitations

As it can be seen in Figure 4-17**,** since the capacitor bank is not capable of consuming reactive power, through this new curve the necessary $Q_{STATCOM}$ and GSC are guaranteed in order to fulfill a lagging power factor of (0.9 1).

Step 5.2: Identification of Inequality Constraints

The first inequality constraint is based on Figure 4-17**:**

$$Q_{\min\_STATCOM} \leq Q_{STATCOM} \tag{4.8}$$

where $Q_{\min\_STATCOM}$ is the requested minimum $Q_{STATCOM}$ rating for a specified GSC in order to fulfill a lagging power factor of $[0.9 \quad 1]$.

Moreover, as presented in the beginning of this chapter a percentage of static and dynamic reactive power capability should be defined. Mainly this constraint should limit the optimal size of the capacitor banks. Without this constraint the optimal $Q_{cap.bank}$ would be higher since the capacitor banks have the lowest price. Imposing an equality constraint for the dynamic reactive power compensation ($Q_{STATCOM}$ + GSC) may lead to an unfeasible solution due to Equation(4.8). Therefore the following inequality constraint is defined:

$$0.3 \cdot (Q_{STATCOM} + Q_{cap.bank} + Q_{GSC}) \leq Q_{STATCOM} + Q_{GSC} \tag{4.9}$$

where $Q_{GSC} = \dfrac{100 \cdot GSC \cdot P_{WT\_rat}}{WF_{baseMVA}}$ is the sum of all the WTs grid side converters rated Q.

It should be stated that for this study case the inequality constraint (4.9) will always be fulfill through inequality constraint (4.8) however when lower inductive power factor are requested (e.g. 0.95) the above equation is requested in order to maintain a desired ration between dynamic and static reactive power compensation.

<u>Step 6: Initial Conditions</u>

Finally, for the initial guess a *flat start* was considered based on the following values:

$$x_0 = [Q_{STATCOM}, Q_{cap.bank}, GSC] \tag{4.10}$$

The optimal power flow algorithm presented above represents the base structure for the next two study cases as well. Applying the algorithm presented above, the following results were obtained:

$$x_{opt} = [0.12, 0.24, 0.3] \tag{4.11}$$

Considering the optimal GSC obtained and the ENTSOE grid code presented in Figure 1-5 the results obtained can be extended for different power factor ranges as shown in Figure 4-18. It can be observed that when the green envelope (power factor range) is reduced to a random ref envelope the necessary Q rating of the STATCOM and capacitor bank is reduced also.

b. <u>Optimization of Cap. Banks and WTs grid side converter Q capability</u>

For this second study case the STATCOM is not considered. Therefore based on the optimization algorithm used for the previous study case, additionally for *Step 5.1* only a new equality constraint was imposed:

$$Q_{STATCOM} = 0 \tag{4.12}$$

Further on the following results were obtained:

$$x_{opt} = [0.2, 0, 0.4] \tag{4.13}$$

Once again, based on ENTSOE grid code and the optimal GSC obtained the results were extended for different power factor ranges as shown in Figure 4-19. As it was expected the value of the capacitor bank Q capability is independent of inductive power factor range.

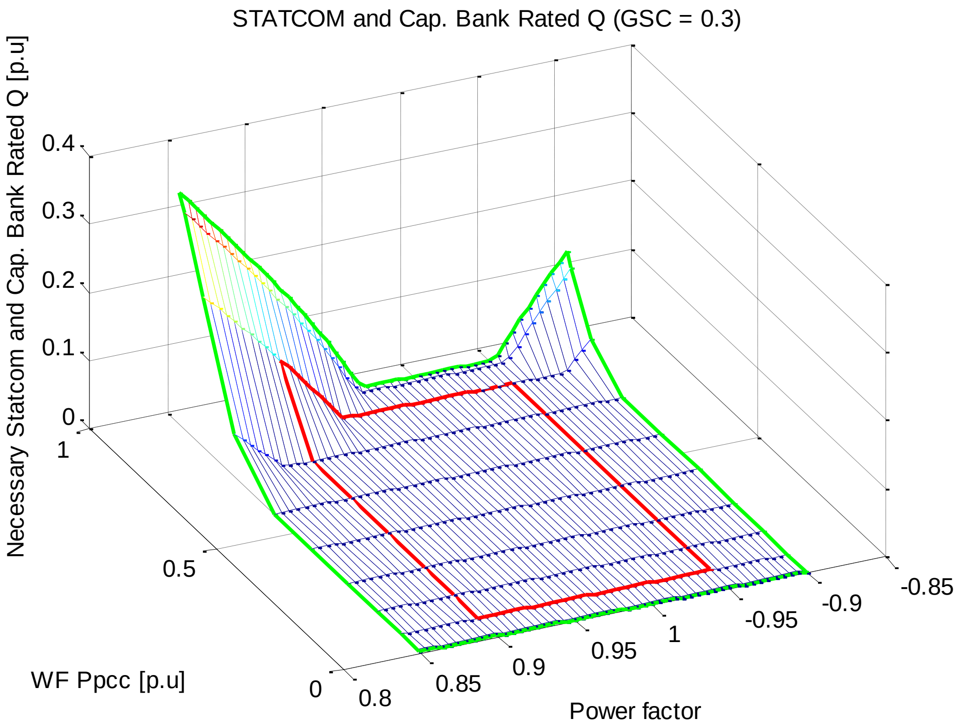

Figure 4-18 Necessary $Q_{ST.+Cap.Banks}$ for different Power factor ranges

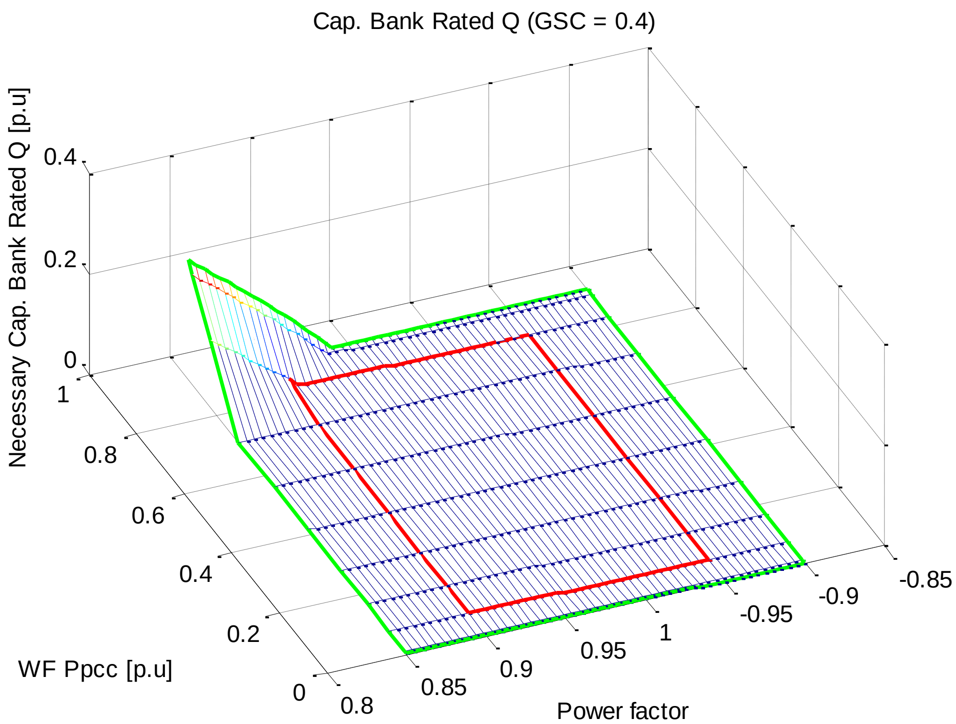

Figure 4-19 Necessary $Q_{Cap.Banks}$ for different Power factor ranges

c. Optimization of STATCOM and Cap. Banks Q capability for a GSC = 0.1

Finally, in the last study case the value of the GSC was considered fixed. Moreover in a similar manner the optimization algorithm will suffer a slight change at *Step 5.1* where:

$$GSC = 0.1 \tag{4.14}$$

is imposed as an equality constraint. Further on the following results were obtained:

$$x_{opt} = [0.27, 0.31, 0.1] \tag{4.15}$$

Once more the ENTSOE grid code from Figure 1-5 is transposed in a 3D plot where the z-axis is defined by the necessary $Q_{ST.+Cap.Banks}$ (see Figure 4-20).

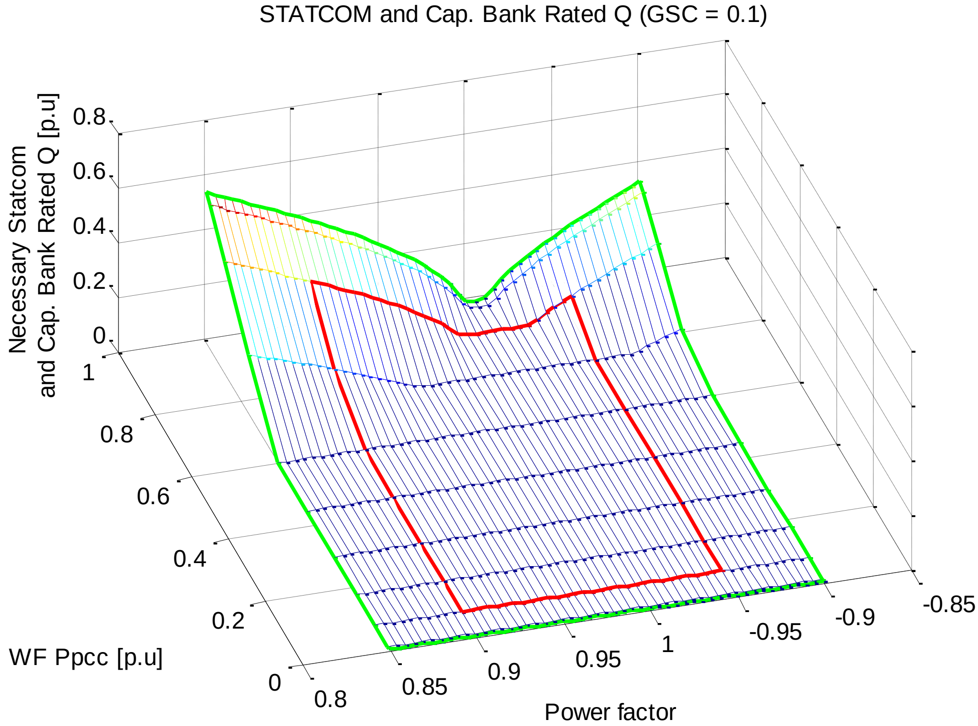

Figure 4-20 Necessary $Q_{ST.+Cap.Banks}$ for different Power factor ranges (GSC=0.1)

Analysis of Results

For a better examination of the results obtained in this second study case, the optimal values obtained for all three situations are summarize in the bellow table. It is worth mentioning that, while GSC represents the upper point in Figure 2-7 (e.g. $0.1 \cdot P$), Q_{GSC} defines the total reactive power capability of all the WT's grid side converter.

Table 4-1 Results

	$Q_{STATCOM}$ p.u	$Q_{cap.bank}$ p.u	GSC	Q_{GSC} p.u
Study Case 1	0.12	0.24	0.3	0.29
Study Case 2	0	0.2	0.4	0.44
Study Case 3	0.31	0.27	0.1	0.09

It can be concluded that the second and third study case are just some particular cases of the first study case. Therefore the next question arises when analyzing the results:

Why is the first Study Case the optimal solution for our WF?

When the first study case is compared with the second one the first impression is that latest one is more convenient since the total rated Q required (0.64 p.u.) is lower in comparison with the first study case (0.65 p.u.). Moreover the STATCOM is missing and the capacitor banks are smaller therefore a significant reduction in cost is achieved for the second study case. However the main difference between the first two study cases is given by the WTs grid side converters price. Not only is the difference of price for the power converters in favor of the first study case but also the changes regarding the power cables in the WF. For a WF row seven cable segments divided in 3 categories were used. For the second study, due to the increase of GSC reactive power capability some cables suffered an increase in diameter and therefore an increase in price. It can be concluded that the increased price of WT's power converters and cables is higher than the reduction in price for the omission of the STATCOM and therefore the first study case remains the optimal one.

Moreover when the third study case is compared with the first one, even if there is a difference in WTS grid side Q rating capability between them, the power cables inside the WF will not change. Thus it can be concluded that the increased price of the STATCOM and capacitor bank is higher in comparison with the reduction in costs obtained due to lower WT's grid side converter.

Finally, for the results obtained in the first study case the following explanations are highlighted. If no constraints were imposed in the optimization algorithm, for the optimal solution the entire necessary reactive power would be given by the capacitor banks because they are the cheapest one. However, due to inequality constraint (4.8) the capacitor banks are decreased at 0.24 p.u. For this value the corresponding sum of Q capability of STATCOM and GSC is almost 0.41 p.u. Moreover, this value is divided between STATCOM and GSC. The optimization algorithm will always try to impose a higher Q capability to the GSC since it is less expensive. Anyway this optimal reference for GSC Q capability is limited also by the cable prices. Therefore, for the first study case, the optimal GSC is 0.3 because this is the highest value for which the WF cable configuration remains unchanged.

Chapter 5 Optimal Power Flow

The purpose of this chapter is to evaluate the performance of the developed WF Controller on different control modes and objectives. In the first part of the chapter validation of the optimal dispatch is presented followed by the comparison between the conventional and optimal power flow. Finally the behavior of the controller is analyzed when a real wind profile is imposed and the lifetime optimization criterion of the WF is considered.

5.1 Optimal Power Flow for one wind sample

The aim of this section is to validate the optimal dispatch of the WF references on different control modes requested by the TSO, when only one wind sample is considered. This section is divided in three parts corresponding to each control mode.

A1. Normal mode with wake effect activated

Before presenting the results of this study case, the simulation conditions have to be mentioned. In Normal Control mode the WT should produce the maximum *P* available from the wind (see Figure 2-9) and the desired *Q* calculated based on TSO PF request in PCC. The wind speed had a value of *14m*/s and the selected wind direction was North. For this case the wake effect was also considered, which means that the wind speed was decreased with *2%* after each WF row. Aiming to have a more realistic distribution of the wind, a small deviation of ± *0.1m/s* was introduced. Therefore, the WTs of each row received slightly different values of wind speed. The Power Factor for this case was set to *0.95*.

The *Optimization Problem* of this study case is similar with the one presented in Chapter 3.3.2 but with some adjustments. For the considered case the following *Objective Function* was utilized:

$$\min f(x) = \left|Q_{dem} + Q_{203}\right| \tag{5.1}$$

From the above equation it can be observed that the WF Controller will provide an optimal dispatch only for the WTs *Q* references, due to the fact that in this Control Mode the WTs *P* references are equal with their maximum capability. Therefore in order to impose this condition to the WF Controller an extra *Equality Constraint* (see Equation(5.2)) was added at the *Optimization Problem*.

$$P_{bus\_i} = P_{\max WT\_j} \text{ for } i = \overline{1,3:199} \text{ and } j = \overline{1:100} \tag{5.2}$$

The results of the optimal dispatch are presented in Figure 5-1. This figure depicts only the results for the 1st, 2nd and last WT of the first two feeders.

From the bellow figure it can be observed that, since the WF Controller is operating in Normal Mode the WTs references in *P* are equal with their maximum capability. Therefore the optimal dispatch can be noticed only in WTs *Q* references.

Analyzing the first feeder it can be seen that the references are dispatched based on the location of the WT. Therefore, the farthest WT will receive the lower reference due to power losses and the nearest WT will receive the highest reference. Following the same principle it can be observed, by comparing the references received by WTs from different feeders, that the WTs belonging to the second feeder have higher references since it is closer to the WF PCC.

Since the wake effect was activated, the results of the optimal dispatch are doubtful. The dispatch of the WTs Q references could be also explained based on the Q capability of each WT. The farthest WTs received the highest wind speed; therefore it had the lower Q capability and consequently received the lower Q reference. To remove all the doubts the Normal Control Mode case was repeated and the wake effect was deactivated.

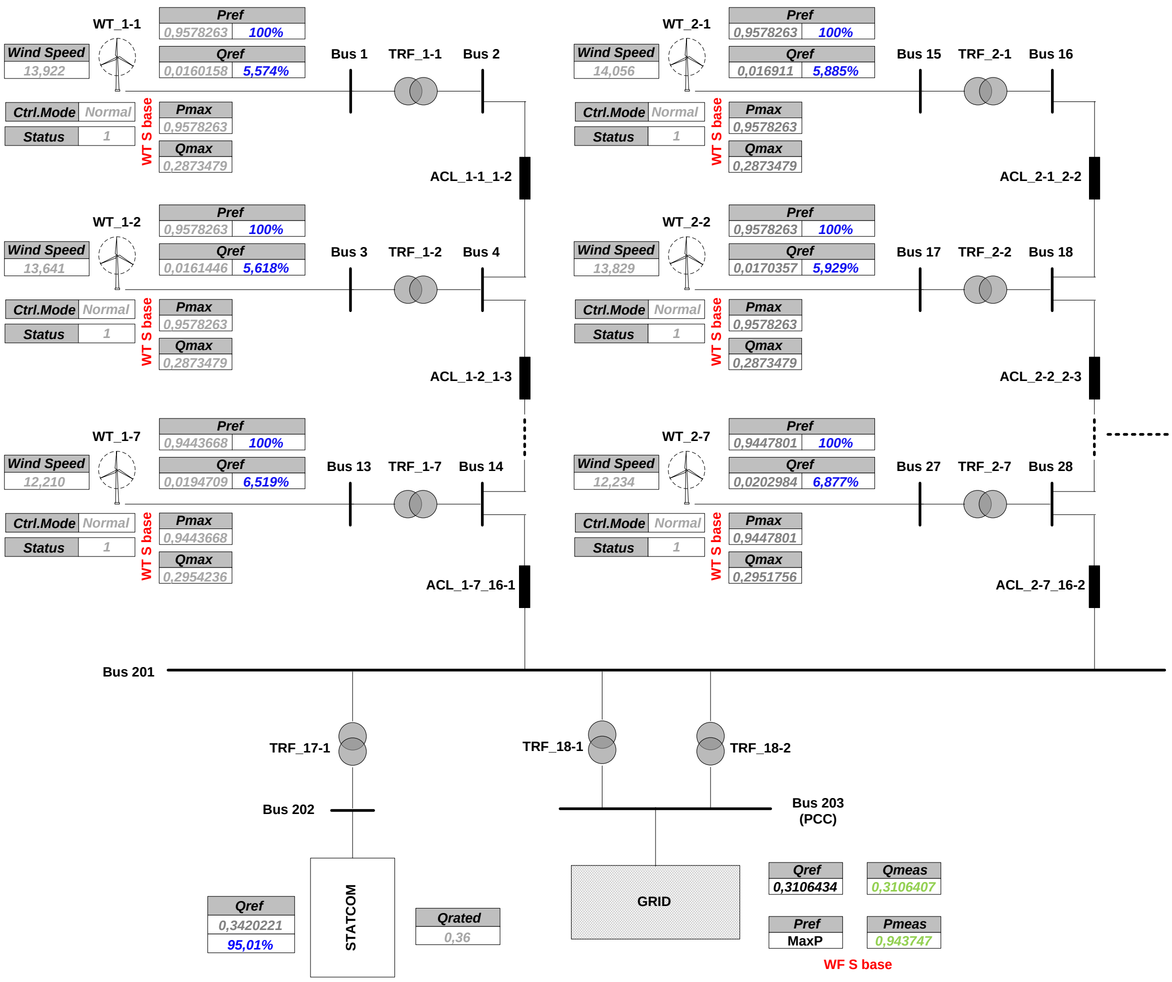

Figure 5-1 Optimal dispatch in Normal Control Mode with wake effect

A2. Normal mode without wake effect

The simulation condition of this study case, were the same with the ones used in study case A1. It had to be mentioned that in this case the wake effect was deactivated; therefore all the WTs received the same wind speed of *14m/s*.

From the results presented in Figure 5-2, it can be noticed that the WT *P* references are unchanged compared with the previous case (equal with the maximum WTs *P* capability). It can also be observed that the WTs *Q* references respect the same principle, the farthest WT will receive the lower reference and the nearest WT will receive the highest reference, even if all the WTs had the same *Q* capability. Therefore, it can be concluded that the results present in Figure 5-2 confirmed that the WTs *Q* references were the results of the optimal dispatch.

The results presented in case A1 and A2 validates that the proposed WF Controller is capable of realizing the optimal dispatch in Normal Control Mode.

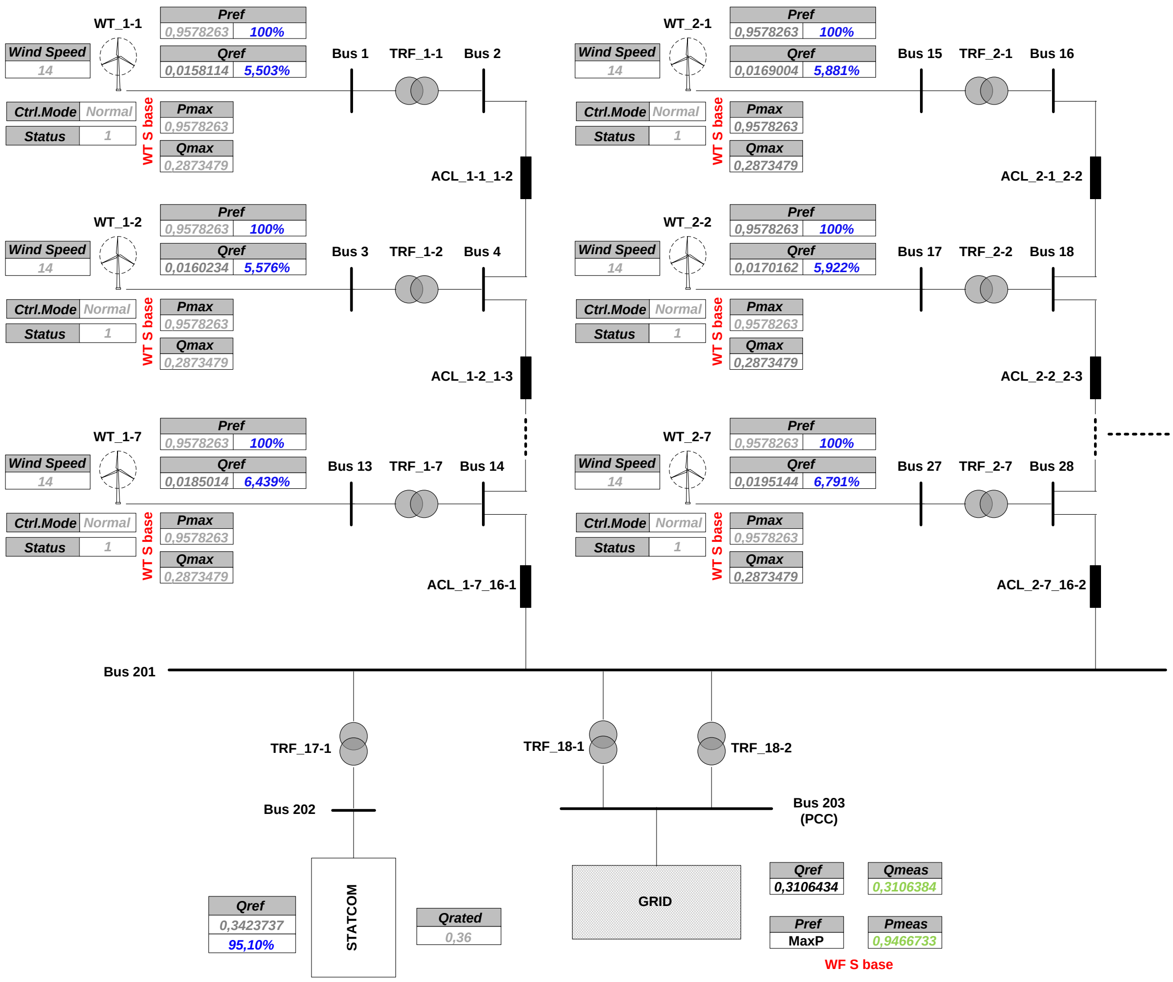

Figure 5-2 Optimal dispatch in Normal Control Mode without wake effect

B. *Delta Control Mode*

For this study case the WF Controller was operating in Delta Control Mode at a delta value of *0.5* imposed by the TSO. This means that the TSO requested to the WF to assure a power reserve of *50%*. The simulation conditions were the same as in the previous cases, with the mention that the wake effect was deactivated.

For this study case the *Optimization Problem* is similar with the one presented in the previous cases but with a new *Objective Function* (see Equation(5.3)).

$$\min f(x) = \left|P_{dem} + P_{203}\right| + \left|Q_{dem} + Q_{203}\right| \tag{5.3}$$

From the above equation it can be observed, that compared with previous case, the WF Controller will provide an optimal dispatch not only for the WTs Q references but also for the WTs P references. In the Delta Control Mode P_{dem} is defined according to the following equation:

$$P_{dem} = \delta \cdot P_{\exp} \tag{5.4}$$

where, $P_{\exp}$ is the estimated value of the P in PCC if the Normal Control Mode was active.

From the results presented in Figure 5-3 it can be observed that the *delta* coefficient decrease from the farthest WT to the nearest one. This means that the farthest WT, due its higher power losses, needs a higher *delta* in order to assure the requested power reserve of *50%* from its capability in PCC.

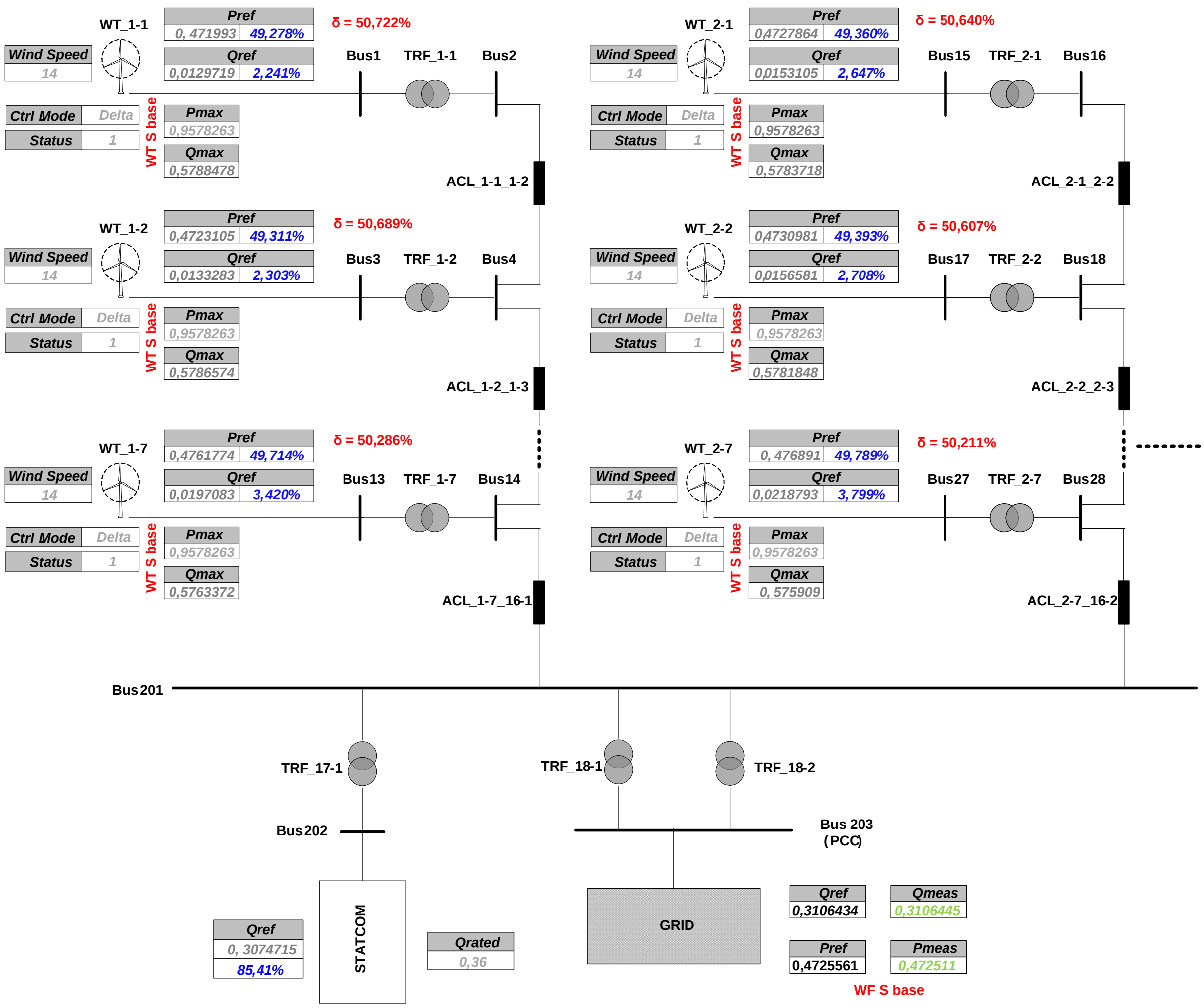

Figure 5-3 Optimal dispatch in Delta Control Mode

C. *Balance Control Mode*

In this Control mode the operator asks the WF Controller to decrease or increase the production at specific levels (see Figure 3-2). For this case the simulation condition was the same as in the previous case and the TSO requested to decrease the WF production at *0.75 p.u.* from its capability.

The *Optimization Problem* for this study case is similar with the one presented in case B, with the mention that for the Balance Control Mode P_{dem} has a fixed value (e.g. 0.75 for the actual study case).

It can be noticed from the results depicted in Figure 5-4 that *P* and *Q* WTs references are optimal dispatched, since the farthest WT received the lowest reference, while the power limit imposed by the TSO in the PCC was fulfilled.

Another fact that can be remarked from the presented study cases refers to *Q* dispatch between the WTs and the STATCOM. Even if the WTs had high *Q* capability the WF Controller the biggest part of the total *Q* demanded in PCC is provided by the STATCOM.

The general conclusion that can be drawn from the presented study cases is that the proposed WF Controller is capable to realize the optimal dispatch of the WTs references for all the demanded control modes.

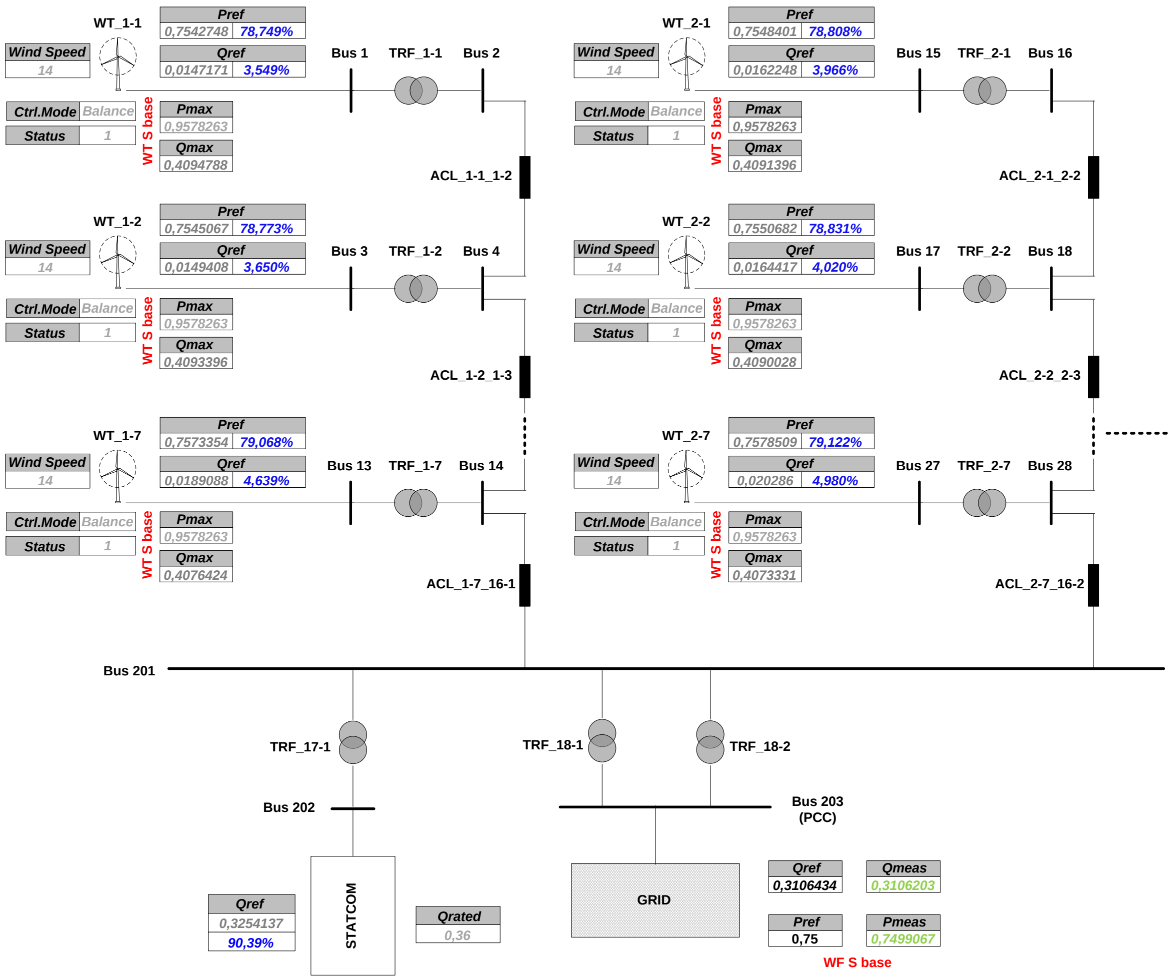

Figure 5-4 Optimal dispatch in Balance Control Mode

5.2 Comparison between Optimal Power Flow and Normal Power Flow

In this sub-chapter the advantages of optimal dispatch for WT's references are presented during Normal WF control mode and Delta WF control mode. Further on the principle of implementing both power flow methods is described.

Conventional Power Flow

For the Conventional Power Flow, first the demanded active (P_{dem}) and reactive power (Q_{dem}) in the WF PCC are defined. Based on these references, the references in active and reactive power for each WT are calculated as follows:

$$P_{ref\_WTj} = \frac{P_{dem}}{N_{WTs}} \tag{5.5}$$

$$Q_{ref\_WTj} = \frac{Q_{dem} - Q_{ST+Cap.Banks}}{N_{WTs}} \tag{5.6}$$

where N_{WTs} is the number of WTs in the WF, and $Q_{ST+Cap.Banks}$ is the Q capability of STATCOM and Capacitor Banks.

Taking into consideration that the wake effect is not activated it can be said that Equation (5.5) is the same with first Equation in (3.1) (the same analogy can be made with Equations (5.6) and the second Equation in (3.1)). However, for the normal power flow proposed in this Chapter the STATCOM and Capacitor Bank were considered in the WF PCC. Therefore as it can be seen in Equation (5.6) for Conventional Power Flow both STATCOM and Capacitor Bank will receive maximum reference (100% of their Q capability). Different study cases when $Q_{ST+Cap.Banks}$ is receiving 75%, 50%, 25% of their Q capability are proposed for Further Work.

Moreover, in the next step of the Conventional Power Flow Algorithm the references presented above are imposed at each WT bus bar. Afterward the active and reactive power in the WF PCC were found: P_{PPC_normal} and Q_{PCC_normal}. As expected, the measured powers in the WF PCC were lower due to power losses inside the WF grid. Consequently for the Optimal Power Flow the demanded active and reactive power in the WF PCC are given by the P_{PPC_normal} and Q_{PCC_normal} instead of P_{dem} and Q_{dem}.

The Conventional Power Flow algorithm is mainly based on the power flow algorithm presented in Chapter 3.3.2. Changing the optimal power flow algorithm into a normal one the following changes were considered:

- for the design variables only the state variables (voltage angle V_{ang_j} and magnitude V_{mag_j} for each bus bar) were considered. Therefore the design variable vector was defined as: $x_{opt} = [V_{mag\_j}, V_{ang\_j}]$ where $j = \overline{1:203}$.
- since there is no active and reactive power demand in the WF PCC the objective function was: $\min f(x) = 0$.
- for the equality constraints the following ones were added:

$$\begin{cases} P_{bus\_i} = P_{ref\_WTj} \\ Q_{bus\_i} = Q_{ref\_WTj} \end{cases} \text{for } i = \overline{1,3:199} \text{ and } j = \overline{1:100} \tag{5.7}$$

where P_{ref_WTj} and Q_{ref_WTj} are the ones presented in Equations (5.5) and (5.6).

- finally, since 100% reference for STATCOM and Capacitor Banks were considered, the following equality constraint was defined:

$$P_{bus\_202} = Q_{ST+Cap.Banks} \tag{5.8}$$

<u>*Optimal Power Flow*</u>

The Optimal Power Flow algorithm is identically with the power flow algorithm presented in Chapter 3.3.2. It should be stated that P_{dem} and Q_{dem} in Equation (3.6) are P_{PPC_normal} and Q_{PCC_normal} from the Normal Power Flow. Through this condition the measured powers in the WF PCC are identically for both Conventional and Optimal Power Flow. As a result, for the same active and reactive power in PCC two different sets of P and Q references for WTs, STATCOM and Capacitor Banks were obtained. Thus a comparison between Normal and Optimal Power Flow is suitable for defining the advantages of WTs reference optimal dispatch.

5.2.1 Power Losses Improvement for Normal WF Control Mode

For Normal WF Control Mode maximum active power is delivered in WF PCC therefore only the optimal dispatch for Q references is influencing the power losses improvement. Moreover in Figure 5-5, the active and reactive power improvement is plotted. In the first 2 sub-plots the active and reactive power losses are presented for both study cases. Next the power losses improvement is presented in p.u. (middle sub-plot) and percentage (bottom sub-plot). It can be concluded from this figure that the power losses improvement due to optimal dispatch is dependent on the average wind speed.

$$\begin{cases} P_{losses\_imp} = f(wind) \\ Q_{losses\_imp} = f(wind) \end{cases} \tag{5.9}$$

As it can be seen, for both active and reactive power, the lower the wind goes the higher the improvement become.

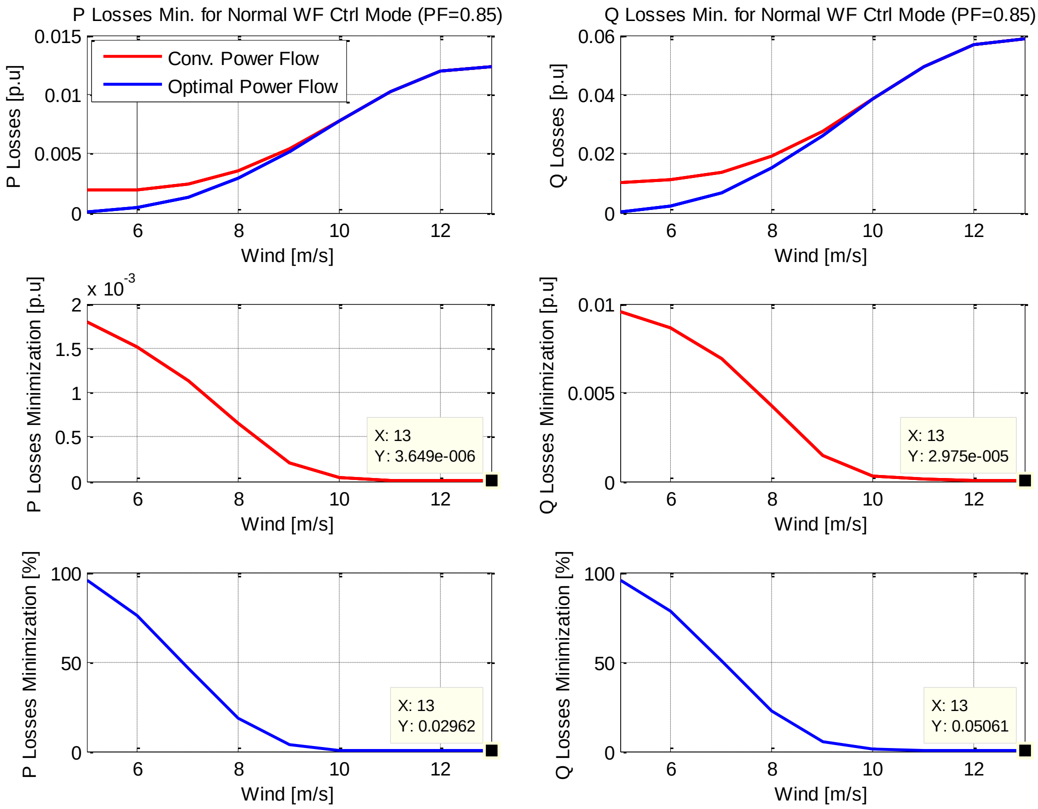

Figure 5-5 Power Losses for Normal WF Control Mode and PF = 0.85

In Figure 5-5 a power factor of 0.85 was requested by TSO in the WF PCC. Moreover the PF is increased to 0.93 and it can be observed from Figure 5-6 that for different power factor different power losses improvement is achieved..

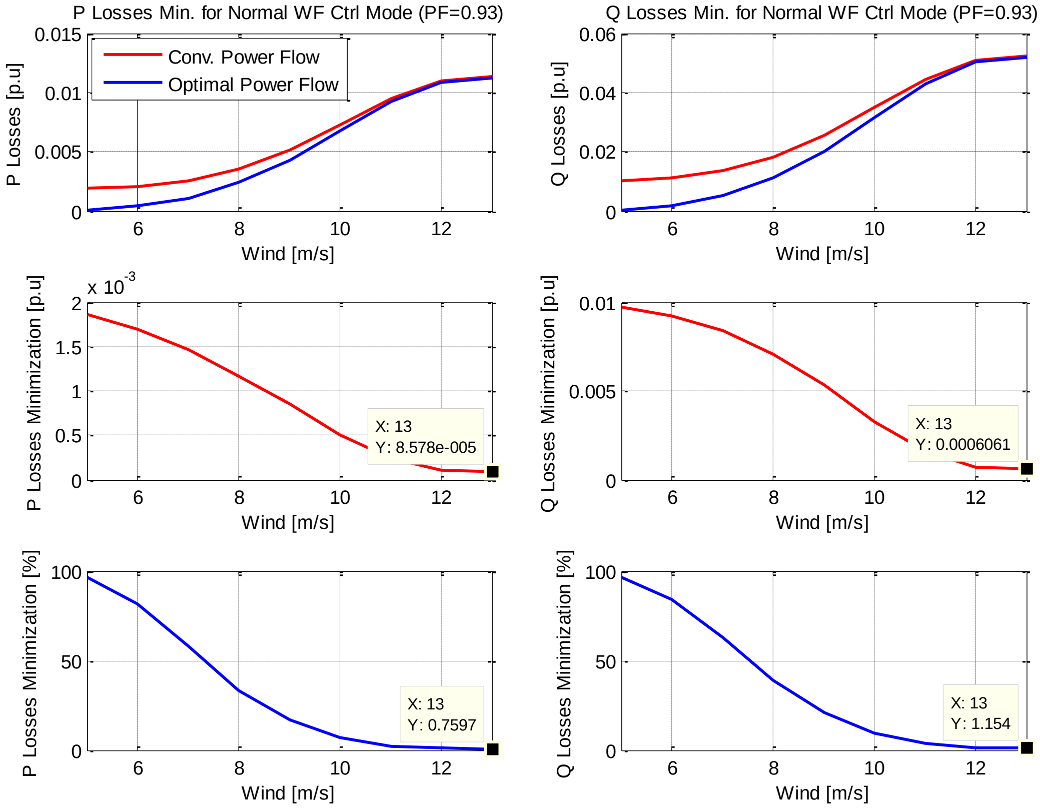

Figure 5-6 Power Losses for Normal WF Control Mode and PF = 0.93

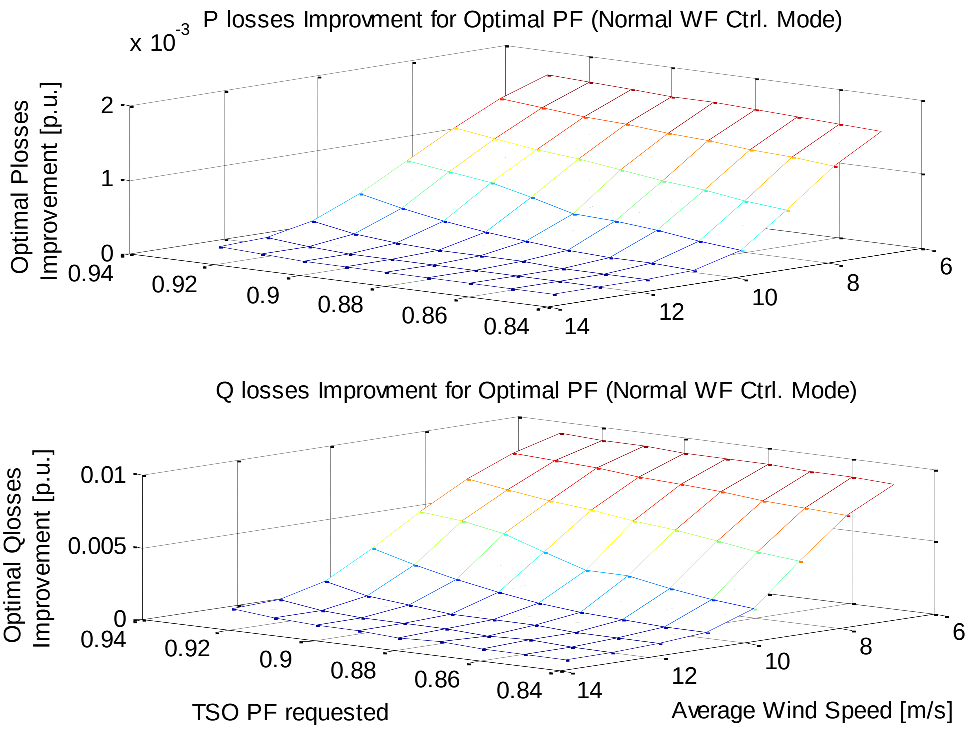

Figure 5-7 Overall Power Losses Improvement for Normal WF Control Mode

When the power factor increases the active and reactive power losses improvement increases as well (both percentage and p.u values). As a consequence, since the power losses is dependent of the PF requested, Equation (5.9) is updated as follows:

$$\begin{cases} P_{losses\_imp} = f(wind, PF) \\ Q_{losses\_imp} = f(wind, PF) \end{cases} \tag{5.10}$$

Finally, based on Equation (5.10) the power losses improvement as a function of wind speed and power factor is presented in a 3d plot in Figure 5-7. As expected, the higher losses improvement is achieved for the lowest wind speed and the highest power factor

5.2.2 Power Losses Improvement for Delta WF Control Mode

For Delta Control Mode, optimal dispatch is valid for both active and reactive power. Therefore, higher power losses improvements are expected for this study case in comparison with the previous one.

In Figure 5-8 power losses improvements are plotted for a delta imposed of 90%. Moreover in Figure 5-9 for a delta of 60% different results are obtained for both active and reactive power. As it can be seen, for lower delta higher losses improvement is achieved thus a new variable is added to Equation(5.10):

$$\begin{cases} P_{losses\_imp} = f(wind, PF, \delta) \\ Q_{losses\_imp} = f(wind, PF, \delta) \end{cases} \tag{5.11}$$

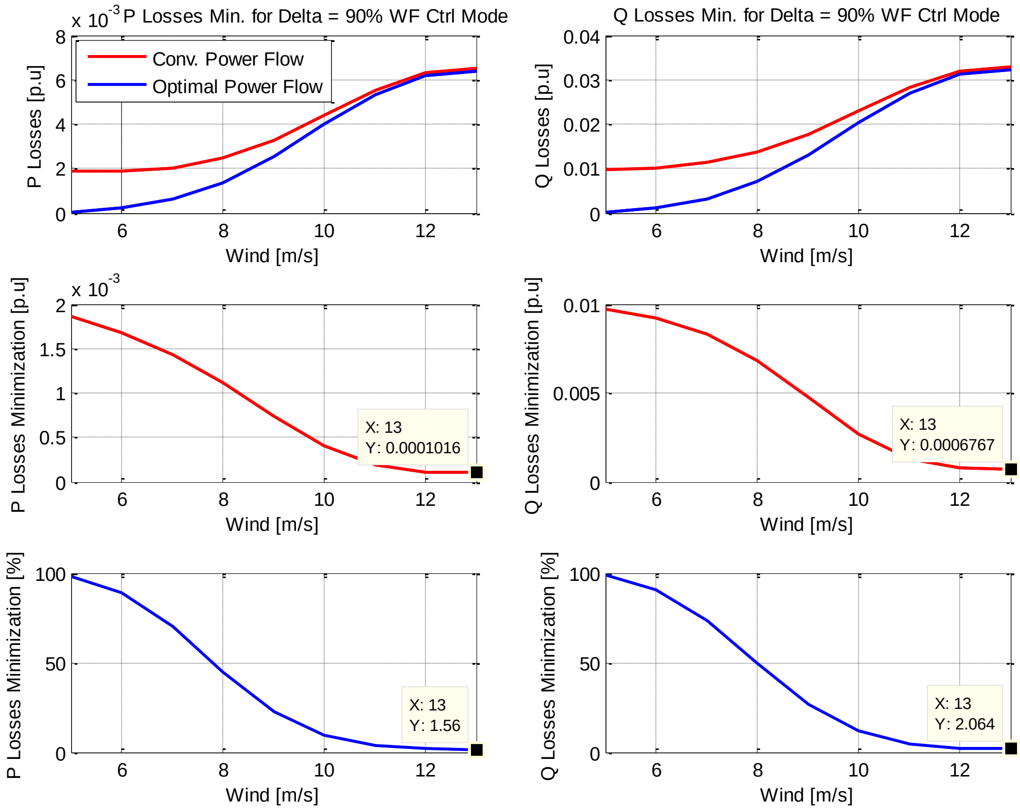

Figure 5-8 Power Losses for Delta = 90% WF Control Mode

In Figure 5-8 and Figure 5-9 the power factor considered was 0.85. Comparing the results of any of these two figures with Figure 5-5 where the power factor considered was also 0.85the following conclusions are highlighted:

- the power losses in Figure 5-8 and Figure 5-9 are lower in comparison with Figure 5-5 because the active and reactive powers requested by the TSO are lower;

- as expected due to the optimal dispatch of active power references the power losses improvements in Figure 5-8 and Figure 5-9 are significantly high in comparison with Figure 5-5;

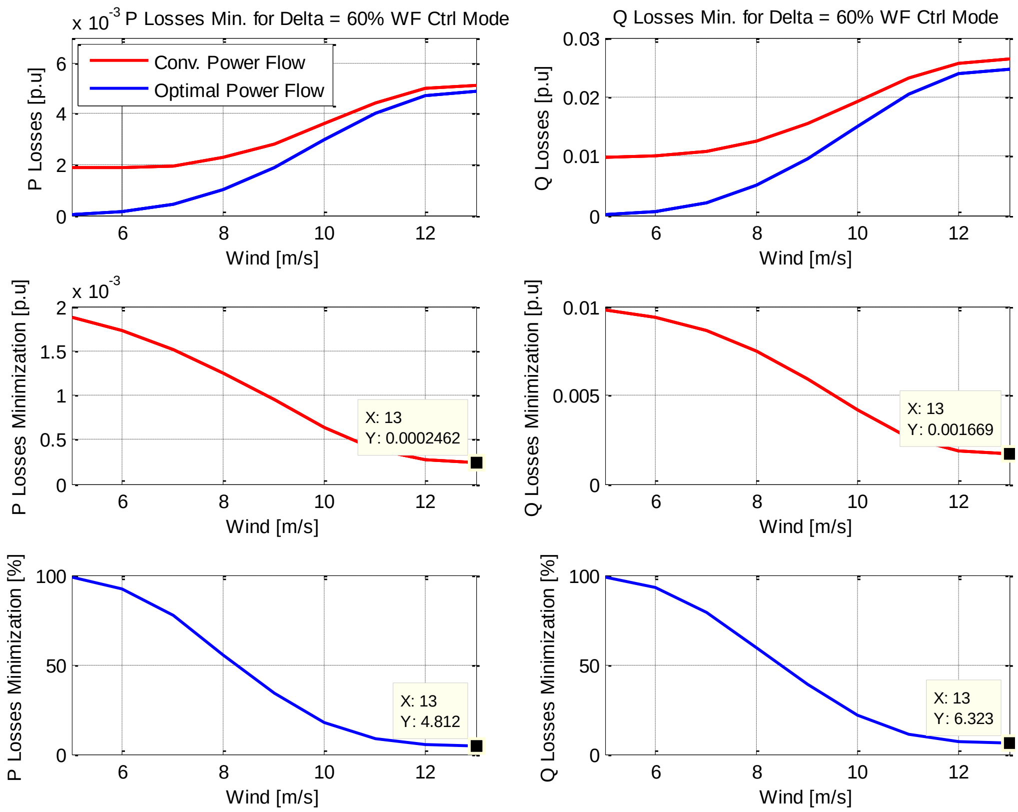

Figure 5-9 Power Losses for Delta = 60% WF Control Mode

Finally, based on Equation (5.11) the power losses improvement as a function of delta and power factor imposed by TSO is presented in a 3d plot in Figure 5-10. The average wind speed considered was 10 m/s. As expected, the higher losses improvement is achieved for the highest power factor and the lowest delta. Moreover the same results are plotted in percentage in Figure 5-11.

Analysis of Results

As concluded in Equation (5.11) both active and reactive power losses improvement is dependent on: average wind speed, power factor and delta. However this dependence can be simplified to active and reactive power requested by TSO in WF PCC. While the wind speed and delta have an effect over the active power demand, the power factor influences the reactive power demand. Therefore Equation (5.11) can be expressed as:

$$\begin{cases} P_{losses\_imp} = f(P_{dem}, Q_{dem}) \\ Q_{losses\_imp} = f(P_{dem}, Q_{dem}) \end{cases} \tag{5.12}$$

Reanalyzing the results obtained, it can be concluded that for a lower reference in active and reactive power a higher improvement in power losses will occur.

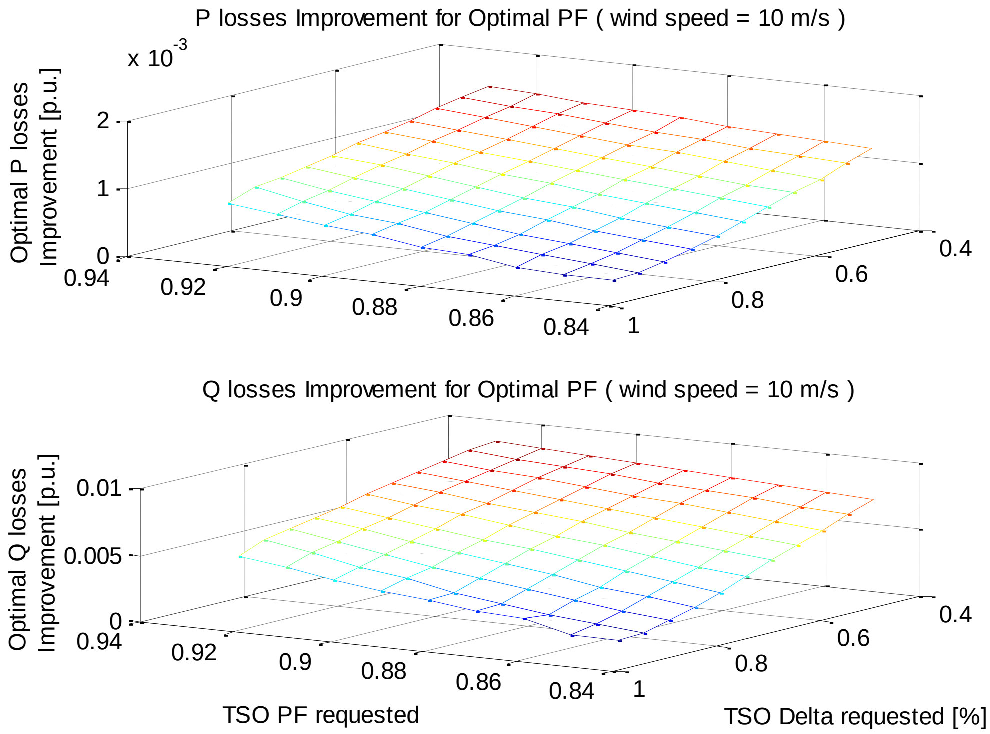

Figure 5-10 Overall p.u. Power Losses Improvement for Delta WF Control Mode

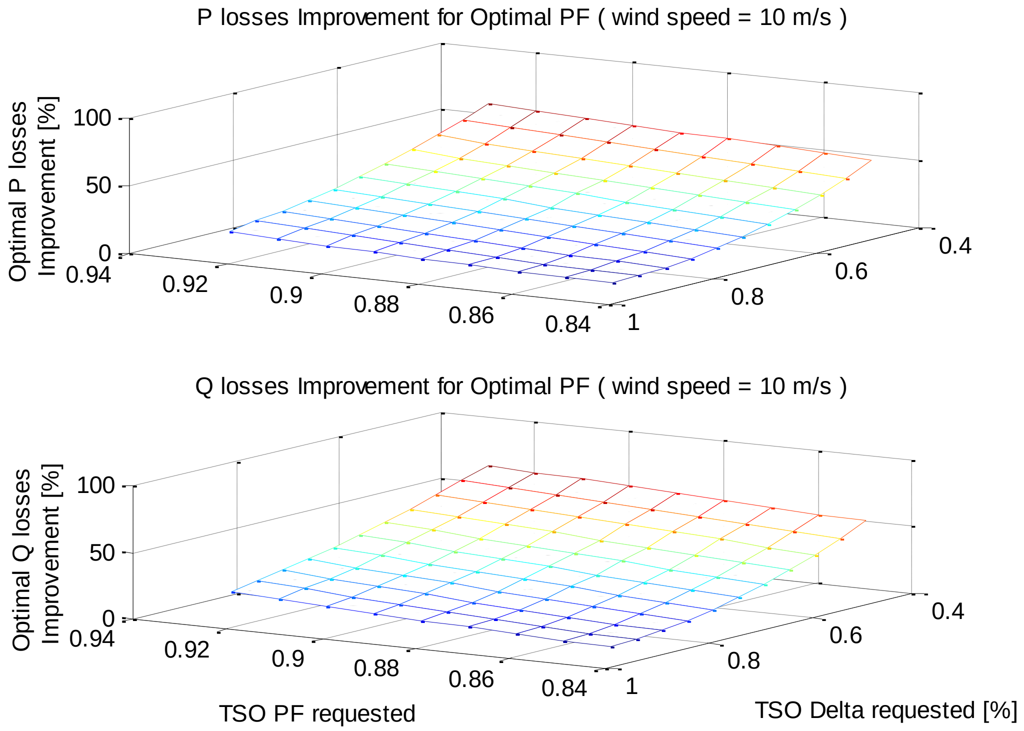

Figure 5-11 Overall Percentage Power Losses Improvement for Delta WF Control Mode

5.2.3 Life Time Power Losses Analysis

This study case was carried out with the intention of presenting the advantages of the optimal power flow over the conventional power flow during a period of 1 year. For the calculation of the energy production a real wind profile was considered, with the wind data's assumed in Figure 5-12 (first sub-plot). Moreover, for the power factor profile, a variation at every 2 hours was considered.

For this study case the following assumptions were considered:

- during the entire period of time, the WF works only in Normal control mode;
- for the power factor profile, a range of 0.85 to 1 was considered. It should be stated that the simulations are made only for capacitive power factor;
- no maintenance profile were considered thus all the WTs were functional;
- wake effect was disabled;
- WF lifetime was considered 20 years;

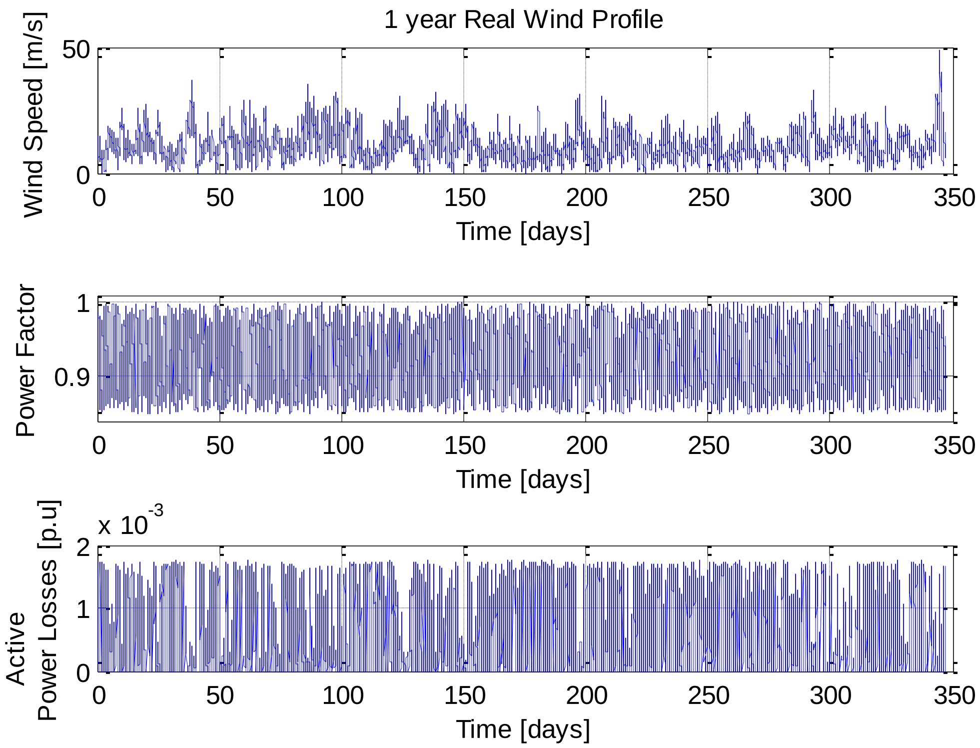

Figure 5-12 Active Power Losses Improvement over 1 year

For each wind sample in Figure 5-12 for the specified power factor requested by TSO a interpolation was realized based on a simillar plot with the one presented in Figure 5-7. If the wind speed was bellow the cut-in speed or above the cut-out speed the losses improvement was considered 0. For a fixed price of 50 €/MWh the results in active power improvement from a financial point of view were around 1 million of € per year.

5.3 Optimal Power Flow for a real wind profile

The previous study cases proved that the WF Controller is capable to operate under different control modes for only one wind sample. Therefore the aim of this study case is to validate the capability of the WF Controller when a real wind profile is considered.

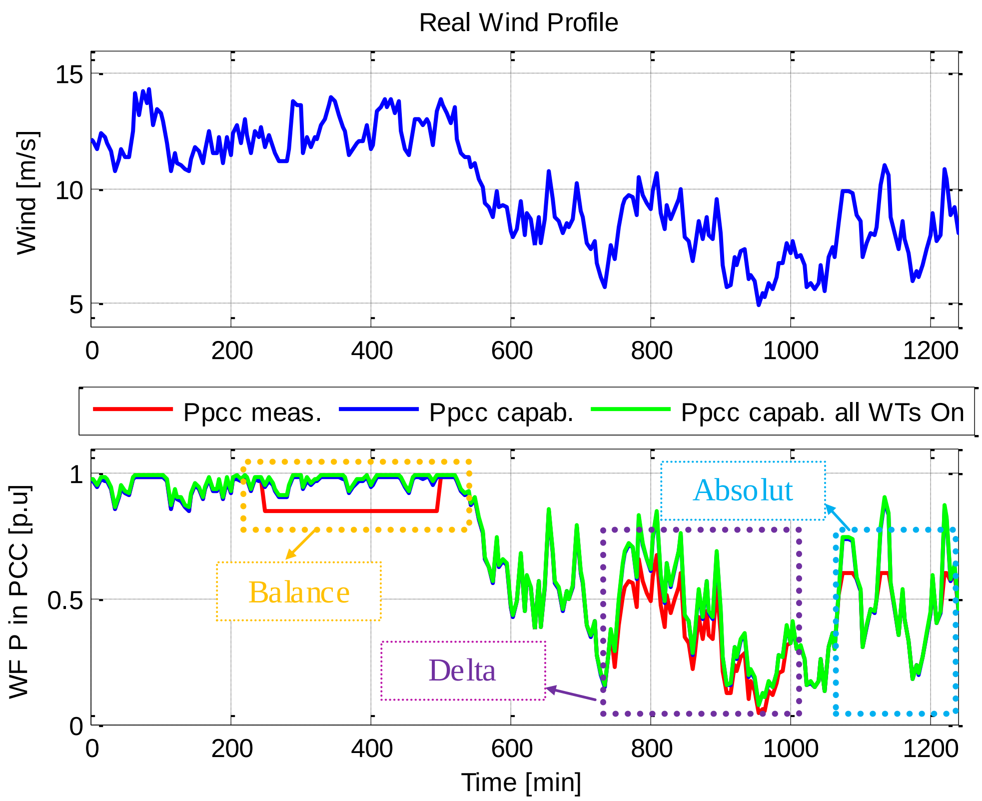

Figure 5-13 Real wind profile and various control modes

The first graph presented in Figure 5-13 depicts the real wind profile for a certain period of time. Based on this wind profile different control modes were scheduled, as it can be observed from the second graph of the same figure. The behavior of the WF Controller during each considered control mode is presented in the next figures.

From Figure 5-14 it can be observed that the WF is operating in Balance Control Mode and is capable to maintain the imposed power level of *0.85 p.u.* Another fact that has to be mentioned is that one WT is in *maintenance*, and this can be noticed from the power difference between the actual WF $P_{capability}$ and the expected WF $P_{capability}$ when all the WTs are running.

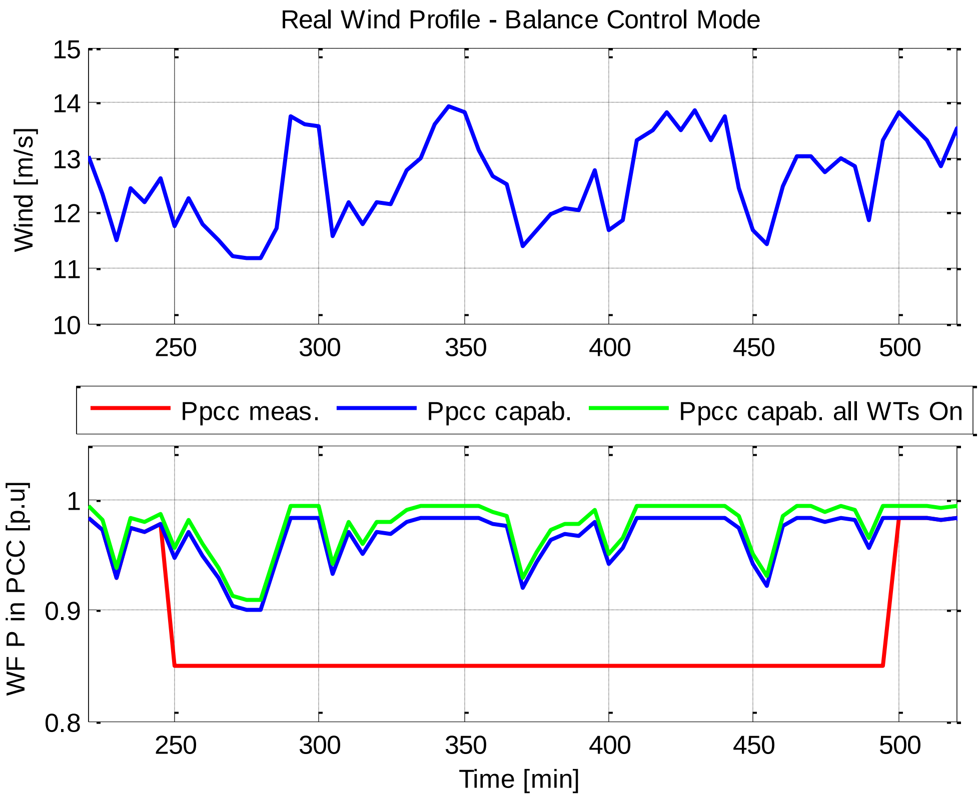

Figure 5-14 Balance Control Mode during a Real wind profile

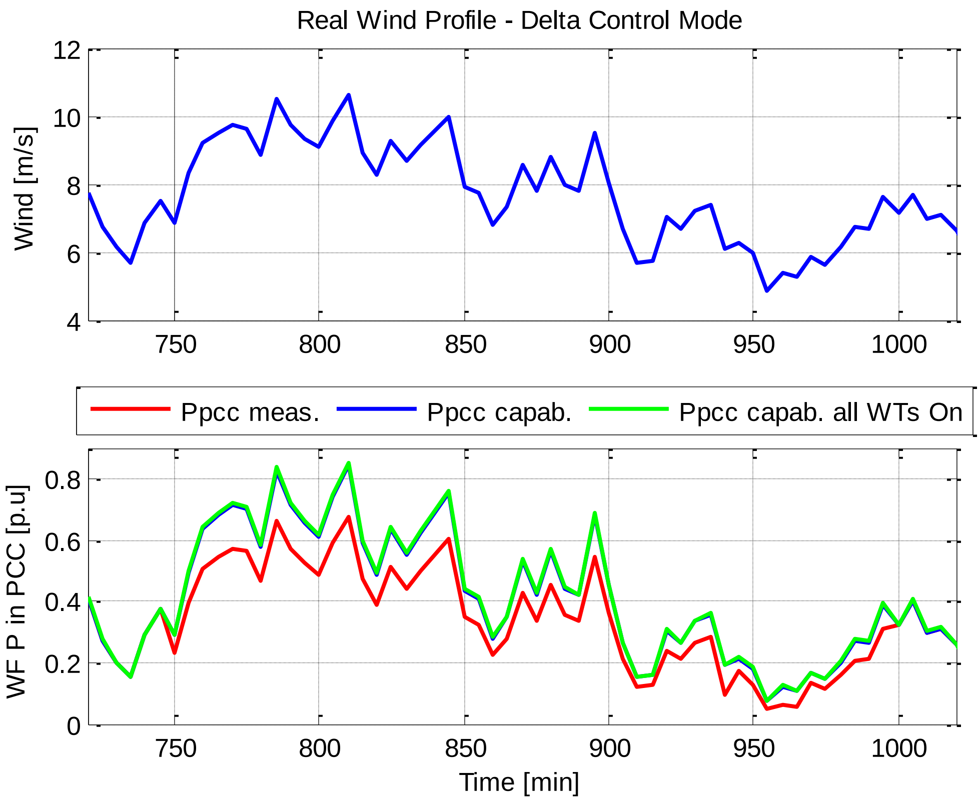

Figure 5-15 Delta Control Mode during a Real wind profile

In Figure 5-15 is presented the behavior of the WF when a Delta Control Mode with a *delta* value of *0.8* is requested.

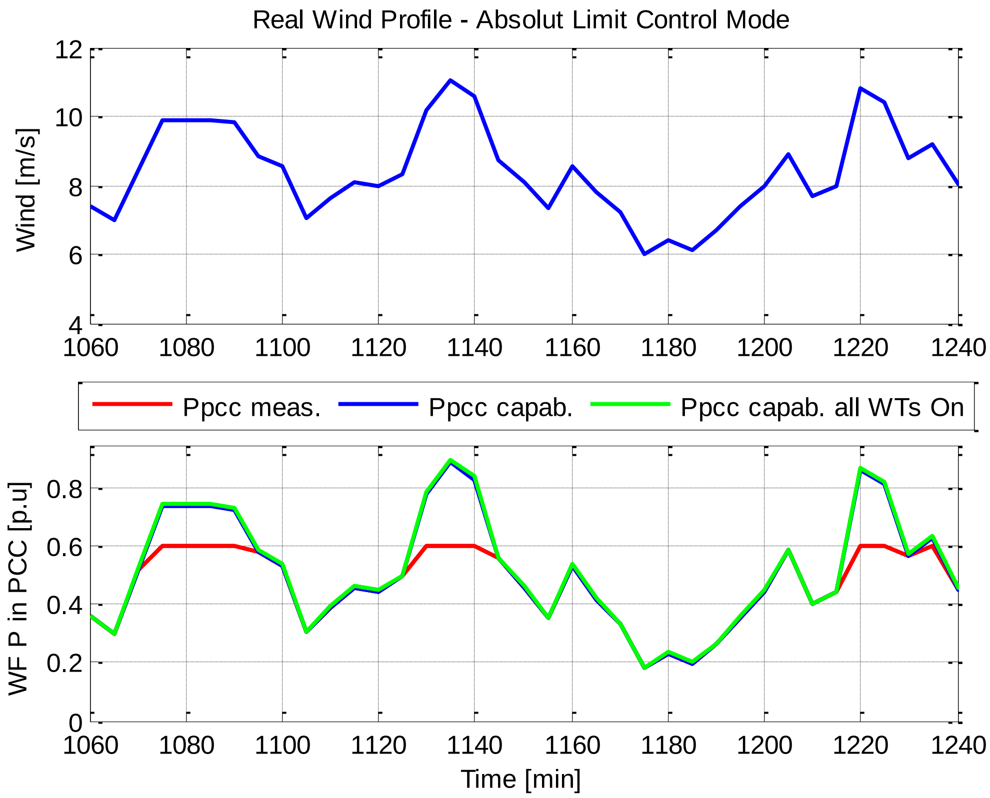

Figure 5-16 Absolute Limit Control Mode during a Real wind profile

The behavior of the WF during the Absolute Limit Control Mode is presented in Figure 5-16. From this figure it can be observed that when this control mode is imposed the WF behaves like in the Normal Control Mode, until the power upper limit of *0.6* is reached.

An observation that can be made based on the above figures is that the *P* profile follows the profile of the wind. The general conclusion that can be drawn from this study case is that the WF Controller can operate under different control modes with a real wind profile.

5.4 Optimal Power Flow with life time optimization

The purpose of this study case is to validate that the WF Controller can realize the Optimal Power Flow when different scenarios, that could improve the WF life time, are considered. Different cases were analyzed in this section: maintenance considerations, static coefficient for each row and WTs shut down.

A. Lifetime optimization through Maintenance considerations

For this study case it was verified if the WF Controller can realizes an OPF considering the maintenance periods of the WTs. The study case was carried out based on the following principle: if the maintenance period of a WT approaches, this WT should operate at its maximum capability during Balance or Delta mode. Therefore if something goes wrong with the respective WT, it will go into maintenance anyway.

The procedure utilized in this case was as follows:

- the number of WTs to be considered was defined (e.g. 10);
- the scheduled maintenance was examined;
- for the first 10 WTs with the closest maintenance *P* and *Q* references were maximized;

For this study case the WF was operating in Balance Control Mode and the results of the simulation are presented in Figure 5-17.

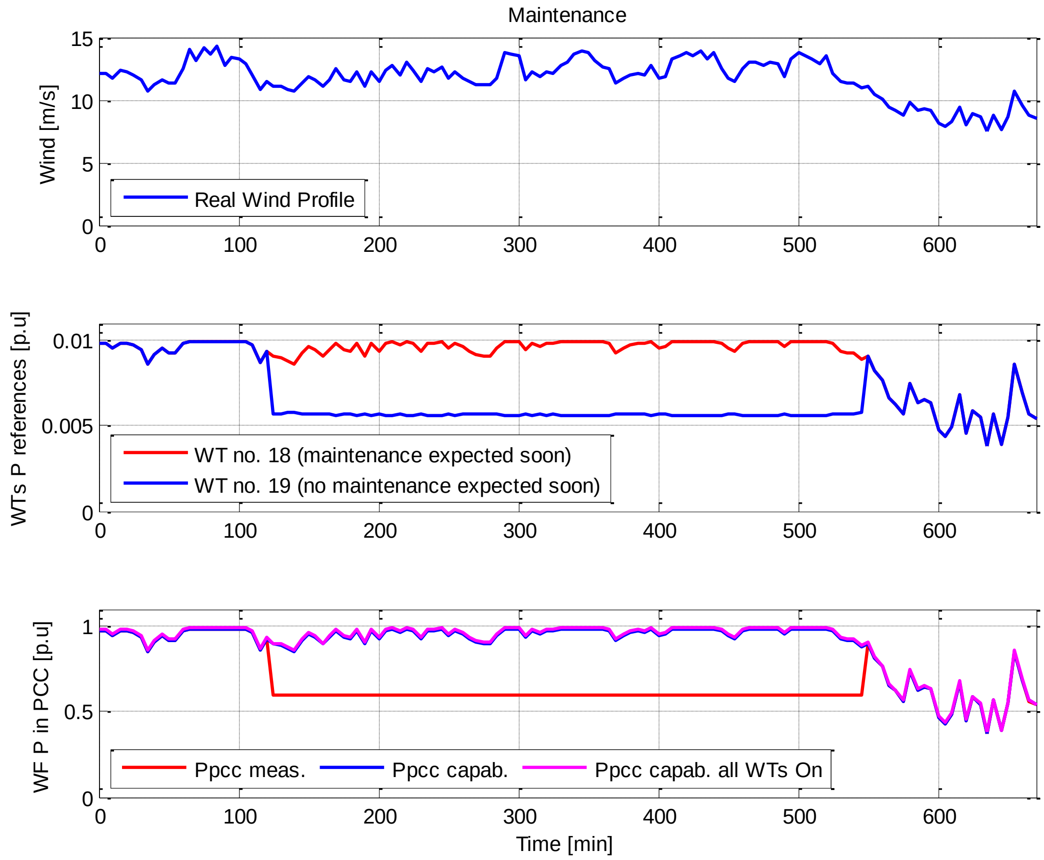

Figure 5-17 OPF with maintenance periods

The first graph of the above figure presents the wind profile over the entire simulation period. In the second graph are presented the *P* references for two WTs (no. 18 and no. 19). For the WT no.18, the *P* reference is maximized because its maintenance period approaches. Since the period maintenance of the WT no. 19 is not in the near future, this WT is operating in Balance mode. The same principle applies for Q references as well.

The last graph of the Figure 5-17 illustrates the PCC power provided by the WF during the simulation. It can be concluded from this graph that the proposed principle doesn't affect the behavior of the WF. Therefore the WF Controller is capable to operate in the demanded control modes and to consider also the Lifetime of the WF, through its maintenance periods.

B. Static coefficients for the WF rows

This study case was build based on the scenario, according to which all the WTs after a certain period of time could crash simultaneously. In order to avoid this situation, static coefficients were given to each feeder of the WF. The WTs belonging to the row with the highest coefficient will receive the highest references, and are expected to crash sooner than the rest of the WTs.

The procedure used in this study case is the following:

- for each WF row a static coefficient is defined;
- the number of WF rows for which the coefficient is considered was specified;
- based on the predefined coefficient new WTs references were imposed;

The results of this study case are presented in Figure 5-18. From the second graph of the above figure, where the *P* references of WTs from different rows are plotted, it can be observed that the WTs with the highest coefficient receive the highest reference. Therefore it can be concluded that the WF Controller respects the proposed principle and in the same time operates in the requested Control Mode.

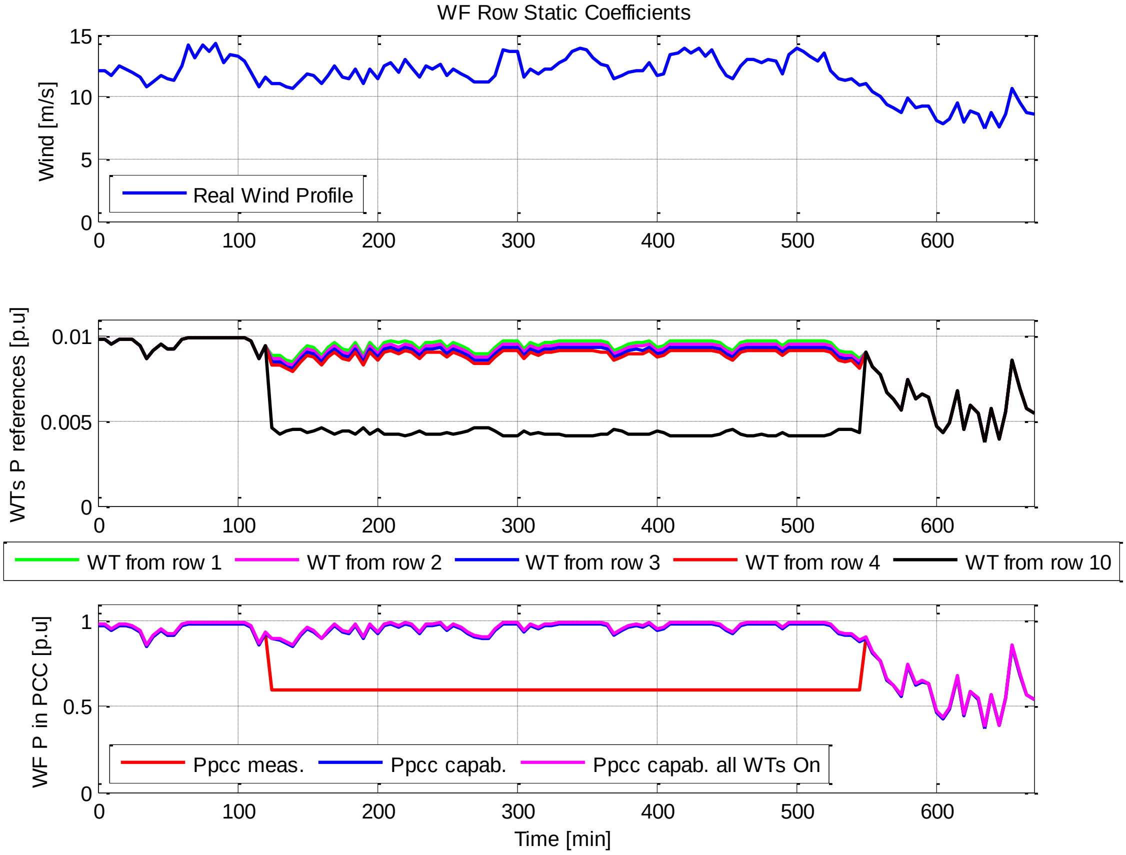

Figure 5-18 Static coefficients for WF rows

C. Lifetime optimization through WTs shut down

This study case is carried out based on the idea that if some WTs are shut downed during the Balance Control Mode the WF Lifetime could be increased. The procedure of this study case is the following:

- for each WT a dynamic (updating continuously) LTC was considered;
- during the Balance Control Mode, based on the imposed WF active power level, the maximum number of WTs that can be shut downed was determined (e.g. 24 WTs);
- moreover the first 24th WTs with the highest LTC were shut downed;

The results of this study case are presented in Figure 5-19. The second graph of the above figure presents the *P* references for WT no.26 in regular Balance Control Mode or when WT no.25 is shut downed according to the proposed procedure. It can be observed that for the same power limit imposed in PCC, the WT no.26 receive a higher *P* reference when some WTs are shut downed. From the last graph it can be observed that even if the WF *P* capability in PCC decreased accordingly with the number of shut downed WTs, the WF is still capable to respect the power level imposed by the TSO.

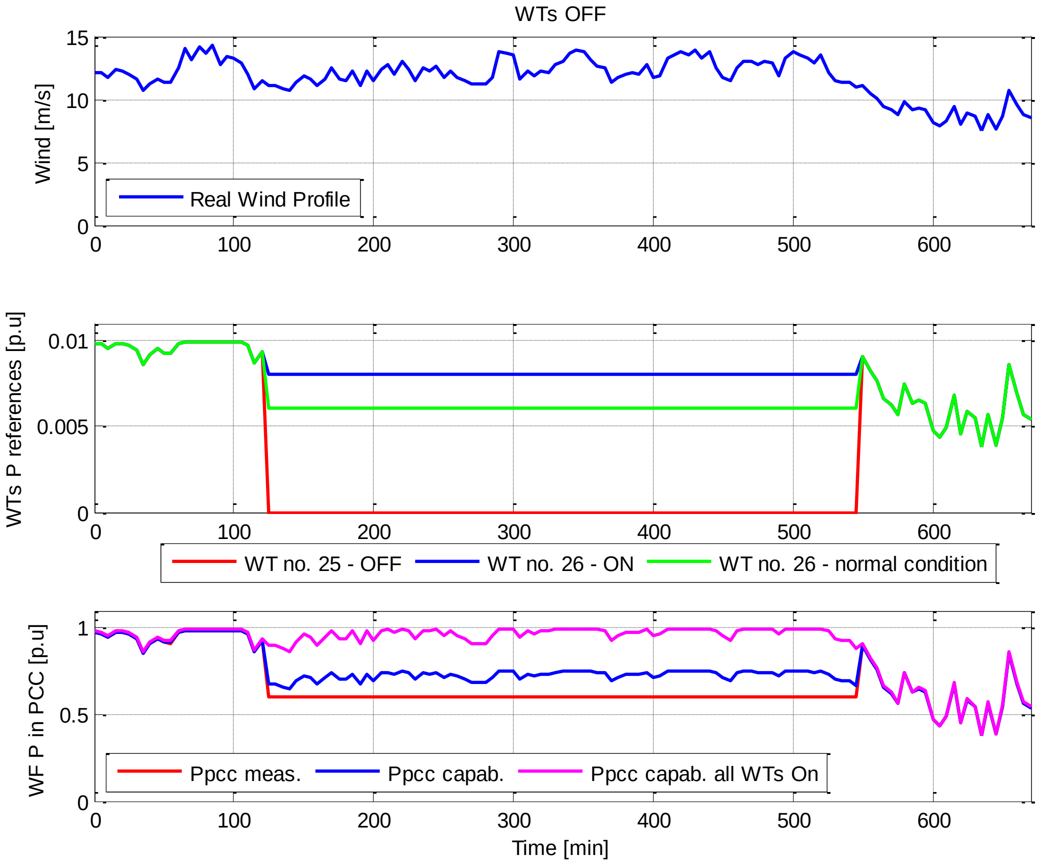

Figure 5-19 Lifetime improvement through LTC

Chapter 6 Conclusions and Further Work

General Conclusions

This research project is focused on the implementation of a wind power plant controller capable to optimize the dispatch of active and reactive power references for each WT. The optimal dispatch was analyzed for different WF control modes (delta, balance, etc) and different control objectives (losses minimization or life time optimization). In order to evaluate the optimal power flow with respect to a benchmark, a conventional power flow was implemented as well.

Moreover, the WF controller had to fulfill the most demanding European grid codes in terms of power factor capability range, according to ENTSOE. Thus, this thesis also investigates the optimal reactive power rating for the STATCOM, Capacitor Bank and the WT's Grid Side Converter, considering a technical and economic analysis.

In order to fulfill these tasks, the process of carrying out this project and the thesis itself has been divided into several parts.

In the first chapter of this thesis general aspects regarding the wind turbine systems were described. The most commonly applied wind turbine configurations were classified, different WT trends were presented and ENTSOE grid codes requirements were highlighted. In the final part of Chapter 1 the problem motivation, the objectives and the limitations of the project were stated. Overall, the main objective for this chapter was to focus on the ENTSOE grid codes since they were used later on for different study cases.

The second chapter was dedicated to the WF description and modeling. Various models of a WPP have been developed in the literature. They have different purposes and therefore, treat different features of a WF. Considering the objectives of this thesis a simplified model has been implemented and in consequence some aspects were neglected. Thus, while the WT model was developed based on the IEC 61400-25 standard series, the rest of the equipment inside the WPP along with the WF topology and measurements were modeled based on IEC 61970 - 301. Even if these standards focus on the communication between the WPP and the WF controller, the necessary WF model was derived only based on the information contained by the XML's developed. It can be concluded that through this chapter, a different perspective for modeling the WPP was proposed.

The third chapter dealt with the control structure of the WPP. Since the focus of the project is not on the WTs, the afferent control structure for each WT was considered ideal. Moreover the emphasis is over the implementation of the WPP controller as an optimization problem. The example presented in the final part of this chapter aimed to describe the design variables, the cost function and the constraints that have to be considered when an optimal power flow control objective is requested. It can be concluded that the proposed optimal power flow method is suitable for all the study cases carried out. However, slightly changes are necessary based on the WF control objectives and WF control modes.

1. Analysis and selection of a suitable STATCOM, Cap. Bank and Grid Side Converter

In the forth chapter of this report general aspects regarding the FACTS devices were described. Moreover a technical and economic analysis was developed, focusing over the optimal Q sizing of STATCOM, capacitor bank and WT`s grid side converters.

For the first study case, minimizations of STATCOM and capacitor banks were considered based on the diminutation of the WF's FFR. Based on this assumption for the optimization problem three different objectives were derived: selection of the highest necessary $Q_{ST.+Cap.Banks}$, paying the TSO's penalties for not providing the requested power factor or decreasing the active power references of the WTs in order to increase the WF's Q capability and to obtain a FFR of 100%. Since decreasing the WTs active power references was not a cost effective method the optimal $Q_{ST.+Cap.Banks}$ was obtained for paying penalties objective. However to study the economic benefits of using an under rated $Q_{ST.+Cap.Banks}$ it is necessary to developed a much more complex cost profile for the penalties. Therefore, it can be concluded that sizing the STATCOM, capacitor bank and WT`s grid side converters by choosing a rating with a FFR smaller that 100% is not recommended.

With the aim of obtaining more realistic results in the last three study cases the FFR was considered 100%. For the first study case the grid side converter, and both STATCOM and capacitor banks were variable. Moreover in the second study case the STATCOM wasn't considered and for the last one the grid side converter was fixed. As it can be seen, the second and third study cases were particular cases of the first study case. However, it can be concluded that the optimal distribution between STATCOM, capacitor banks and GSC was given by the first study case. Additionally, for the first study case, it is worth mentioning that the optimal capacitor bank Q capability was decreased to 0.24 p.u due to the necessary fulfillment of the lagging power factor. Moreover, the optimal distribution of STATCOM and GSC Q capability was realized mainly based on the evolution of cables price. Therefore, for the first study case, the optimal GSC was 0.3 because this was the highest value for which the WF's cable configuration remains unchanged.

2. *Optimal Power Flow for different WF control modes and control objectives*

The purpose of the last chapter was to evaluate the capability of the developed WF Controller for different control modes and objectives. From the first part of this chapter it can be concluded that the WF Controller was capable to realize the optimal dispatch of WTs references when optimal power flow was considered. For any WF control mode (normal, delta, etc.), when losses minimization was activated the farthest WT always received the lowest reference.

Moreover, in order to evaluate the performances of the optimal power flow with respect to a benchmark, a conventional power flow method was implemented. As a result, for the same active and reactive power in PCC two different sets of P and Q references for WTs, STATCOM and Capacitor Banks were obtained. Thus a comparison between Conventional and Optimal Power Flow was suitable for defining the advantages of WTs reference optimal dispatch. As concluded in Chapter 5 also, both active and reactive power losses improvement were dependent on active and reactive power requested by TSO in WF PCC: for a lower reference in active and reactive power a higher improvement in power losses occurred.

Further on, a comparison in energy production between conventional and optimal power flow was performed. As a result, for a 1 year period of time, the optimal power flow had an average increase of 2.3 *MWh* in comparison with the conventional power flow.

Finally, the purpose of the last study cases was to validate the WF Controller implementation for different WF control objectives. Different control hypothesis were proposed in this section. For the first study case the maintenance periods of the WTs were taken into account. This study case was carried out based on the idea that a WT should operate at its maximum capability if a scheduled maintenance period was coming in the near future. Moreover the second study case was developed in order to avoid a simultaneously crash of all the WTs when the lifetime of the WF is approaching to an end. In order to avoid this situation, static coefficients were given to each feeder of the WF. Consequently, the highest the coefficient was the highest the references imposed for the WTs belonging to the row were. As a final hypothesis, the last study case was carried out based on the idea that some WTs should be shut downed, during the Balance Control Mode, based on the individual LTC assigned for each WT.

Further Work

As always, the possibility for future work remains. The work can be evolved in many directions. There are several lines of research arising from this work which should be pursued. First, it should be stated that this thesis was not focused on the selection of the most favorable optimization method. Therefore, from this point of view different optimization methods can be considered in order to improve the WF controller response (accuracy, number of iterations, etc).

A second line of research, which follows from the project limitations, is the utilization of an ESS in the WF PCC. Therefore, the capability of the ESS and the fluctuations of energy prices in the spot market where the WPP is participating in, should be considered in the optimization criterion.

Other WT topologies (e.g. DFIG) could be studied by considering different PQ capability curves. Moreover, as stated in Chapter 3, for the MV/HV power transformers the ratio tap changers should be considered for a more realistic voltage level regulation.

Different study cases could be performed when different loading percentages (75%, 50% and 25%) for STATCOM and capacitor bank are considered in the implementation of the conventional power flow method. Further on, in order to analyze the impact of the proposed methods for life time optimization, the simulation time for the study cases should be extended.

A new line of research, which follows the initial project proposal, would be the implementation on a real time platform of the WF controller developed in this thesis.

Bibliography

[1] T. Ackermann, *Wind Power in Power Systems*: John Wiley & Sons, 2005.

[2] *BTM Consult: World Market Update 2009 Forecast 2010-2014*. Available: www.btm.dk

[3] EWEA, "Powering Europe: wind energy and the electricity grid," 2010.

[4] EWEA, "Wind Energy - The Facts " 2009.

[5] M. I. Blanco, "The economics of wind energy," *Renewable and Sustainable Energy Reviews 13 (2009) 1372–1382,* 2008.

[6] EWEA, "Pure Power: Wind energy targets for 2020 and 2030," 2009.

[7] R. Teodorescu, *et al.*, *Grid Converters for Photovoltaic and Wind Power Systems* 2011.

[8] ETNSOE, "Requirements for Grid Connection Applicable to all Generators," ed, 2010.

[9] T. Ackermann, *Wind Power in Power Systems* John Wiley Chichester, West Sussex, England, 2005.

[10] C. Zhe, *et al.*, "A Review of the State of the Art of Power Electronics for Wind Turbines," *Power Electronics, IEEE Transactions on,* vol. 24, pp. 1859-1875, 2009.

[11] H. Li and Z. Chen, "Overview of different wind generator systems and their comparisons," *Renewable Power Generation, IET,* vol. 2, pp. 123-138, 2008.

[12] H. Aoyang, *et al.*, "Study of the factors affected the rotor over-current of DFIG during the three-phase voltage dip," in *Electric Utility Deregulation and Restructuring and Power Technologies, 2008. DRPT 2008. Third International Conference on*, 2008, pp. 2647-2652.

[13] A. Causebrook, *et al.*, "Fault Ride-Through of Large Wind Farms Using Series Dynamic Braking Resistors (March 2007)," *Power Systems, IEEE Transactions on*, vol. 22, pp. 966-975, 2007.

[14] "IEC 61400-25," ed. Switzerland, 2006.

[15] "IEC 61970-301," ed. Switzerland, 2009.

[16] A. D. H. Florin Iov, Poul Sørensen, Frede Blaabjerg, *General Model for Representing Variable SpeedWind Turbines in Power System Dynamics Simulations*, 2004.

[17] H. K. Vladislav Akhmatov, "An aggregate model of a grid-connected, large-scale, offshore wind farm for power stability investigations - importance of windmill mechanical system," *Electrical Power and Energy System 24,* 2001.

[18] A. Sode-Yome and N. Mithulananthan, "Comparison of shunt capacitor, SVC and STATCOM in static voltage stability margin enhancement," *International Journal of Electrical Engineering Education 41/2,* 2004.

[19] M. Ciobotaru, *Reliable Grid Condition Detection and Control of Single-Phase Distributed Power Generation Systems*, 2009.

[20] A. Larsson, *The Power Quality of Wind Turbines*, 2000.

[21] I. Munteanu, *et al.*, *Optimal Control of Wind Energy Systems Towards a Global Approach*, 2008.

[22] F. D. Bianchi, *et al.*, *Wind Turbine Control Systems*, 2007.

[23] A. D. H. Poul Sørensen, Kenneth Thomsen, Thomas Buhl, Poul Erik Morthorst, Lars Henrik Nielsen, Florin Iov, Frede Blaabjerg, Henrik Aalborg Nielsen, Henrik Madsen and Martin H. Donovan, *Operation and control of large wind turbines and wind farms - Final report*, 2005.

[24] T. K. Mohsen Soltani, Thomas Bak, "Modeling and Simulation of Offshore Wind Farms for Farm Level Control," 2009.

[25] R. G. de Almeida, *et al.*, "Optimum generation control in wind parks when carrying out system operator requests," *Power Systems, IEEE Transactions on,* vol. 21, pp. 718-725, 2006.
[26] J. A. Momoh, *Electric Power Distribution, Automation, Protection and Control*, 2008.
[27] H. C. Pedersen, "AAU Lecture: Optimisation Theory," 2010.
[28] N. G. Hingoranl and L. Gyugyi, *Understanding FACTS*, 1999.
[29] X.-P. Zhang, *et al.*, *Flexible AC Transmission Systems: Modelling and Control*, 2005.
[30] F. F. Li, *et al.*, "A Preliminary Analysis of the Economics of Using Distributed Energy as a Source of Reactive Power Supply," 2006.
[31] E. David, *et al.*, "Distributed Energy Resource using FACTS, STATCOM, SVC and Synchronous Condenser for Dynamic System Control of VAR," 2005.
[32] R. P. a. T. Lettenmaier, "Alternative Design Study Report: WindPACT Advanced Wind Turbine Drive Train Designs Study," 2002.
[33] R. D. Guide, "Simulating the Manitoba Hydro Power System using RTDS."

Appendix A - CD Content

The content on the CD is sorted into different folders as shown below:

- Report
  - Word Version
  - Pdf Version
- Results
  - Matlab Figures
  - .mat files
- References

Appendix B - ENTSOE Parameters

Parameters for Voltage/Frequency diagram (400kV)

	Synchronous Area				
	Continental Europe	**Nordic**	**Great Britain**	**Ireland**	**Baltic States**
$V_{p\min}$	0.9 pu	0.9 pu	0.9 pu	0.9 pu	n/a
$V_{t\min 1}$	0.875 pu	n/a	n/a	n/a	n/a
$V_{t\min 2}$	0.85 pu	n/a	n/a	n/a	n/a
$V_{t\max}$	1.1 pu	1.1 pu	1.10 pu	1.118 pu	n/a
$V_{p\max 2}$	1.05 pu	n/a	1.05 pu	n/a	n/a
$V_{p\max 1}$	1.0875 pu	1.05 pu	Not defined	n/a	n/a
$f_{p\min}$	48 Hz	49 Hz	48.5 Hz	49.5 Hz	n/a
$f_{t\min 1}$	47.5 Hz	47.5 Hz	47.5 Hz	47.5 Hz	n/a
$f_{t\min 2}$	46.5 Hz	n/a	47.0 Hz	47 Hz	n/a
$f_{p\max}$	51.5 Hz	51 Hz	51.0 Hz	50.5 Hz	n/a
$f_{t\max 1}$	51.5 Hz	52 Hz	51.5 Hz	52 Hz	n/a
$f_{t\max 2}$	53.0 Hz	52.5 Hz	52.0 Hz	n/a	n/a
t1	3 h	n/a	n/a	n/a	n/a
t2	30 min	n/a	n/a	n/a	n/a
t3	10 s	n/a	20 sec	5 min	n/a
t4	10 min	30 min	90 min	60 min	n/a
t5	30 min	30 min	90 min	60 min	n/a
t6	10s	3 min	15 min	60 min	n/a
t7	1 h	60 min	n/a	n/a	n/a

Parameters for Reactive power capacity diagram

Synchronous Area	Range of $Q/P_{\max}$	Range of steady state voltage level in pu
Continental Europe	**0.75**	**0.225**
Nordic	**0.95**	**0.150**
Great Britain	**0.95**	**0.100**
Ireland	**1.08**	**0.218**
Baltic States	**Not defined yet**	**Not defined yet**

Appendix C – WPP Parameters

WT Parameters

Parameters	Values
No. of WTs	**100**
No. of feeders	**15**
WT Rotor Diameter	**100(m)**
Row/Column distance	**500(m)**
WT Rated Power	**5(MW)**
Cut-in Speed	**4(m/s)**
Cut-out Speed	**25(m/s)**
Rated Speed	**13(m/s)**

WT Power Profile parameters [33]

Wind speed (m/s)	WT Power (p.u)
0	**0**
3	**0**
4	**0.0168**
5	**0.0864**
6	**0.1854**
7	**0.3066**
8	**0.4548**
9	**0.6102**
10	**0.771**
11	**0.9024**
12	**0.9822**
13	**1**
25	**1**
26	**0**

Power Transformers parameters

Winding parameters

Parameters	WT Transformers	WPP Transformers	STATCOM Transformer
R p.u	0.01	0.01	0.01
X p.u	0.1	0.07	0.07
Rated S (MVAr)	5.52	325	182
Rated U (kV)	4/33	33/125	3.3/33

¶

WPP Transformer Tap changer parameters

Parameters	Values
High step	**9**
Low step	**-9**
Neutral step	**0**
Neutral Voltage (kV)	**125**
Step voltage increment p.u	**1.67**

ACLine parameters

Conductor CSA (mm^2)	Conductor Resistance AC 90°C (ohm/km)	Inductance (mH/km)	Current Rating (A)	Power Rating (MVA)
120	**0.20**	**0.41**	**325**	**18.6**
150	**0.16**	**0.40**	**365**	**20.9**
185	**0.13**	**0.38**	**449**	**25.7**
240	**0.10**	**0.37**	**513**	**29.3**
300	**0.08**	**0.36**	**572**	**32.7**
400	**0.06**	**0.35**	**637**	**36.4**
500	**0.05**	**0.33**	**659**	**39.7**
630	**0.04**	**0.32**	**776**	**44.4**
800	**0.03**	**0.31**	**838**	**47.9**

STATCOM Parameters

Parameters	Values
Capacitive rating $(MVAr)$	**182**
Inductive rating $(MVAr)$	**182**
Control mode	**“Reactive Power”**

Grid Parameters

Parameters	Values
Grid Inductance (μH)	**50**
Grid resistance $(mOhm)$	**0.1**

Appendix D – CimTool Schemes

WT CimTool schema

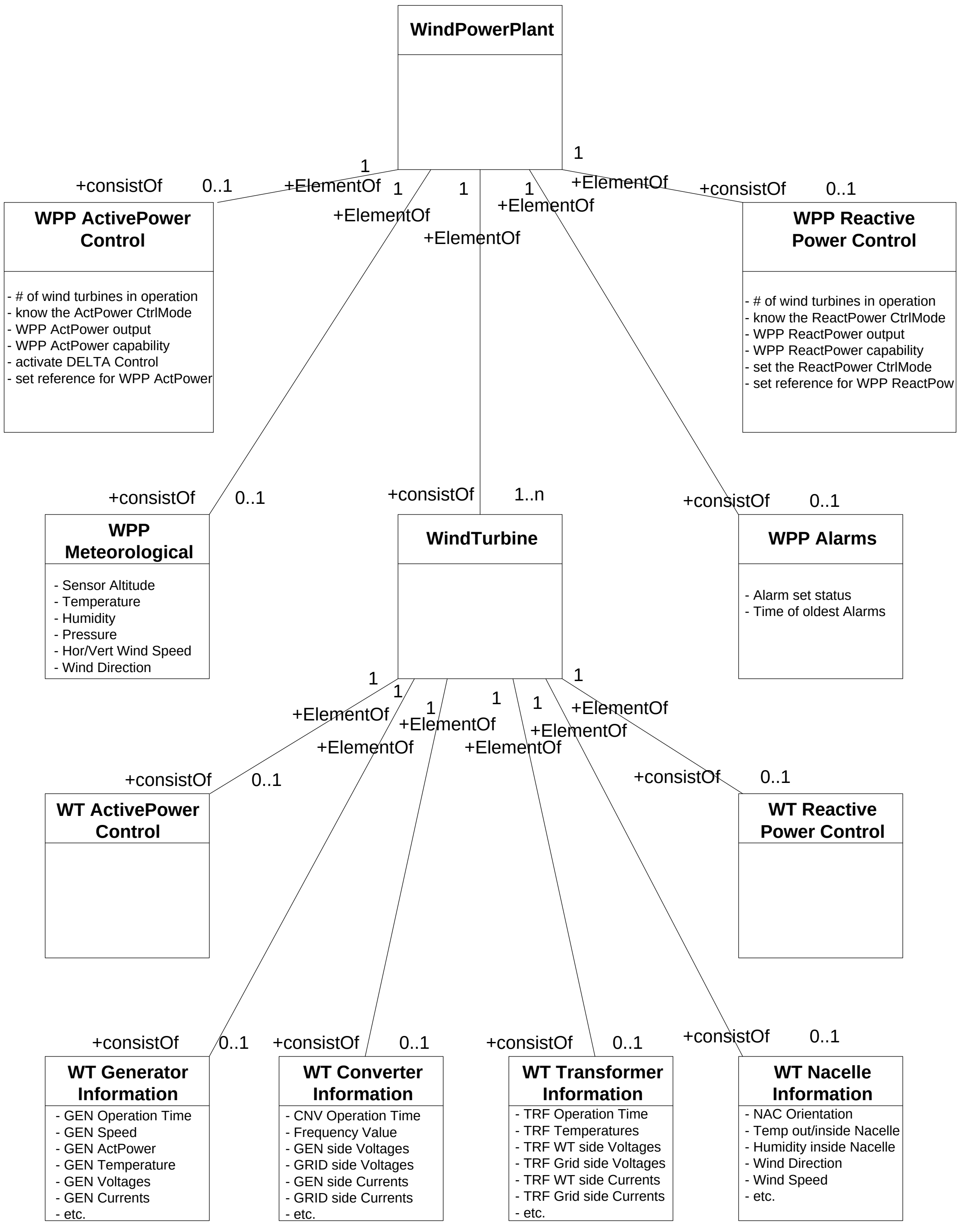

Overview of the inheritance hierarchy of the CimTool model

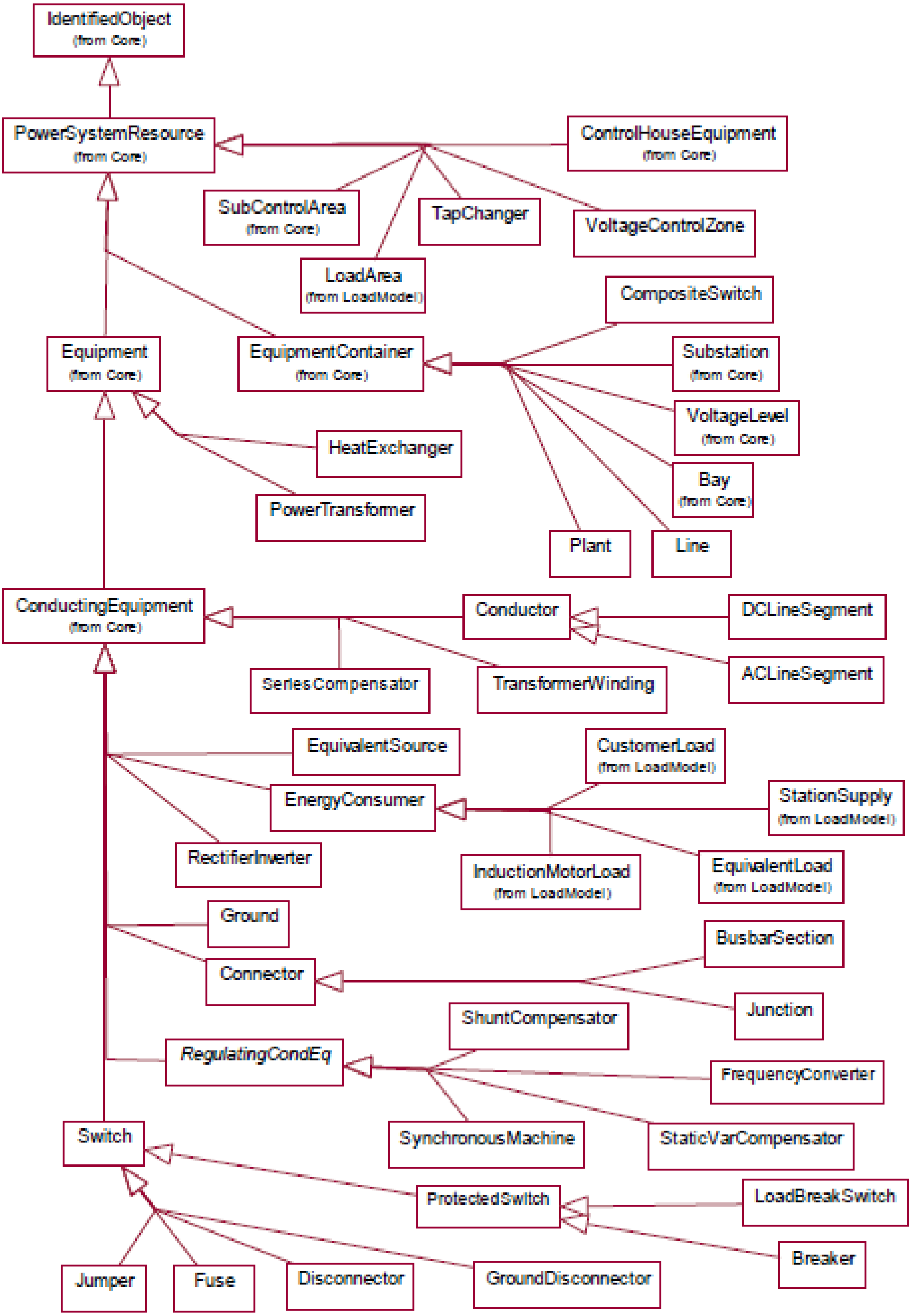

Appendix E – Project Proposal

Coordinated Control of Wind Turbines

Background

Large wind installations are requested to behave like a modern power plant, i.e. being integrated in the power system planning and control tools. Consequently, the control of the wind power plant needs to be carefully designed to meet the requirements from system operators in terms of grid code compliance and participation in grid controls.

Project's objectives

The project shall develop a wind power plant controller to meet grid requirements in different countries in Europe. Starting from the wind turbines' technology, the project shall evaluate the possibilities of the plant to provide reactive power and design control schemes for regulating output power (both active and reactive) of the plant. The existence of Flexible AC Transmission Systems (FACTS) and energy storage systems (ESS) at the point of common coupling shall be also considered in design.

Scope and focus of the project

The project should focus on the following key points:

- design and implement a real time wind farm controller for a large scale wind power plants
- consider the constraints on response time imposed by the system operators
- consider the constraints of the communication technologies used (or to be used) in a wind power plant (i.e. fiber optic, radio communication, etc.)
- consider the existence of FACTS and ESS at the plant premises
- implement a few control strategies for the plant to show compliance with grid codes in Europe

Deliverables

The project deliverables should include

- A design of the wind power plant controller
- Implementation of the controller in Simulink
- Technical report